FIELD VERIFICATION OF STANDARD INSTALLATION DIRECT DESIGN (SIDD) METHOD FOR CONCRETE PIPE

FINAL REPORT

OHIO DEPARTMENT OF TRANSPORTATION
U.S. DEPARTMENT OF TRANSPORTATION, and
FEDERAL HIGHWAY ADMINISTRATION

Principal Investigators:
Shad M. Sargand
Glenn A. Hazen

Graduate Research Assistants:
Mohammed Haque
Elangovan Vaithianathan

Ohio University
Ohio Research Institute for Transportation and the Environment
Civil Engineering Department

August 1998

1. Report No.	2. Government Accession No.	3. Recipient's Catalog No.
FHWA/OH-98/010		

4. Title and Subtitle	5. Report Date
FIELD VERIFICATION OF STANDARD INSTALLATION DIRECT DESIGN (SIDD) METHOD FOR CONCRETE PIPE	April, 1998
	6. Performing Organization Code
	8. Performing Organization Report No.
7. Author(s)	10. Work Unit No. (TRAIS)
Shad M. Sargand, Glenn A. Hazen	
9. Performing Organization Name and Address	11. Contract or Grant No.
Ohio University Department of Civil Engineering Athens, OH 45701	State Job No. 14528(0)
	13. Type of Report and Period Covered
	Final Report
12. Sponsoring Agency Name and Address	14. Sponsoring Agency Code
Ohio Department of Transportation 25 S. Front St. Columbus, OH 43215	

15. Supplementary Notes

Prepared in cooperation with the U.S. Department of Transportation, Federal Highway Administration

16. Abstract

Concrete pipes play a significant role in highway construction. The economics of manufacturing, durability of pipe, and rigidity under a load make them an attractive choice in many situations. As a direct result of substantial use, these pipes have been subjected to continuing research over a number of years. The American Concrete Pipe Association has developed a Standard Installation Direct Design (SIDD) method for the structural design of reinforced concrete pipe. SIDD is a user friendly software program that employs an elastic solution with an assumed pressure distribution around the pipe. There is considerable interest in comparing SIDD calculations to measured values since a greater choice of installation methods is available.

In this study, four steel reinforced concrete pipes were fully instrumented and tested in the load cell facility of the Ohio Research Institute for Transportation and the Environment (ORITE). Pipes were tested with two diameters and two backfill conditions. The behavior of these pipes was compared to two instrumented pipes that were installed in the field and with theoretical calculations. Theoretical values were calculated from finite element program Culvert Analysis and Design (CANDE) and design program Standard Installation Direct Design (SIDD).

SIDD calculations were in good agreement with experimental measurements when compared to loading before the concrete walls cracked. Furthermore, at design depth the agreement of moment was excellent. However, there was agreement with thrusts in the pipe walls at only the initial load steps.

17. Key Words	18. Distribution Statement
Concrete Pipe, Deep Burial, SIDD, and CANDE	No Restrictions. This document is available to the public through the National Technical Information Service, Springfield, Virginia 22161

19. Security Classif. (of this report)	20. Security Classif. (of this page)	21. No. of Pages	22. Price
Unclassified	Unclassified		

FIELD VERIFICATION OF STANDARD INSTALLATION DIRECT DESIGN (SIDD) METHOD FOR CONCRETE PIPE

TABLE OF CONTENTS

LIST OF FIGURES

LIST OF TABLES

ACKNOWLEDGMENTS

The authors are grateful to the many individuals who contributed to this effort. The Indiana-Kentucky-Ohio Concrete Pipe Association contributed to the pipe design and furnished the pipes. A special note of appreciation to Joe Neidhardt. The cooperation of the Ohio Department of Transportation personnel in District 10 and in the research office is also recognized.

CHAPTER 1

INTRODUCTION

1.1 GENERAL STATEMENT

Concrete pipe plays a significant role in highway construction. The economics of manufacturing, durability of pipe, and rigidity under a load make them an attractive choice in many situations. As a direct result of substantial use, these pipes have been subjected to continuing research over a number of years. In this study, four, steel reinforced, concrete pipes were fully instrumented and tested in the load cell facility of the Ohio Research Institute for Transportation and the Environment (ORITE). Two pipes of different diameters were embedded under two compactions. Then the load responses of these pipes were compared to two instrumented pipes, installed in the field and theoretical calculations. Theoretical values were calculated by the finite element program Culvert Analysis and DEsign (CANDE) [1] and design program Standard Installation Direct Design (SIDD) [2].

With advancement in computational capacity and sensor technology, new software for design and analysis of engineering problems, such as concrete pipe design, has been developed. This new software, however, has not gained wide usage by practicing engineers or others. To ensure acceptance and replace existing empirical methods of design, this software must be verified.

The American Concrete Pipe Association has developed a Standard Installation Direct Design (SIDD) method for the structural design of reinforced concrete pipe. SIDD is a user friendly software program that employs an elastic solution with an assumed pressure distribution around the pipe. There is considerable interest in comparing SIDD calculations to measured

values since a greater choice of installation methods is available.

1.2 LITERATURE REVIEW

The most commonly used empirical method for the design of reinforced concrete pipe is to determine the earth loads on the pipe employing the Marston-Spangler theory; and then to convert the loads to the equivalent loads in a 3-edge bearing test; and finally to design the pipe for these loads. This approach is referred to an indirect design method. Application of the indirect design method is described in the American Concrete Pipe Association Handbook [3].

Another approach is the direct method where the pressure distribution around the pipe is calculated from a finite element formulation or assumed on the basis of numerous finite element solutions. Pipe response can be computed for either condition.

The direct design methodology called Soil Pipe Interaction Design and Analysis (SPIDA) was developed based on the finite element method with a soil-structure concept [4]. SPIDA was developed for the design and analysis of complicated soil-structure problems, where assumptions in the installation procedures, material properties, and live loads can be taken into account. The two suppositions that require particular care, when formulating an analysis, are describing the constitutive relationships for backfill materials and crack formulation in concrete pipe. In modeling backfill materials it is well known that the effect of compaction activities in the construction sequence is difficult if possible to describe. In addition, all failure modes in concrete cannot be accommodated by finite element programs. Yet, to date only a few installations, designed to match field conditions to the direct design methodology, have been instrumented and monitored.

Krizek and McQuade [5] studied the response of buried concrete pipes in eight different

field locations where the investigation looked at stress distribution at the soil-pipe interface with change in pipe geometry. The stresses and strains in the soil adjoining the pipe were also calculated. A comparison was made to a developed mathematical model by Anderson [6]. The data was collected with stress cells, mechanical strain gages, electric strain gages and settlement plates. The tests were done for both embankment and trench installations. Good agreement was obtained when compared to field measurements. The mathematical model predicted higher normal stresses just below the pipe and significant horizontal stresses at the springline when compared to the field data. Other results were consistent and agreed qualitatively with engineering intuition.

In another study, Roschke and Davis [7] performed a rigid culvert trench experiment and finite element analysis to determine the allowable fill depth for varying pipe strengths. Circumferential soil pressures, pipe strains, and displacements were monitored. Fluid settlement platforms and stress meters were also utilized. Roschke and Davis observed that accurate prediction of soil behavior with a finite element method (FEM) analysis required a nonlinear soil model. However, calculations done with simplified, symmetrical meshes give normal pressures at the interfaces and diameter deflections of the same order of magnitude as full scale investigations. Rigid culvert behavior was found to be influenced more by the gradients of soil pressures than their absolute magnitudes. The behavior of the periphery of the culvert resulted from all applied forces.

In this study, Roschke and Davis required a general purpose program to efficiently handle many elements. They compared the Reinforce Earthwork Analysis (REA) to the Culvert Analysis and Design (CANDE) for the analysis of a rigid concrete culvert. They concluded that REA was a more appropriate program than CANDE because of the following additional features:

- three beam elements that meet at a node,
- special constitutive relations of low-modulus materials,
- excavation models of soil elements from trenches, and
- stiffness matrices with half-bandwidth greater than ninety columns.

Selig and Packard [8] have reported comprehensive studies on buried concrete pipe embankment and trench installation analysis. They concluded that the hyperbolic soil model, using bulk modulus and Young's modulus adequately described soil responses.

Penman, et al. [9] measured the earth pressure on a rigid, reinforced concrete culvert placed 53 m (174 ft) below a rock fill. He measured culvert crown pressure of 176% of the geostatic pressure when construction was complete.

As a simplification to the finite element programs, the design program, SIDD, includes a model for earth pressure distribution around a rigid pipe, based on results provided by SPIDA. The modeling of backfill materials is difficult with incorporation of compaction activities in the construction sequences. In addition, all failure modes in concrete pipe have not yet been accommodated by models used in these finite element programs. Yet, to date, only a few installations, designed to compare the direct design methodology (SIDD), have been instrumented and monitored.

1.3 OUTLINE OF RESEARCH

Chapter 2 describes in detail the six concrete pipes that were evaluated in this project, including instrumentation. Attachment procedures and data collection for sensors were essentially the same for all six pipes. Embedment procedures are also described for both load tests and field installations.

Chapters 3, 4 and 5 report the results of load tests on the 610 mm (24 in.) concrete pipes, load tests on the 1520 mm (60 in.) concrete pipes, and field tests on the 1520 mm (60 in.) concrete pipes, respectively. Experimental and field measurements are presented. The moments and thrusts are computed and presented for each loading. For purposes of design, SIDD and finite element (CANDE) comparisons are made.

Discussion of results and conclusions are presented in Chapter 6. Comparison of concrete pipe bedding and backfill parameters are made. Possible implementation of results is suggested.

CHAPTER 2

INSTRUMENTATION

2.1 INTRODUCTION

Under simulated field conditions, reinforced concrete pipe was instrumented and monitored during incremental loading in the ORITE load cell facility. Two different size pipes, one 1520 mm (60 in.) in diameter and one 610 mm (24 in.) in diameter, each with two different backfill compactions were studied (Pipe Test 1 through 4). Pipes were supplied by the Ohio Concrete Pipe Association. Two 1520 mm (60 in.) diameter pipes were installed under 13.1 m (43 ft) of cover on the continuation of the four-lane highway of Meigs County, S.R. 7, Sta. 516+45 (MEIG-7); located just northeast of Pomeroy, Ohio (Pipe Tests 5 and 6). The description of test pipes is given in Table 2.1.

Table 2.1 Description of Test Pipes

Pipe Property	Test 1	Test 2	Test 3	Test 4	Test 5	Test 6
Nominal Size	610 mm (24 in.)	610 mm (24 in.)	1520 mm (60 in.)	1520 mm (60 in.)	1520 mm (60 in.)	1520 mm (60 in.)
Nominal Thickness	76 mm (3 in.)	76 mm (3 in.)	172 mm (6.75 in.)	172 mm (6.75 in.)	172 mm (6.75 in.)	172 mm (6.75 in.)
No. of Layers of Reinforcing Steel	1	1	2	2	2	2
Type of Test	Load Cell	Load Cell	Load Cell	Load Cell	Field	Field
Compaction (SIDD)	Type 1	Type 3	Type 1	Type 3	Type 1	Type 1

For each test, the pipe-backfill system stabilized after 15 minutes and the following data were recorded three times for each load increment at an interval of five minutes:

1. Strains at the inside and outside concrete surfaces of the pipe wall, and on the steel reinforcement cage at equally spaced locations around the circumference at the middle of the pipe.
2. Additional circumferential and longitudinal strains at the cross section located 254 mm (10 in.) away from the middle of the pipe.
3. Pressure at the interface between soil and pipe-wall at the crown, invert and springline.
4. Deflected shape of the pipe at the middle.
5. And, the movement of the loading platform.

2.2 PIPE DETAILS

Pipes for the load cell tests were manufactured using a centrifugal forming process whereas pipes placed on the MEIG-7 project were manufactured with stationary forms.

2. 2.1 Concreting and Curing

The instrumented steel circular cages for Tests 1 through 4 were transported to the concrete pipe manufacturing plant. The pipe form was a metal circular shape with a fixed base. The expanded end of the cage was placed over the base of the pipe form and shutters tightened. The wires of the strain gages, cemented to the steel cage, were carefully routed to a safe exit through a hole drilled in the top of the pipe form. Then the pipes were formed with a standard packerhead. The forms containing the concreted pipes were carefully transported to a nearby space provided for curing. After removing the forms by unlocking the shutters, the concreted pipes stood upright. Before curing, any gaps were filled and the outer surface of the pipe was smoothed. A thermally insulated mobile tent provided the required curing temperature over a

seven-day period.

Concrete forming for the Tests 5 and 6 was accomplished by closing forms around the two steel cages and discharging concrete into the upper gap while the forms were vibrated; a process known as dry cast vibration. Wires were carefully routed to the top of the forms. The concrete in the forms was allowed to harden for 24 hours. Then the forms were removed for instrumentation of the pipe. Concrete test cylinders were produced with the pipes to evaluate failure stress and elastic modulus of the cured concrete. These cylinders were cured under environmental conditions equivalent to the tested pipes.

2.2.2 Pipe Properties

Two 610 mm (24 in.) diameter, reinforced concrete pipes were tested in the load cell. Each concrete pipe was reinforced with a single circular steel cage of 686 mm (27 in.) in diameter and 2.39 m (7.83 ft) in length. These pipes were designed for 7.9 m (26 ft) of fill. When delivered, the pipes were inspected to record any anomalies that might affect test results.

Uniaxial compression tests were conducted on the concrete cylinder specimens. To record longitudinal strain, two electrical strain gages were cemented diagonally opposite, at the mid-length of the specimen. Strain gages were connected to a strain indicator to record the strains from both gages simultaneously. Stress was calculated from the cross-sectional area and the load applied; corresponding strain was computed as the average of the strains from the two strain gages. An average modulus of elasticity for concrete of 36 GPa (5.2×10^6 psi) was used in all calculations. The average failure stress was 44.1 MPa (6,400 psi) for Tests 1 through 4 and 53.8 Mpa (7,800 psi) for Tests 5 and 6.

The tensile strength of concrete is essential to determine the level of cracking during the

loading sequence. Because of the non homogeneity of the material, it is impossible to predict the tensile strength of concrete accurately. The maximum tensile strain in concrete was assumed to be between 0.0001 and 0.0002 mm/mm.

2.3 SENSOR INSTALLATION FOR 610 mm (24 in.) PIPE

The concrete pipe tested had an overall length of 2.4 m (8 ft), nominal diameters of 610 mm (24 in.) and wall thicknesses of 73 mm (2.875 in.). The 610 mm (24 in.) pipe was reinforced at the center of the wall thickness with a circular wire cage. The wire was spaced 150 mm (6 in.) in the circumferential direction and 50.8 mm (2 in.) in the longitudinal direction. Wire reinforcement was sized at 5.1 mm (0.200 in.) in both the circumferential as well as the longitudinal direction.

The pipe was instrumented with a total of 58 uniaxial strain gages at two cross sections; 34 gages at the primary cross section located in the middle, and 24 gages at the secondary cross section located 254 mm (10 in.) away from the primary cross section. The purpose of instrumenting the secondary cross section was to provide a duplication of the strain field and measurements of longitudinal strain variations. At the primary cross section, eight locations were selected to install the gages in both the circumferential and the longitudinal directions at the extreme interior and exterior surfaces of the concrete and at the steel wire cage. At the secondary cross section, the strain gages were also cemented to the concrete surfaces and the steel wire cage. Gages were concentrated at the crown, the springlines, and the invert. Figures 2.1 and 2.2 illustrate a cross-sectional view of the strain gage installation plans at primary and secondary cross sections, respectively.

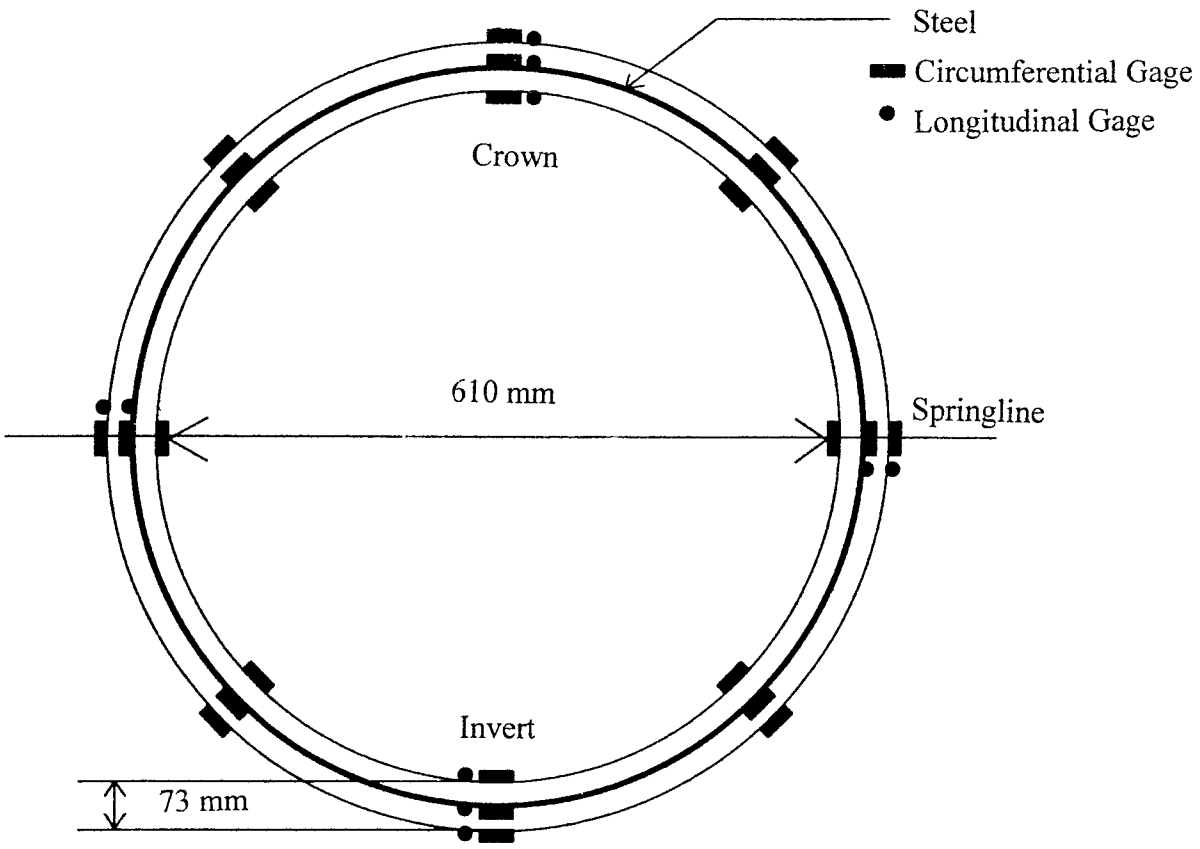

Figure 2.1 Primary Section of Concrete Pipe (34 Gages)

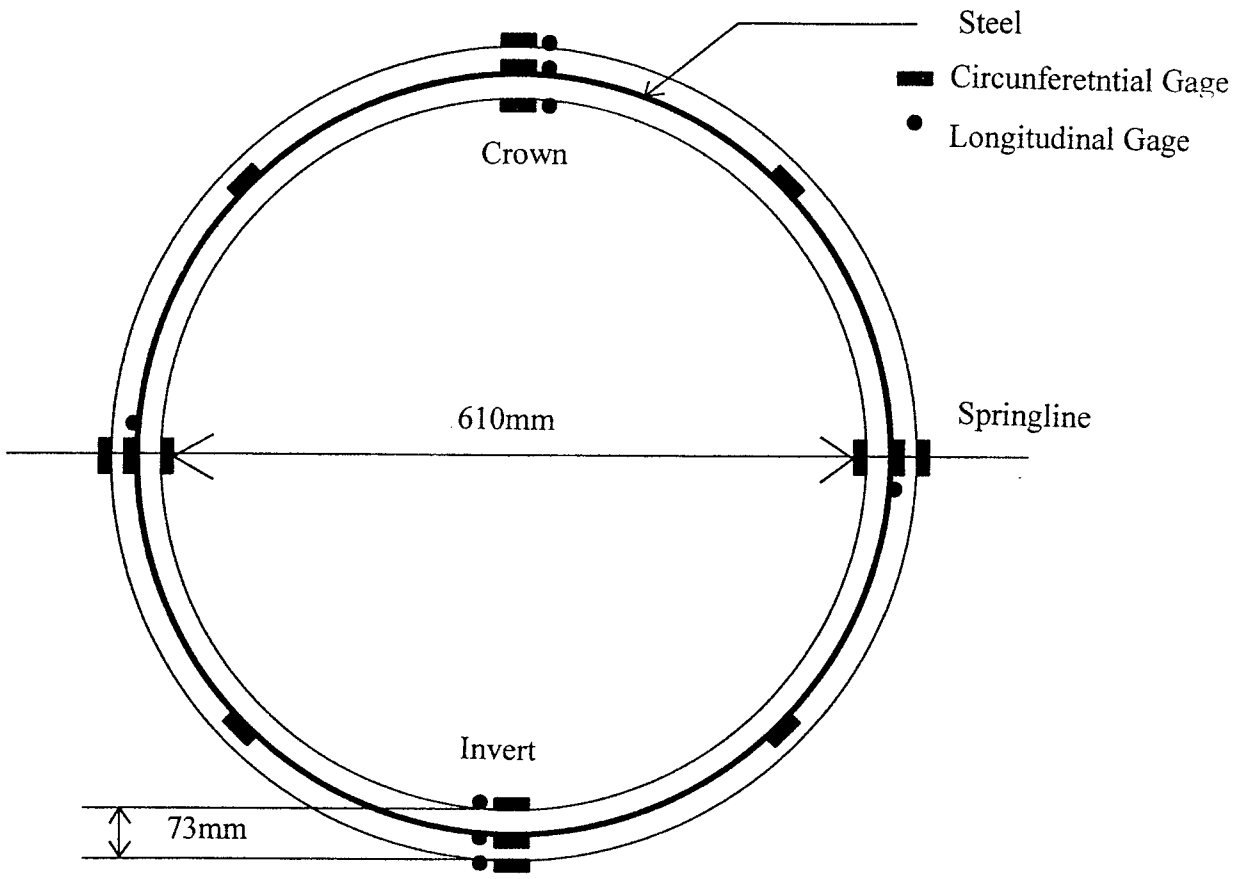

Figure 2.2 Secondary Section of Concrete Pipe (24 Gages)

2.3.1 Steel Cage

All strain gages had a 350-ohm resistence to minimize the error due to lead wire resistance. The type of electrical strain gage selected for measurement of strain in the steel reinforcement wires had a gage length of 13 mm (0.5 in.) and pre soldered lead wires of 3 m (9.8 ft). Lead wires were protected with heat shrinkable tubing before epoxying to reinforcing steel. Care was taken to cement lead wires on the longitudinal reinforcement to model correctly the contact area of the more important transverse reinforcement wires.

Strain gages selected to measure the longitudinal strain were installed on the longitudinal steel reinforcement near the transverse strain gage for each location. Adequate strain relief was provided to the wires to avoid debonding during pipe manufacture. It was also mandatory to provide protection to the gages against moisture and sharp edges of gravel in the concrete mix while concreting. All internal gages were covered with Teflon film first, then butyl rubber, and last neoprene rubber. Gages were further covered with aluminum tape and a nitride rubber coating for moisture protection.

2.3.2 Concrete Surface

Two types of uniaxial gages were employed to instrument the concrete pipe surface. For the primary cross section a gage was used with a gage length twice the maximum dimension of the gravel used in the concrete mix. Hence, the 27 mm (1.0625 in.) gages were applied to the concrete at the primary cross section and 14 mm (0.5625 in.) gages were applied to the concrete at the secondary cross section. Because of the mounting technique used for all gages, it was felt that the 14 mm (0.5625 in.) gages would give accurate readings.

The installation procedure involved preparing the surface before cementing the gages in

place. An epoxy was used to fill the concrete pores. The coating was smoothed before gage application. A standard protection was applied to the gages: layers of Teflon and wax covering; and aluminum tape and nitride rubber coating as an additional precaution against moisture penetration.

2.4 SENSOR INSTALLATION FOR 1520 mm (60 in.) PIPE

The same sensor installation plan was followed for the larger diameter pipe with the exception that larger pipe was reinforced with two steel cages. Both steel reinforcement cages were instrumented. As shown in Figure 2.3, cages were installed 32 mm (1.25 in.) from the inside and outside concrete surfaces, respectively. The concrete pipes tested had nominal dimensions of 2.4 m (8 ft) length, 1520 mm (60 in.) inside diameter, and 172 mm (6.75 in.) wall thickness. Circumferential wires cages were spaced 50 mm (2 in.) in the longitudinal direction and 203 mm (8 in.) in the circumferential direction. For the inner steel cage, the circumferential steel wire was 7.8 mm (0.305 in.) in diameter and the longitudinal steel wire was 5.7 mm (0.225 in.) in diameter. Similarly, for the outside cage, the circumferential steel wire was 5.5 mm (0.215 in.) in diameter and the longitudinal steel wire was 5.1 mm (0.200 in.) in diameter.

The dimensions of the pipe placed in Tests 5 and 6 were similar to the pipe of Tests 3 and 4 and the reinforcement wire spacing was the same. However, the reinforcement was sized slightly different. For the inner steel cage, the circumferential steel wire was 8.7 mm (0.341 in.) in diameter and the longitudinal steel wire was 5.9 mm (0.232 in.) in diameter. For the outer cage, the circumferential steel wire was 6.7 mm (0.262 in.) in diameter and the longitudinal steel wire was 5.1 mm (0.200 in.) in diameter.

Each 1520 mm (60 in.) pipe was instrumented with a total of 64 uniaxial, electrical strain gages at two cross sections: 48 gages at the primary cross section located at the mid-length, and

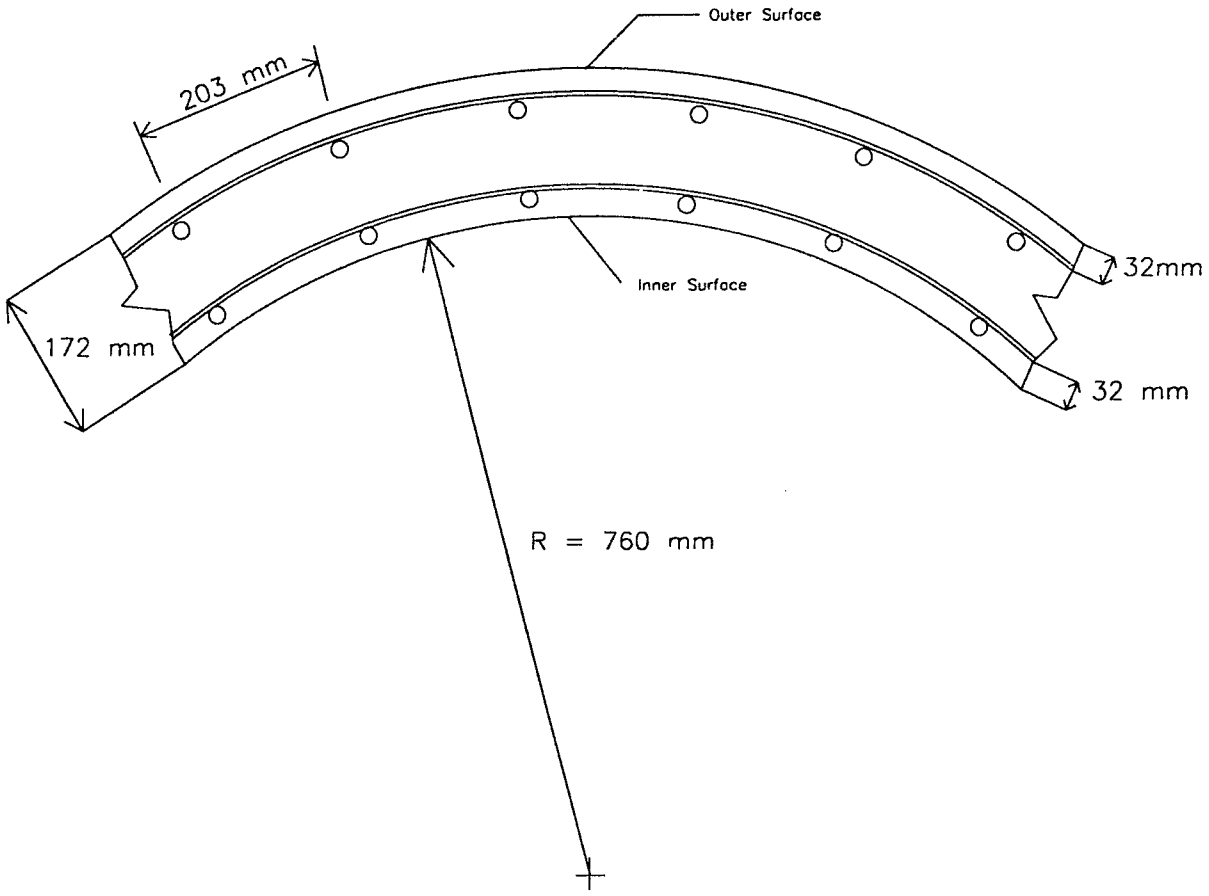

Figure 2.3 Reinforced Concrete Pipe Details

16 gages at the secondary cross section located 254 mm (10 in.) away from the primary cross section. The pipes at final instrumentation for field installation are shown in Figure 2.4.

2.5 PRESSURES AT THE PIPE-SOIL INTERFACE

During pipe installation, earth contact pressure cells were installed around the pipe at the primary cross section. Pressure cells were installed at the crown, invert and both springlines for all tests. This allowed for a comparison of springline pressures to be made. When very little difference in the readings was recorded, the readings were averaged to obtain the springline pressure.

The pressure cells consisted of two stainless steel, circular plates welded together around the periphery and filled with an antifreeze solution. Several laboratory tests were conducted on the optimum embedment and calibration procedure to use. For the application of interface pressure, it was determined that embedment into a 76 mm (3 in.) sand lense gave equal pressure readings for the internal fluid which balanced the external pressure that acted on the cell. Vibrating wire pressure transducers were used because of their long-term stability.

2.6 DEFLECTIONS

Although the deflection of rigid pipe is small, deflection is a prime criterion for evaluation of the pipe-soil system. The deformed shape of the pipe was recorded at each load step by recording the deflection profile three times at five minute intervals. Horizontal and vertical changes in diameter were calculated from the profile shape recorded.

The deflected shapes for most tests were determined using a Linear Voltage Differential

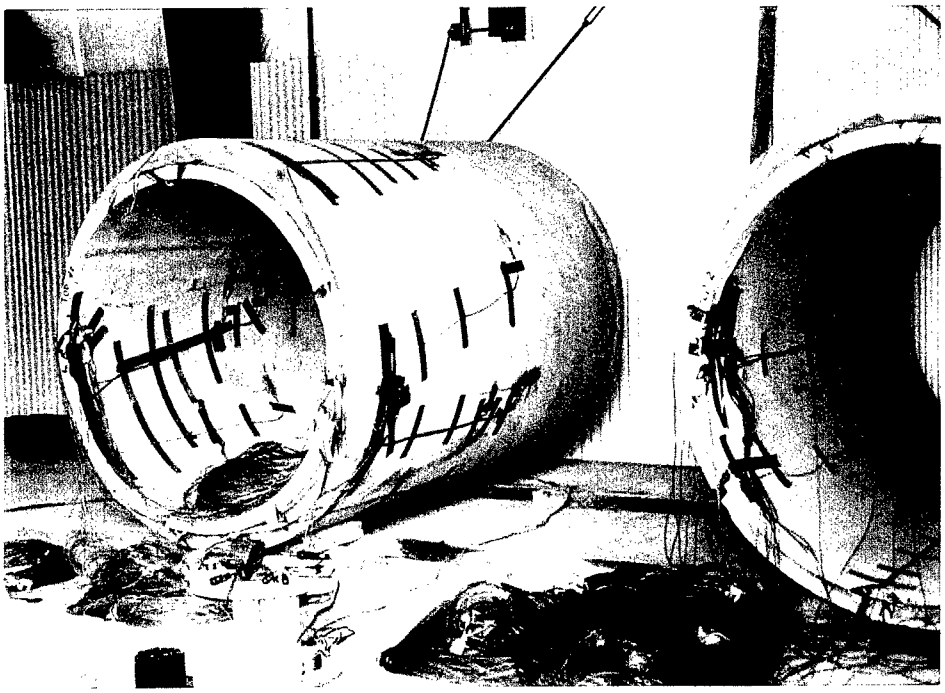

Figure 2.4 Application of Pipe Instrumentation at Manufacturing Site

Transformer (LVDT). The LVDT had a linear range of ±13 mm (0.5 in.) with an accuracy of 0.1 mm (0.004 in.). One end of the LVDT arm had a roller that swept the inner surface of the pipe. The LVDT arm was attached to the shaft of a DC motor that was mounted on one end of a metal beam. To locate the center of rotation of the LVDT arm with the center of the pipe, the other end of the beam was fixed into an adjustable support. The deformed pipe was monitored 150 mm (6 in.) from the instrumented secondary cross section to avoid the strain gage lead wires. As the LVDT arm rotated, the LVDT compressed or elongated defining the deflected shape of the pipe.

Output voltages from the stepper motor were recorded at each rotated position of the LVDT (5 degrees). Readings were taken until the LVDT arm lodged in a crack. When the rotating LVDT became inoperable, horizontal and vertical diameters were measured directly with a portable Linear Voltage Differential Transformer (LVDT) attached to a spacer rod.

Direct measurement was also employed in the field test. The change of diameters in the vertical and horizontal directions at the primary cross section of each pipe was measured by using a portable LVDT device. The portable LVDT was set to show 0.0 volt when set for initial reading (1520 mm (60 in.) inside diameter). The change of the pipe diameter under additional backfill caused a change in LVDT voltage reading. The linear relationship between voltage and deflection was determined in the ORITE laboratory prior to field and load cell acquisition of data.

2.7 PROFILEMETER MEASUREMENTS

A vibrating-wire profilemeter was used to monitor the settlement of the loading platform during testing. This system was used for all load-cell pipe tests. The difference in voltage potential was recorded after each load increment. The settlement was then determined from the

potential difference value using calibrations performed prior to each test. Temperature change was also accounted for in calculating the platform deflection since temperature has a large effect on reading accuracy.

2.8 TEMPERATURE

Temperature readings were available from the pressure cells which would read temperature as well as pressure. Since the field tests were conducted over an extended period of time, it was felt that a change in temperature could introduce a substantial magnitude of residual stress into the pipes. Consequently, to read any variation in temperature, thermistor were installed at the invert, springlines, and crown at the primary cross sections for Test 5 and Test 6. For load cell tests, which were usually conducted over a two day interval and scheduled when rain was not expected, temperature readings were not taken.

2.9 DATA ACQUISITION SYSTEMS

Several data acquisition systems were used, depending on the physical measurements being recorded. Most of the electric strain data were recorded using a Hewlett-Packard, powered bridge system. This system uses an HP computer to control data acquisition and record data. A total of 130 channels can be read sequentially and recorded to an HP computer. This system employed a three-wire system to minimize temperature and lead wire error. Sampling error was mitigated by collecting five data points for each gage reading. For collecting data at the load cell facility, the system was attached to the sensors when the pipe was placed. Then at intervals during backfilling and loading, all data were recorded. The data collection routine was similar for the field study conducted in Test 5 and Test 6. For this investigation, the system was connected

when the pipes were placed. Then, over a five week period, the site was visited and data recorded. When backfill reached design height, the system was disconnected.

Deflection profile was programed so that the step interval of rotation was set and the LVDT deflection versus the rotation angle was recorded to the computer. As a backup an LVDT, attached to a rod, provided a manual reading of pipe deflection.

Pressures and settlement of the loading platform were read manually during the backfilling and application of load. Soil pressures and profilemeter were read with a factory provided readout. Each pressure cell was connected in series and the pressure and the temperature were recorded manually.

2.10 GENERAL

The same sensor installation procedure was used for all pipes whether the pipes were tested in the ORITE test facility or in the field. Electrical strain gages were installed to measure strains from which the thrust and moment in the pipe were calculated. Other measurements taken were pressure on the crown, invert and springlines, and deflections of the vertical and horizontal diameters. In addition, for the load cell tests, deflection of the surface load platform and the profile of the pipe were also measured. These quantities would indicate soil failure and unsymmetric loading.

CHAPTER 3

PIPE INSTALLATION

3.1 Introduction

The purpose of this project was to verify the performance of the reinforced concrete pipes in two of the four installation conditions specified by SIDD and SIDD-HT software manual, under the application of large surface pressures. The experimental simulation was achieved by using the unique test facility of ORITE at Ohio University, Athens, Ohio.

3.2 Structural Load Cell

The principal focus of the test facility was the load cell comprising four concrete columns spaced nearly 8 m (25 ft) center to center which supported the steel I-beams, as shown in Figures 3.1 and 3.2. These concrete columns rested on shaley bedrock that provided a firm foundation to the pipe. The I-beam framework consisted of two main W36x280 I-beams connected on the top of the columns and two W36x260 I-beams that intersected beneath the mid-span of the main beams. The main beams were fastened to the bedrock through eight 35 mm (1.375 in.) diameter grouted tension rock anchors of 60 feet in length. These anchors have a minimum uplift capacity of 828 kN (186 kips) each. After extending the pit, the geometry of the system was compatible with the 4.9 m (16 ft) long jointed, 610 mm (24 in.) diameter, reinforced concrete pipes for burying and testing. To test the 1520 mm (60 in.) concrete pipes the pit was widened to 4 m (13 ft) and elongated to allow the burial of a 7.3 m (24 ft) long jointed section with access to both ends of the pipe.

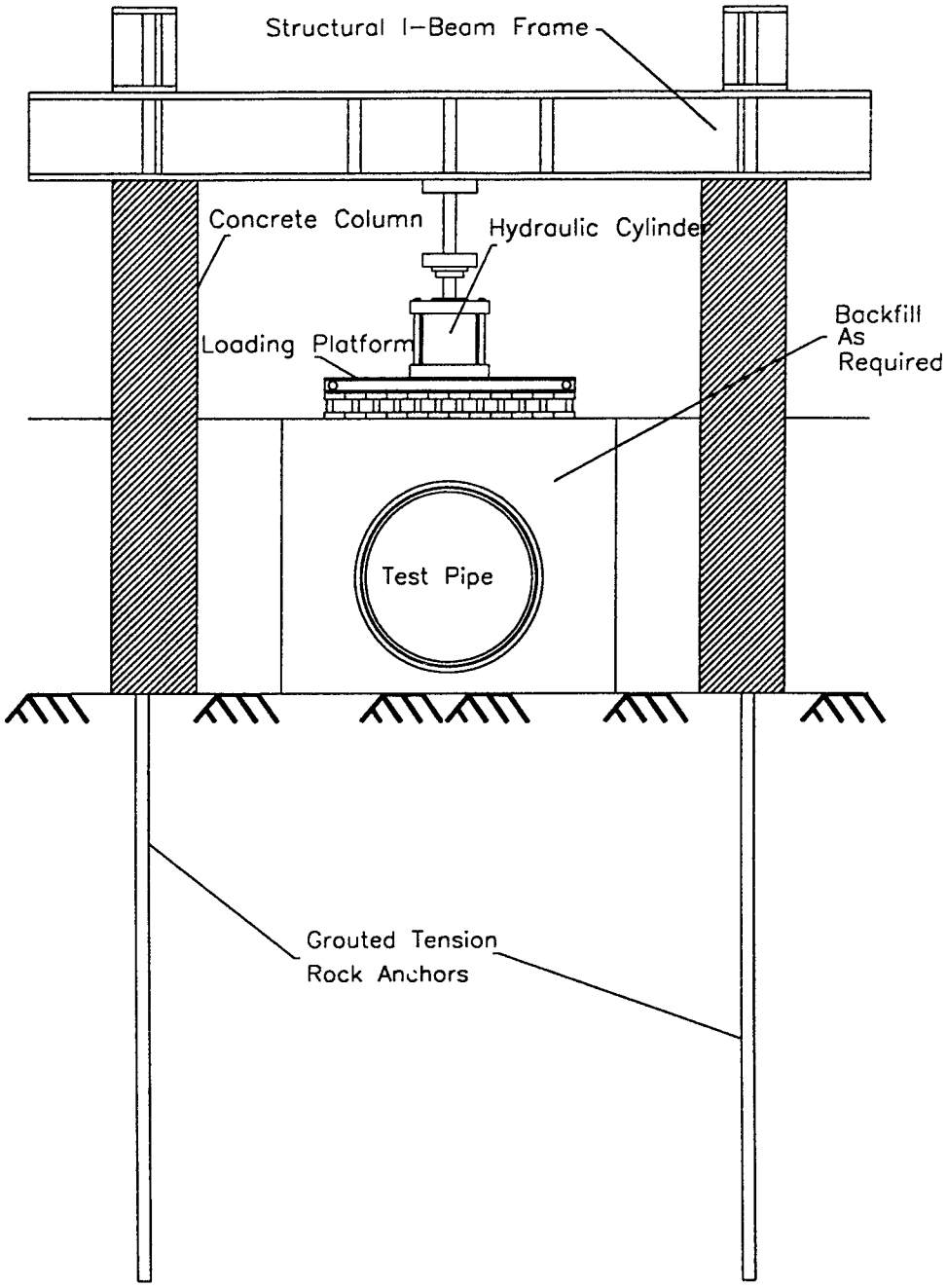

Figure 3.1 Front View of the Load Frame Facility

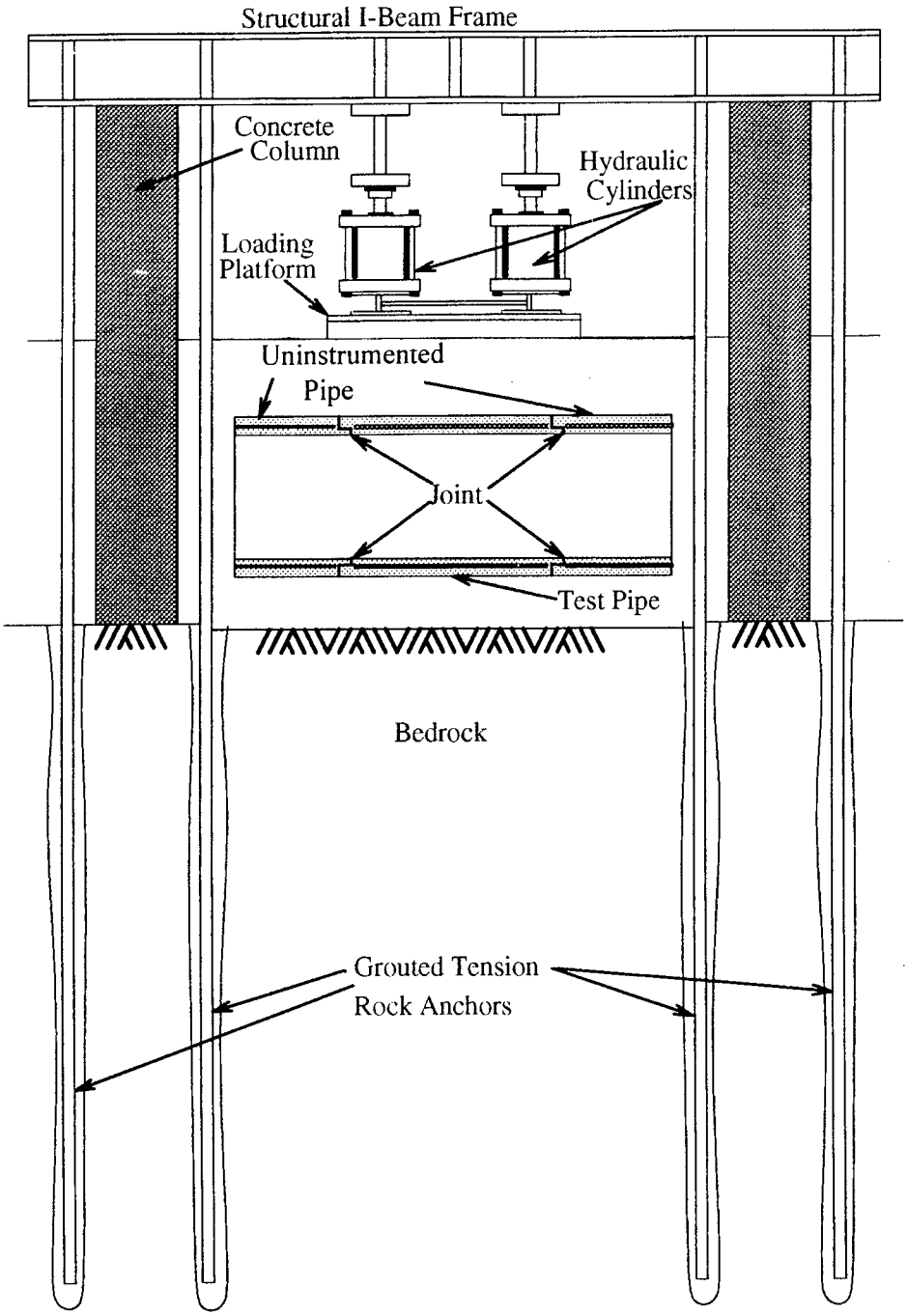

Figure 3.2 Side View of the Load Frame Facility

3.3 Hydraulic System

Beneath each intersection of I-beams, a 2.0 MN (230 ton) capacity hydraulic cylinder was attached to the lower flange for the application of a load to the pipe-soil system as shown in Figures 3.1 and 3.2. These cylinders have a 356 mm (14 in.) bore, a 610 mm stroke (24 in.), and a 178 mm (7 in.) diameter piston rod. The cylinder was connected to a hydraulic power supply/control unit for a synchronized operation. Maximum pressure of 18.6 Mpa (2700 psi) can be achieved.

To ensure uniform pressure distribution on the top of the soil, pressure from the two cylinders was transferred to a two-tier loading platform devised by welding I-beams along their lengths. The lower part of the loading platform was 1.8 m (6 ft) by 2.7 m (9 ft). The platform was fabricated from eight, 2.7 m (9 ft) long I-beams welded along the edges of their flanges. They were held together by two 25 mm (1 in.) diameter rods running through their webs. The upper part of the loading platform was made of two I-beams. On top of the flange two circular metal discs were placed to provide contact surfaces for the hydraulic cylinders. Again, when the 1520 mm (60 in.) pipes were tested the load platform was enlarged to 2.4 m (8 ft) by 3.7 m (12 ft) to prevent soil failure. Soil failure was found when pipe diameter exceeded 1.2 m (4 ft) for the smaller platform. The smaller and larger platforms contributed 4.6 kPa (0.66 psi) and 5.7 kPa (0.83 psi), respectively, to the surface load applied to the pipe.

3.4 Bedding and Backfilling

Installation was performed to simulate two of the installation conditions specified in SIDD and SIDD-HT users manual. Before transporting the complete instrumented pipe carefully to the testing site, a rectangular area sufficient to install the test pipe was excavated under the

load frame. Trench excavation was performed until shaley bedrock was encountered. The trench was enlarged from 2.4 m (8 ft) to 3.7 m (12 ft) to accommodate the larger pipe. Since the trench walls were stable, additional care was not necessary to secure them.

Crushed limestone was the common embedment material used in all pipes tested at the load cell facility. Both crushed limestone - Gradation No. 57 and sand - #310.02 Grading A, used in the pipe installation, satisfied the 1995 specifications for ODOT 603.02 for Pipe Backfill and Bedding Granular Material. The specific weight of the crushed limestone - No. 57 and sand #310.02 Grading A was γ_{d_max}= 2.05 g/cm^3 (128 lb/ft^3) and γ_{d_max}= 1.84 g/cm^3 (114.8 lb/ft^3), respectively. For both tests on 610 mm (24 in.) pipes, crushed limestone was directly laid over the bedrock and sand, ODOT #310.02 Grading A served as the bedding layer. Embedment material was placed in layers with each layer being leveled and compacted using a vibrating plate compactor. For Test 1 and Test 2, sand was placed in the bottom of the trench to provide cushioning for the pipe as shown in Figure 3.3. Two 1.2 m (4 ft) lengths of concrete pipe were jointed at both ends to the instrumented pipe to provide a uniform test length.

For Test 3 and Test 4, after the crushed limestone layer was placed and compacted, a 685 mm (27 in.) wide trench, 150 mm (6 in.) deep was dug and filled with uncompacted sand. The instrumented pipe was then carefully positioned in the trench until the center of the pipe was aligned with the center of the load frame. Two 2.4 m (8 ft) lengths of pipe were used to extend from the instrumented pipe.

Backfilling with crushed limestone, ODOT #310.02 Grading A, commenced after the pipes were placed. For all pipe tests, conducted in the ORITE load cell test facility, the sand cone method, AASHTO T191-86, was used to determine moisture content and density of the backfill. This test was conducted at the alternate sides of the pipe for every lift of constructed backfill.

Ottawa sand that passed through sieve No. 30 and retained in sieve No. 40 was used in the sand cone apparatus. Density of the Ottawa sand was determined in the laboratory ($\gamma_{sand} = 1.47$ g/cm^3). The sand cone apparatus was calibrated in the laboratory before using in the field. The sample from top of each layer after compaction was collected by using a hole template and digging tools (i.e., spoon, screwdriver). Sample soil was secured in a pre-weighed plastic container by closing it with a plastic lid to retain moisture content. Weight and volume of the soil was measured in the field to compute field density. The moisture content and the dry density were determined in the laboratory from the soil specimen collected for every layer.

As shown in Figure 3.3, the bottom pressure cell was inserted in the bedding before the pipe was placed. During the backfill operation, the remaining three earth contact pressure cells were positioned to monitor the earth pressure around the instrumented pipe.

3.4.1 Backfill Placement Procedure for Load Cell Test Facility

The pipes were embedded, in an appropriately sized trench, following the extremes of expected contractor installation procedures. These were modeled as the Type I and Type III installation procedures described by SIDD:

1. Placement of a well compacted, bedding layer over the bedrock, using a crushed limestone material.

2a. Dumping of a sandy material to form a 150 mm (6 in.) thick, loose layer; for Test 1 and Test 2. Bedding installation is shown in Figures 3.3 through 3.5.

2b. Excavating of 150 mm (6 in.) By 685 mm (27 in.) furrow and filling with a loose, sandy material for Test 3 and Test 4. The bedding installation is shown in Figures 3.6 and 3.7.

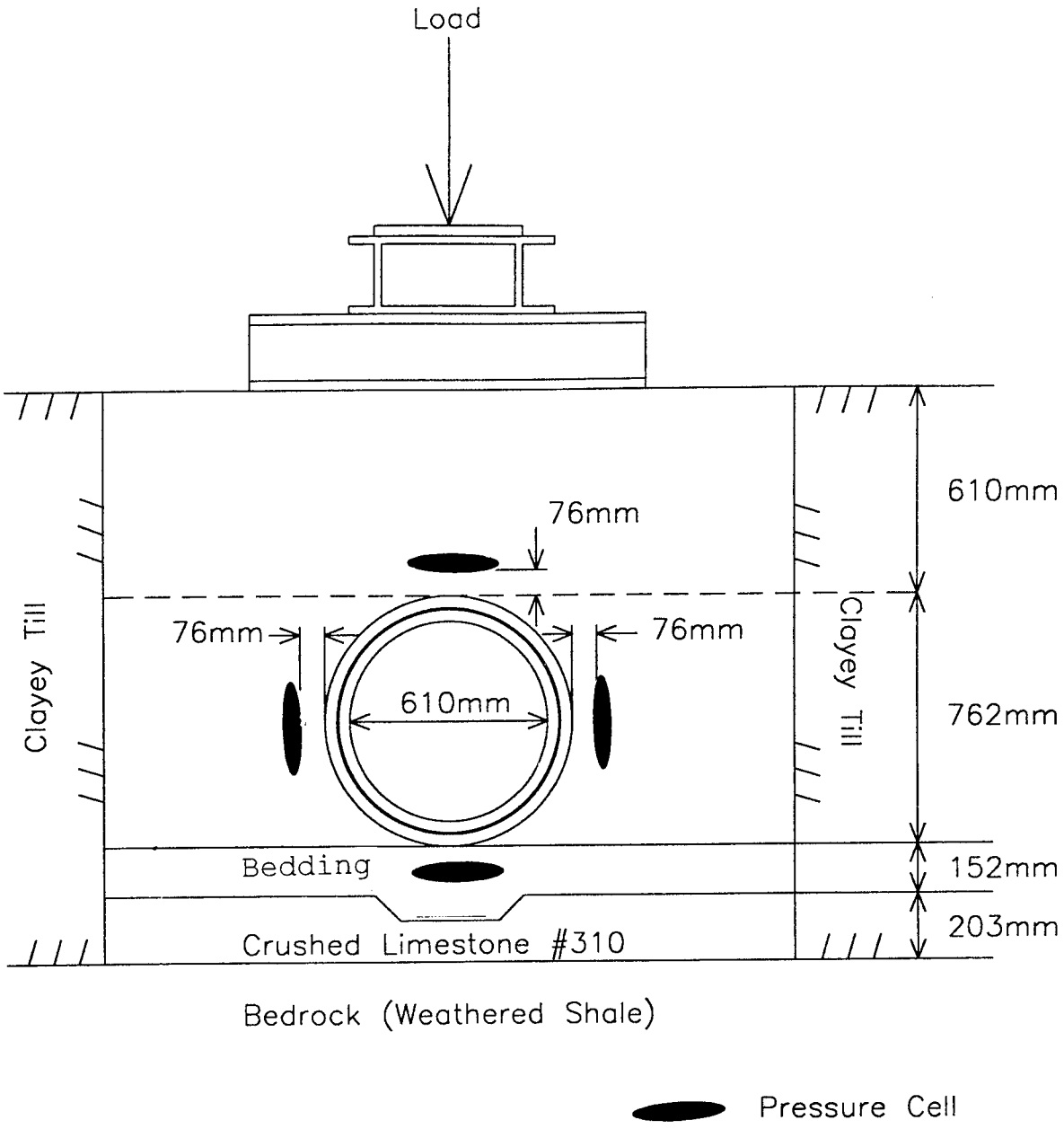

Figure 3.3 Earth Pressure Cell Locations Surrounding Pipe

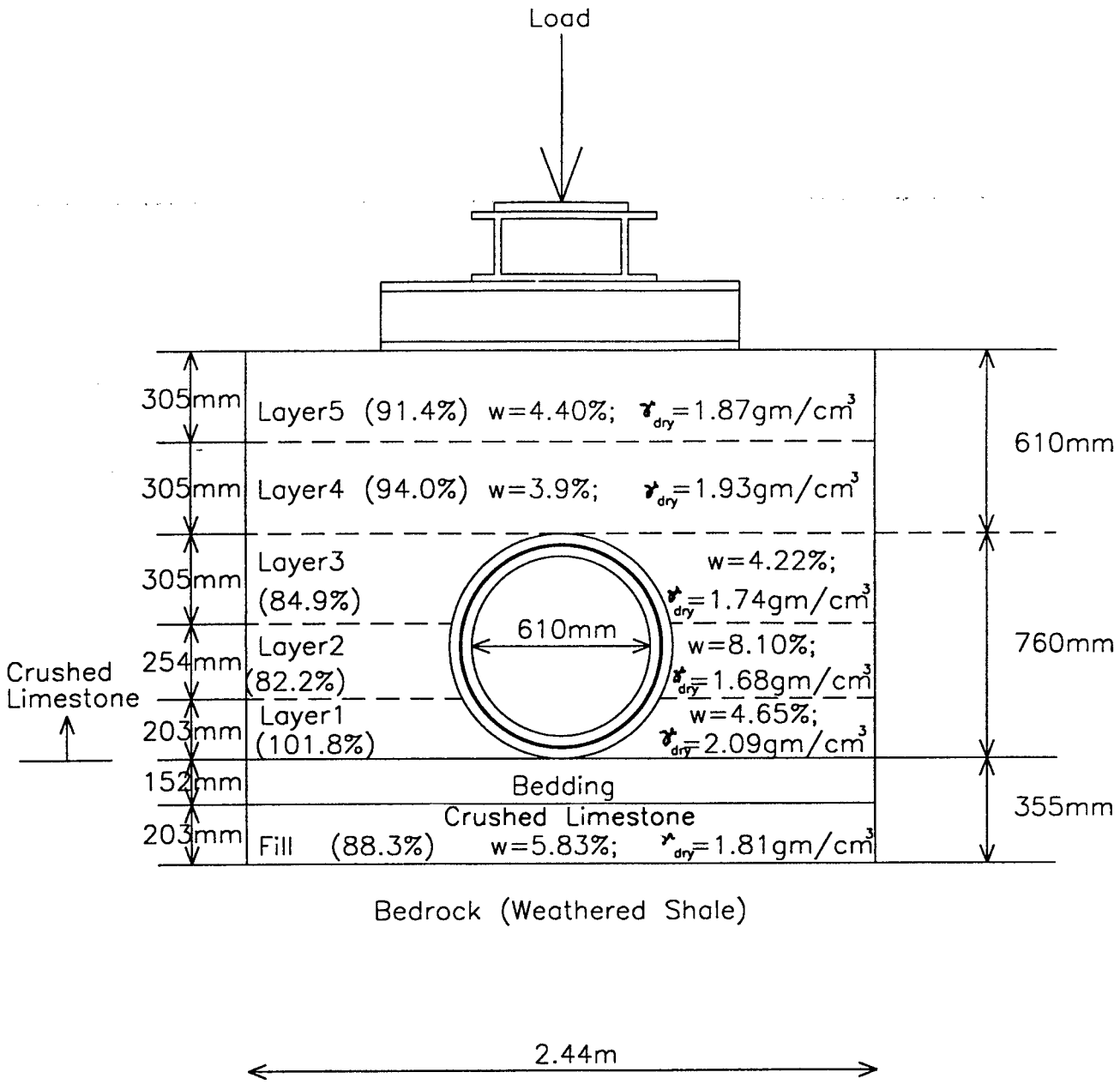

Figure 3.4 Detail of Each Layer of Backfill (Type 3) for Test No. 1

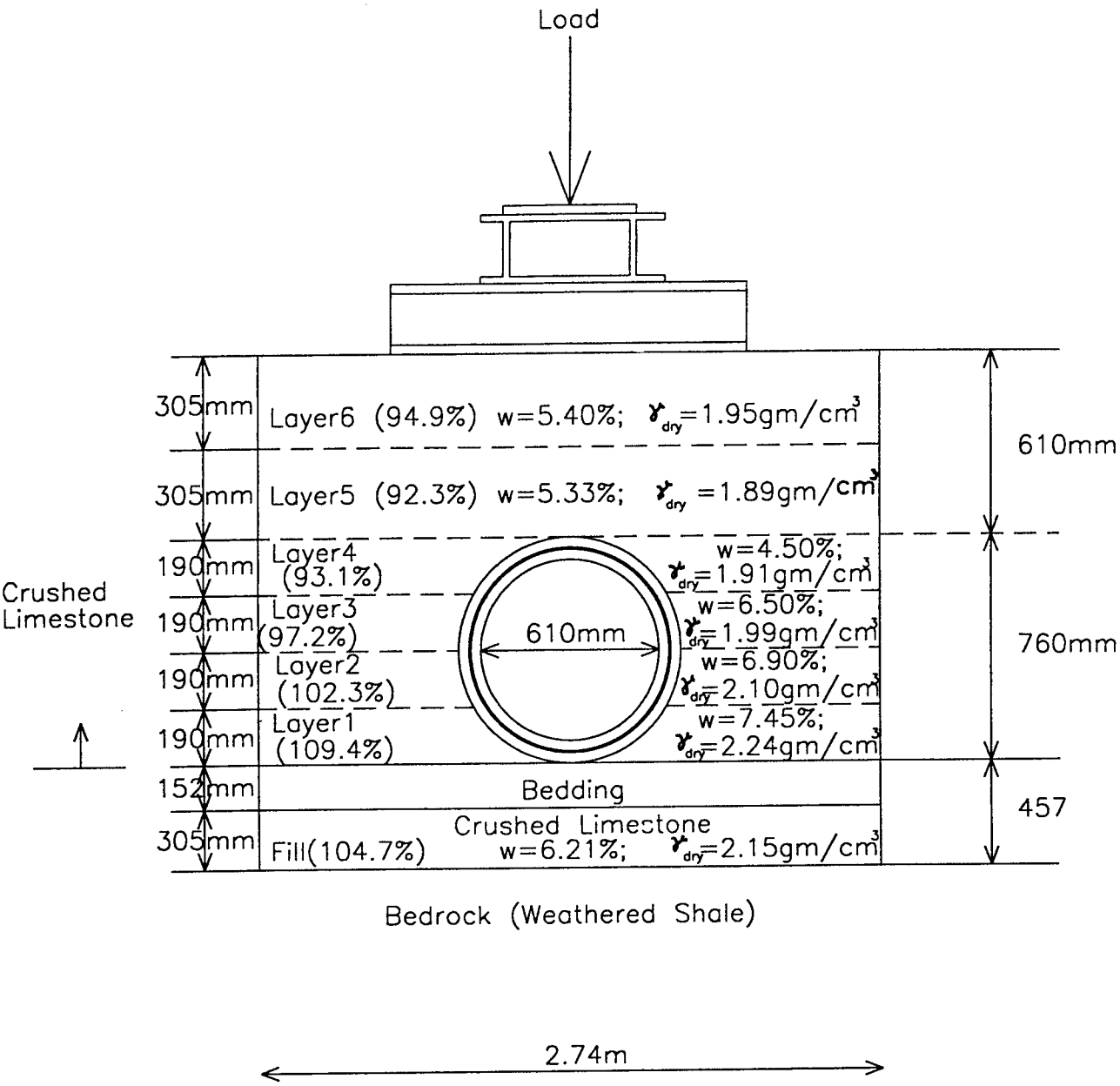

Figure 3.5 Detail of Each Layer of Backfill (Type 1) for Test No. 2

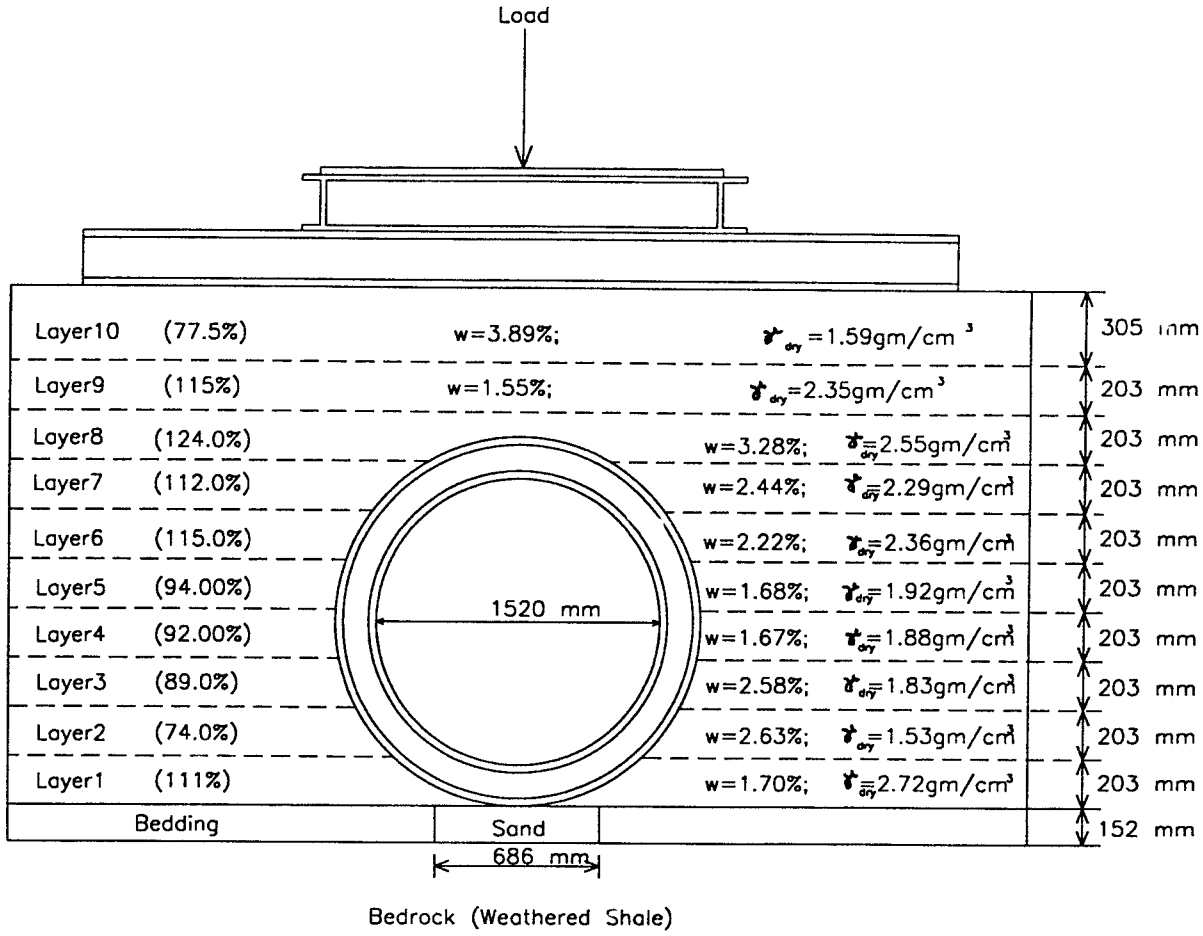

Figure 3.6 Detail of Each Layer of Backfill (Type 1) for Test 3

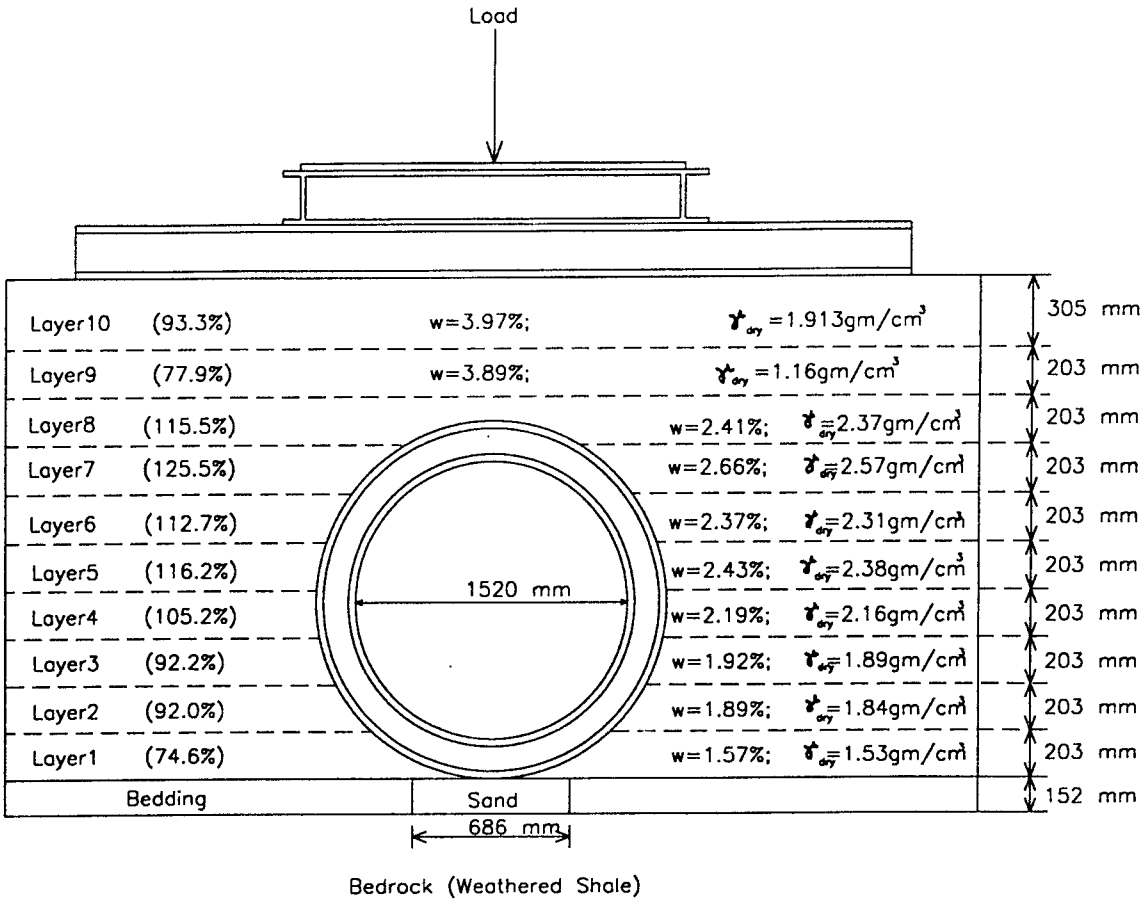

Figure 3.7 Detail of Each Layer of Backfill (Type 3) for Test 4

3. Placing of the concrete pipe on top of the sandy bedding layer.

4. Placement of crushed limestone layers, no more than 305 mm (12 in.) thick, up to a level of the pipe crown (four passes by the compactor were applied to each layer to achieve a 95% Proctor density and one pass was applied to each layer to achieve a 85% Proctor density). The density at the top of each layer was measured during placement and recorded on Figures 3.4 to 3.7.

5. Placement of crushed limestone layers, no more than 305 mm (12 in.) thick up from the pipe top to the surface level. Soil was compacted with at least two passes of the compactor for Type 1 installations and one pass of the compactor for Type 3 installations.

Extensions to the pipe were placed with the pipe and backfilled according to the prescribed procedure. All sensor leads were connected to data acquisition with the placement of the pipe. Subsequently, data was recorded during the placement of each backfill layer.

3.4.2 Backfill Placement Procedure for Field Test

Pipes for Tests 5 and 6 were designed for a positive projection installation mode as required ODOT. The pipes were positioned in August 1996 as shown in Table 3.1. Backfilling continued for 52 days until the depth of 13.1 m (43 ft) was attained. A silty loam fill, was placed and compacted in accordance with highway construction practices. A Type 1 Installation was followed:

1. A trench, approximately 1 m (40 in.) deep, was excavated.

2. At the bottom of the trench a bedding channel was excavated and filled with loose

sand.

3. At the location where measurements were to be taken, a pressure cell was embedded in the sand channel.
4. As the pipe was laid into place, inside and outside lead wires were separated.
5. Upon the positioning of the instrumented pipes, as shown in Figure 3.8, lead wires from the inside sensors were routed through the lift holes of adjacent pipes. All wires were then continued along the outside of the pipes to the data acquisition units, located at the entrance.
6. River gravel, used as backfill, was deposited in layers of 200 mm (8 in.) and compacted with hand held vibratory compactor. Below the springline the average compaction was 94% and moisture content was 4.2%. Above the springline the compaction was 93% and the moisture content was 6.2%. At each level of fill, the Proctor density was read at several locations to ensure uniform compaction.

Pressure cells were installed according to same procedures as used in pipe installation in the load cell facility testing. There were eight pressure cells installed around the primary sections of the two pipes during the placement of backfill. The positioning of the top pressure cells is shown in Figure 3.9. Data on pipe response was collected as compaction of each layer was completed. Data was then collected as construction took place. As shown in Table 3.1, backfilling was completed in 53 days.

Figure 3.8 Pipe Installation for Test 5 and Test 6

Figure 3.9 Pressure Cell Placement for Test 5 and Test 6

Table 3.1 Height of Fill as Construction Progressed

Day	Date	Time	Height of Fill Above Bottom (m)
1	8/30/95	12:30	Initial (Invert)
1	8/30/95	14:30	0.46
1	8/30/95	16:30	0.72
1	8/30/95	17:30	0.93 (Springline)
2	8/31/95	9:10	0.93
2	8/31/95	11:30	1.24
2	8/31/95	16:00	1.40
3	9/1/95	11:20	1.87 (Crown)
3	9/1/95	14:35	2.24
8	9/6/95	11:50	2.48
8	9/6/95	15:30	4.09
14	9/12/95	11:30	6.13
16	9/14/95	11:30	6.32
29	9/27/95	12:35	8.72
52	10/20/95	13:45	13.72

CHAPTER 4

DATA ACQUISITION AND ANALYSIS

4.1 INTRODUCTION

The instrumented pipes were subjected to loading, and experimental data were collected using data acquisition systems. The field data comprised output voltages, which were then post processed using application programs and spreadsheets to derive design variables. For Tests 1 through 4, the deflection measurement system was positioned near the primary section and made measurements at load steps. Similarly, for Tests 5 and 6 the vertical and horizontal pipe diameters were taken manually at intervals in the backfilling process.

The temperature variations for Test 1, Test 2, Test 3, and Test 4 were assumed too small to affect any calculations except for platform deflection, since these Tests were conducted over two or three days. As Test 5 and Test 6 were longer tests taking 52 days to complete, the temperature was measured. The maximum variation at the invert was 10° Celsius, at the crown was 17° Celsius, and at the springlines was 11° Celsius. Thus, for these tests as well, the temperature change was not included in calculations.

4.2 STRAIN GAGE OBSERVATIONS

The principle of any conductor is that the potential difference across a conductor is proportional to resistance of the conductor. The data acquisition system functioned on this principle by recording voltage response to the change in resistance. Thus, a strain reading may be obtained from,

$$\frac{\Delta R_1}{R_1} = S_g * \varepsilon \qquad (4.1)$$

where R_1 = change in strain gage resistance

R_1 = change in strain resistance

ε = strain

S_g = gage factor

The amplifier of the data acquisition system has a built-in Wheatstone Bridge to balance the resistance. The change in voltage of a gage was calculated from the equation,

$$\Delta V = V_{br} * \frac{R_1 * R_2}{(R_1 + R_2)^2} * \frac{\Delta R_1}{R_1} \qquad (4.2)$$

where, ΔV = change in voltage

V_{br} = bridge voltage

R_2 = resistance of the internal precision resistor

The following equation, resulting from the previous two equations, is used to compute the strain values:

$$\varepsilon = \frac{\Delta V * (R_1 + R_2)^2}{V_{br} * S_g * R_1 * R_2 * G} \qquad (4.3)$$

where G is a dimensionless variable used to control the voltage values to fall within the range of the data acquisition system. The value G can be changed during a test to bring the Wheatstone in balance.

In the HP data acquisition system, the strain gage responses were stored as voltages and saved in the system generated files. For every data file, the HP system recorded 5 voltage values within the sampling period for all channels supported on the test. Stresses, bending moments and thrusts were determined from the computed strains using a spreadsheet.

4.3 CALCULATION OF BENDING MOMENT AND AXIAL THRUST

From mechanics of materials, circumferential stresses at the inside and the outside walls of the pipe, due to beam bending and axial forces are expressed as follows:

$$\sigma_i = \frac{P}{A} + \frac{M*c}{I} \qquad (4.4)$$

$$\sigma_o = \frac{P}{A} - \frac{M*c}{I} \qquad (4.5)$$

where σ_i, σ_o = circumferential stresses at the inside and outside of the pipe, respectively,

P = axial thrust per unit length of the pipe

A = cross-sectional area per unit length of the pipe

M = bending moment per unit length of the pipe

c = distance from the neutral axis to location

I = moment of inertia per unit length of pipe wall

Since the stress is related to strain by Young's modulus, the following relationships are obtained when the equations are solved for thrust and moment:

$$P = \frac{\varepsilon_i + \varepsilon_o}{2} * E * A \qquad (4.6)$$

$$M = \frac{\varepsilon_o - \varepsilon_i}{2 * c} * E * I \qquad (4.7)$$

The sign convention followed depicts thrust to be positive in tension and moment to be positive when the outside of the pipe is in compression. An example of the wall section considered for Test 1 is shown in Figure 4.1.

4.4 APPLIED LOADING ON THE PIPES

As described earlier, the test pipe was subjected to loading controlled by a hydraulic system. The load was applied until one of the following conditions were met:

(1) Maximum capacity of the load cell facility was achieved, or

(2) Most of the electric strain gages had failed, or

(3) The LVDT deflection monitoring system could not rotate because of extensive cracking on the inside surface.

The pipe-backfill system was loaded at the surface using an I-beam platform , 1.83 m (6 ft) perpendicular to the test pipe by 2.74 m (9 ft) along the length of the test pipe for Test 1 and Test 2. The equivalent height of backfill was calculated by assuming the specific weight of soil to be 1.92 g/cm^3 (120 lb/ft^3) .

The testing for Test 1 and Test 2 proceeded until the crown pressure of 367.9 kPa (53.3 psi) and 395.2 kPa (57.3 psi), respectively, was achieved. At this pressure, the springlines of the pipe of Test 1 (Type 3) crushed. The pipe of Test 2 (Type 1) had cracks at the crown and invert, obstructing rotation of the LVDT; and most of the electric strain gages were giving inconsistent readings. The surface pressure, equivalent fill height, and total applied load are given in Tables

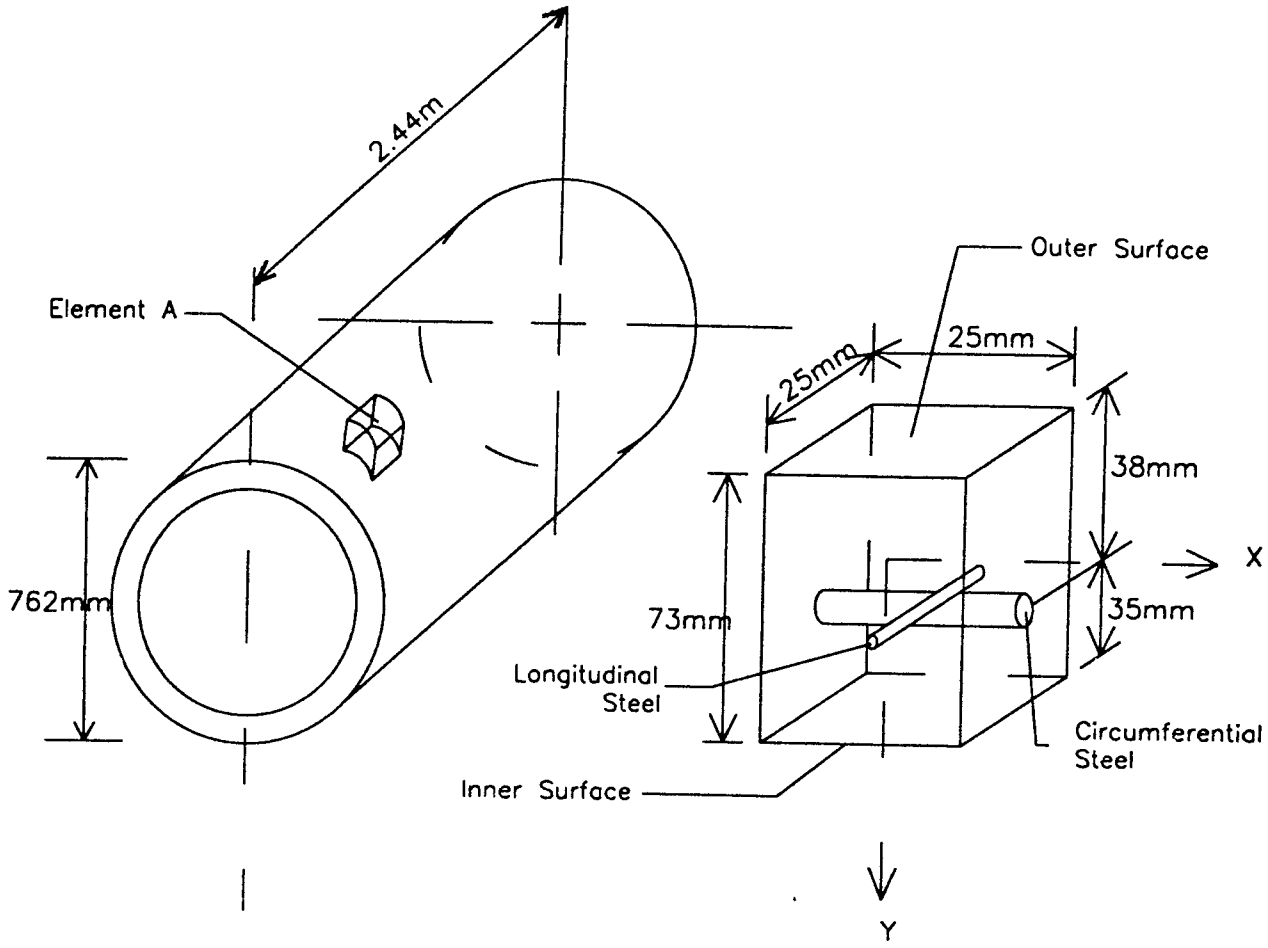

Figure 4.1 Cross Section of Concrete Pipe for Test 1 and Test 2

4.1 and 4.2.

Testing for Test 3 proceeded until a crown pressure of 365.2 kPa (53.1 psi) was reached, which was the capacity of the load cell. A hairline crack appeared, along the invert and crown, at a surface pressures of 119.7 kPa (17.4 psi) and 149.6 kPa (21.7 psi), respectively. These cracks did not widen beyond 1.5 mm (0.0625 in.).

Testing for Test 4 proceeded until the pipe walls crushed at both springlines. Hairline cracks appeared at both invert and crown at 89.8 kPa (13.0 psi) surface pressure. Shear failure appeared at the joint at 209.4 kPa (30.4 psi). Finally, wall crushing of springline occurred at the surface pressure of 359.0 kPa (52.1 psi). The surface pressure, fill height, and total applied load are given in Table 4.3.

As shown in Table 4.4 the final backfill depth for Test 5 and Test 6 was 13.7 m (45 ft) above the trench. The final backfill operation was completed 52 days after the pipe was placed. Vertical and horizontal diameter changes and soil-pipe pressures were recorded during backfilling and for several months after completion. Minor longitudinal cracks were noted on the inside surface of Test 5 at locations of 20° clockwise rotation from the crown. No cracks were observed for Test 6. Because the invert accumulated sediment and water, no observations were made at the invert.

4.5 SETTLEMENT OF LOAD PLATFORM

Settlement of the load platform (I - beam) was monitored by the profilemeter. Figure 4.2 shows the settlement of the loading platform for Test 1 and Test 2. Settlement of the platform exhibited a linear relationship up to surface pressure of 273 kPa (39.6 psi) in both tests. From Figure 4.2 it can also be observed that, after initial consolidation, the slopes of both curves are

Table 4.1. Test 1 -- Loading Sequence for 610 mm (24 in.) Concrete Pipe, a Type 3 Installation

Load Increment	Surface Pressure kPa (psi)	Fill Height above Crown m (ft)	Total Applied Load MN (kip)
1	78.5 (11.4)	5.0 (16.2)	0.329 (73.9)
2	94.9 (13.8)	5.8 (19.0)	0.411 (92.4)
3	122.2 (17.7)	7.3 (23.8)	0.548 (123.2)
4	149.5 (21.7)	8.7 (28.5)	0.685 (153.9)
5	176.8 (25.6)	10.2 (33.3)	0.822 (184.7)
6	204.1 (29.6)	11.6 (38.0)	0.959 (215.5)
7	231.3 (33.6)	13.1 (42.8)	1.096 (246.3)
8	258.6 (37.5)	14.5 (47.5)	1.233 (277.1)
9	285.9 (41.5)	16.0 (52.3)	1.370 (307.9)
10	311.8 (45.2)	17.3 (56.8)	1.507 (338.7)
11	340.6 (49.4)	18.9 (61.8)	1.644 (369.5)
12	367.9 (53.3)*	20.3 (66.5)	1.780 (400.2)

* Pipe wall at springlines crushed.

Table 4.2. Test 2 -- Loading Sequence for 610 mm (24 in.) Concrete Pipe, a Type 1 Installation

Load Increment	Surface Pressure kPa (psi)	Fill Height above Crown m (ft)	Total Applied Load MN (kip)
1	93.0 (13.5)	5.7 (18.7)	0.356 (80.1)
2	94.9 (13.8)	5.8 (19.0)	0.411 (92.4)
3	122.2 (17.7)	7.3 (23.8)	0.548 (123.2)
4	149.5 (21.7)	8.7 (28.5)	0.685 (153.9)
5	176.8 (25.6)	10.2 (33.3)	0.822 (184.7)
6	204.1 (29.6)	11.6 (38.0)	0.959 (215.5)
7	231.3 (33.6)	13.1 (42.8)	1.096 (246.3)
8	258.6 (37.5)	14.5 (47.5)	1.233 (277.1)
9	285.9 (41.5)	16.0 (52.3)	1.370 (307.9)
10	340.6 (49.4)	18.9 (61.8)	1.644 (369.5)
11	395.2 (57.3)	21.8 (69.3)	1.917 (431.0)

* LVDT failure due to cracks at crown and invert.

Table 4.3. Test 3 and Test 4 -- Loading Sequence for 1520 mm (60 in.) Concrete Pipe, Type 1 and Type 3 Installation, Respectively

Load Increment	Surface Pressure kPa (psi)	Fill Height m (ft)	Total Load MN (kip)	Comments
1	44.7 (6.5)	4.3 (13.9)	0.322 (72.3)	
2	67.1 (9.7)	5.5 (17.9)	0.515 (115.8)	
3	97.1 (14.1)	7.1 (23.0)	0.773 (173.8)	
	119.7(17.4)	8.1 (26.6)	0.972 (218.6)	Initial cracks in Test 3
4	126.9 (18.4)	8.6 (28.2)	1.031 (231.8)	
	149.6 (21.7)	9.7 (31.9)	1.230 (276.5)	Initial cracks in Test 4
5	156.8 (22.7)	10.2 (33.4)	1.289 (289.8)	
6	186.7 (27.1)	11.8 (38.6)	1.546 (347.6)	
7	216.6 (31.4)	13.4 (43.8)	1.804 (405.6)	
8	246.8 (35.8)	15.0 (49.1)	2.064 (464.0)	
9	276.5 (40.1)	16.7 (54.81)	2.320 (521.6)	
10	306.4 (44.4)	18.2 (59.7)	2.577 (579.3)	
11	335.3 (48.8)	19.8 (65.0)	2.835 (637.3)	
12	365.2 (53.1)	21.4 (70.2)	3.092 (695.1)	Capacity of Load Cell

Table 4.4. Backfill Loading Sequence for 1520 mm (60 in.) Concrete Pipe — Test 5 and Test 6

Load Increment	Backfill Height above Crown m (ft)	Backfill Height above Trench m (ft)
1	0.36 (1.2)	2.23 (7.3)
2	0.51 (1.7)	2.38 (7.8)
3	0.60 (2.0)	2.48 (8.1)
4	2.22 (7.3)	4.10 (13.4)
5	4.26 (14.0)	6.13 (20.1)
6	4.44 (14.6)	6.31 (20.7)
7	6.85 (22.5)	8.72 (28.6)
8	11.85 (38.9)	13.72 (45.0)

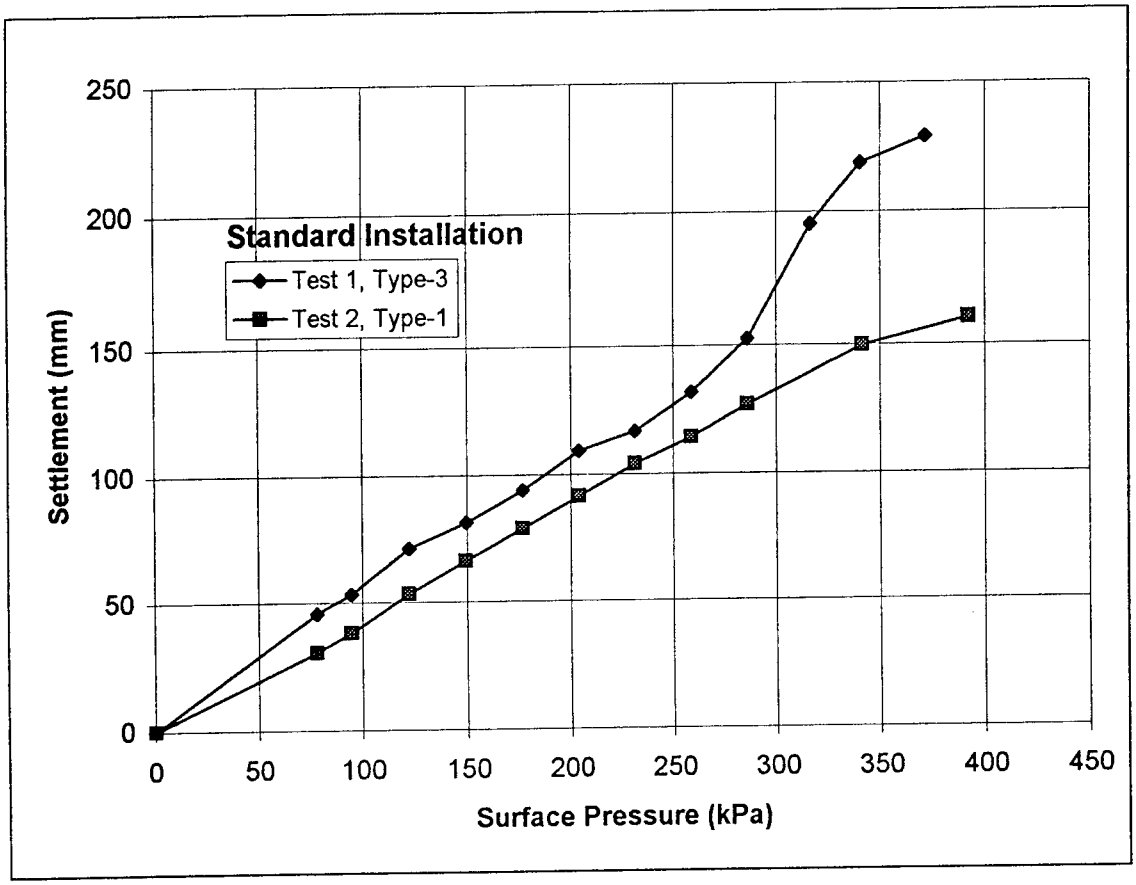

Figure 4.2 Settlement of the Loading Platform for the 610mm Test Pipes

approximately equal despite the average compaction of Test 1 (Type 3) being greater than Test 2 (Type 1). Due to instrumentation failure the settlement of the load platform for Test 3 was not measured. By observation the settlement was approximately the same as for Test 4. The platform settlement of the 1520 mm (60 in) pipe is shown in Figure 4.3. Platform settlement was about 30% of the settlement that measured for the 610 mm pipes. Again the deflection is approximately linear with respect to applied surface pressure.

4.6 DEFLECTION RESULTS

The deflected shapes at load levels for Test 1 are shown in Figure 4.4. Figure 4.5 represents the graphical comparison of percentage horizontal and vertical deflections. Measured horizontal and vertical deflections are presented in Table 4.5. All the figures show change of deflection before and after crushed limestone, Gradation No. 57, was placed. Similar results are shown for Test 2 in Figure 4.6, Figure 4.7 and Table 4.6.

In Test 1 a maximum vertical deflection of 3.23% and a maximum horizontal deflection of 2.79% were observed at an applied surface pressure of 285.9 kPa (41.5 psi), beyond which the rotated LVDT was not operational. Whereas, in Test 2, a maximum vertical deflection of 4.14% and a maximum horizontal deflection of 1.85% was recorded at an applied pressure of 341.3 kPa (49.5 psi), beyond which the rotated LVDT refused to function properly. In Test 1, the horizontal deflections were higher than the vertical deflections at the initial stages, as reflected by their ratio given in Table 4.5. This may have resulted from backfill compaction above the crown being higher than the compaction at the springline and haunch. In contrast, for Test 2 the ratio of horizontal to vertical deflection was less than for Test 1, possibly, because the average compaction of the backfill at the springline and haunch level was greater than the compaction

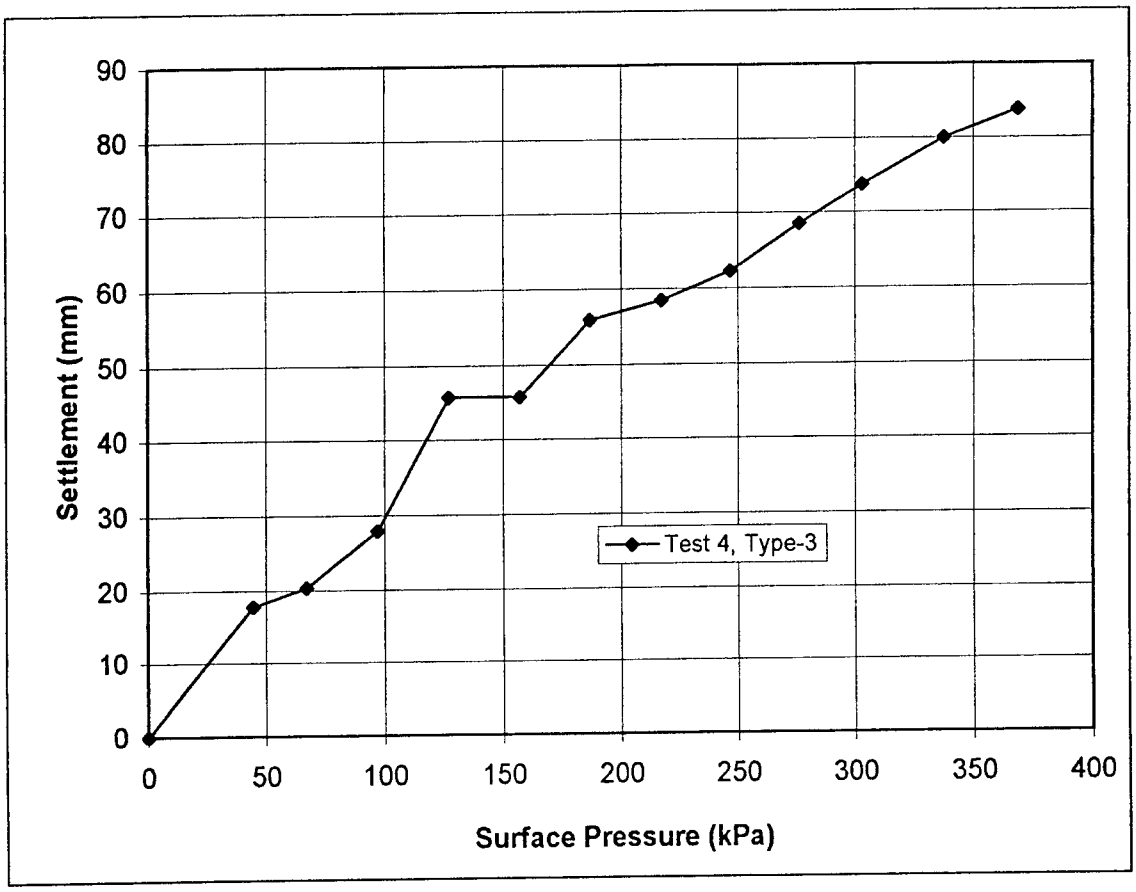

Figure 4.3 Settlement of the 1520 mm Pipe Loading Platform

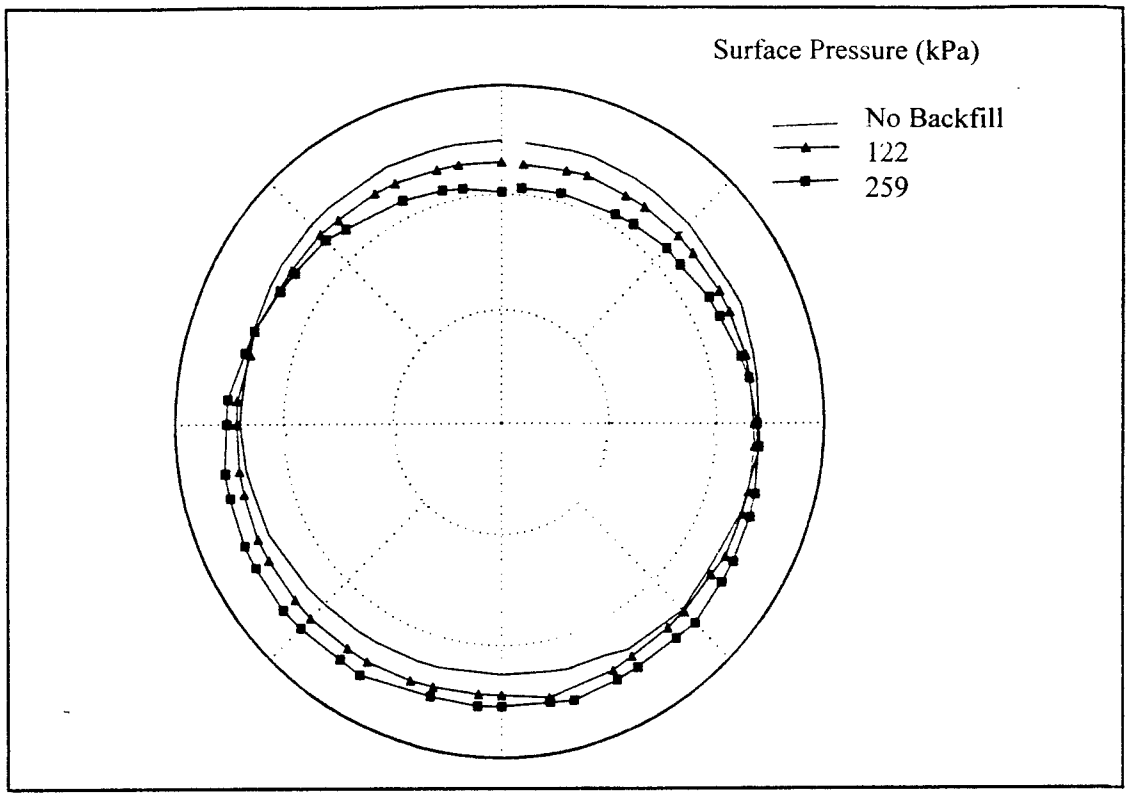

Figure 4.4 Deformed Shapes for 610 mm (24 in.) Concrete Pipe for Test 1

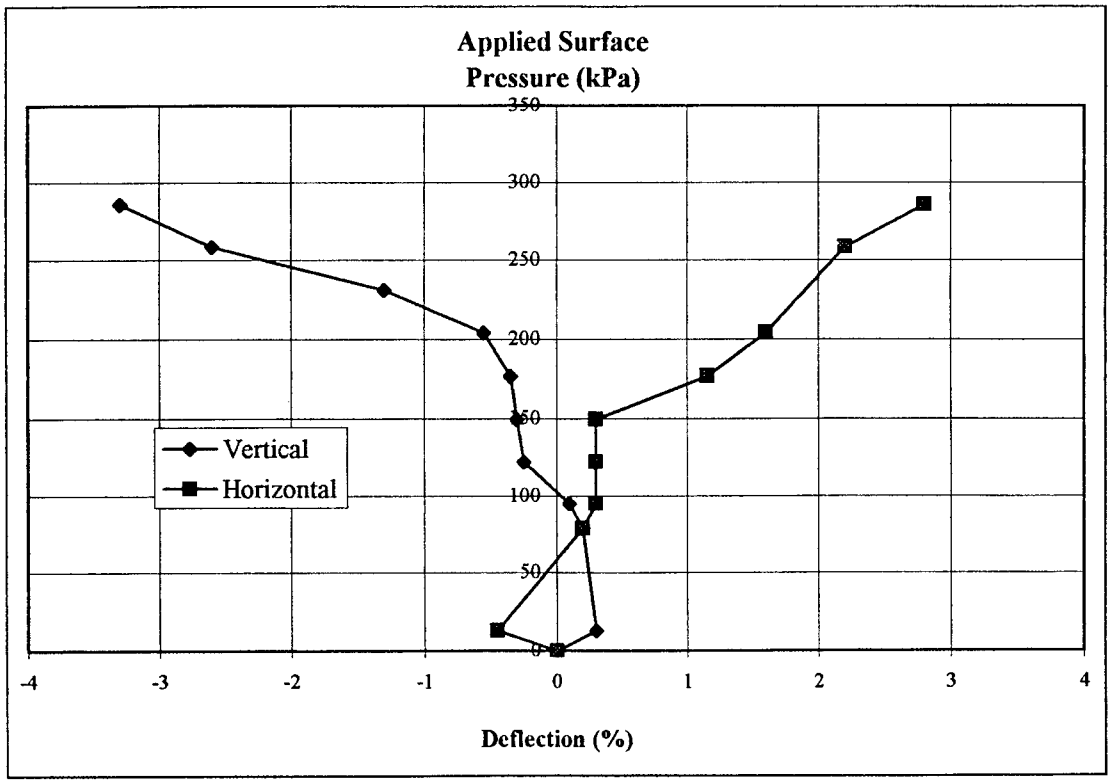

Figure 4.5 Deflection of the 610 mm Concrete Pipe for Test 1

Table 4.5. Experimental Deflections for 610 mm (24 in.) Diameter Reinforced Concrete Pipe — Test 1

Surface Pressure kPa (psi)	Horizontal Diameter mm (in.)	Vertical Diameter mm (in.)	Experimental Deflection		Ratio of Horizontal Deflection to Vertical Deflection
			Horizontal %	Vertical %	
0*	609.3 (23.99)	600.7 (23.65)	0	0	0
13.0 (1.9)	606.6 (23.88)	602.5 (23.72)	-0.47	0.28	1.64
78.5 (11.4)	610.4 (24.03)	601.7 (23.69)	0.16	0.17	0.99
94.9 (13.8)	611.1 (24.06)	601.5 (23.68)	0.30	0.10	2.88
122.2 (17.7)	611.4 (24.07)	599.4 (23.60)	0.32	-0.24	1.36
149.5 (21.7)	611.4 (24.07)	599.2 (23.59)	0.34	-0.27	1.25
176.8 (25.6)	616.2 (24.26)	598.7 (23.57)	1.13	-0.35	3.26
204.1 (29.6)	619.3 (24.38)	597.4 (23.52)	1.62	-0.56	2.90
231.3 (33.6)	-----	592.8 (23.34)	----	-1.33	----
258.6 (37.5)	622.8 (24.52)	585.2 (23.04)	2.20	-2.58	0.85
285.9 (41.5)	626.4 (24.66)	581.4 (22.89)	2.79	-3.23	0.86

* Surface pressure includes the dead weight above the pipe.

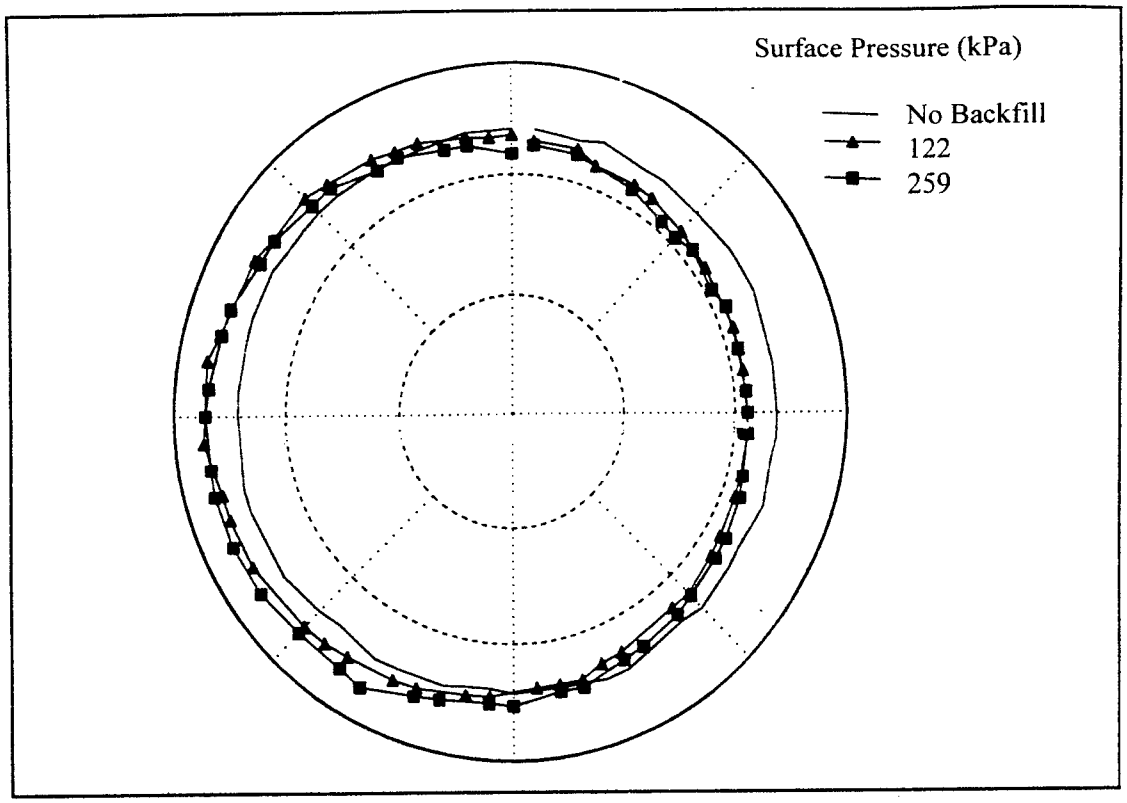

Figure 4.6 Deformed Shapes for 610 mm (24 in.) Concrete Pipe for Test 2

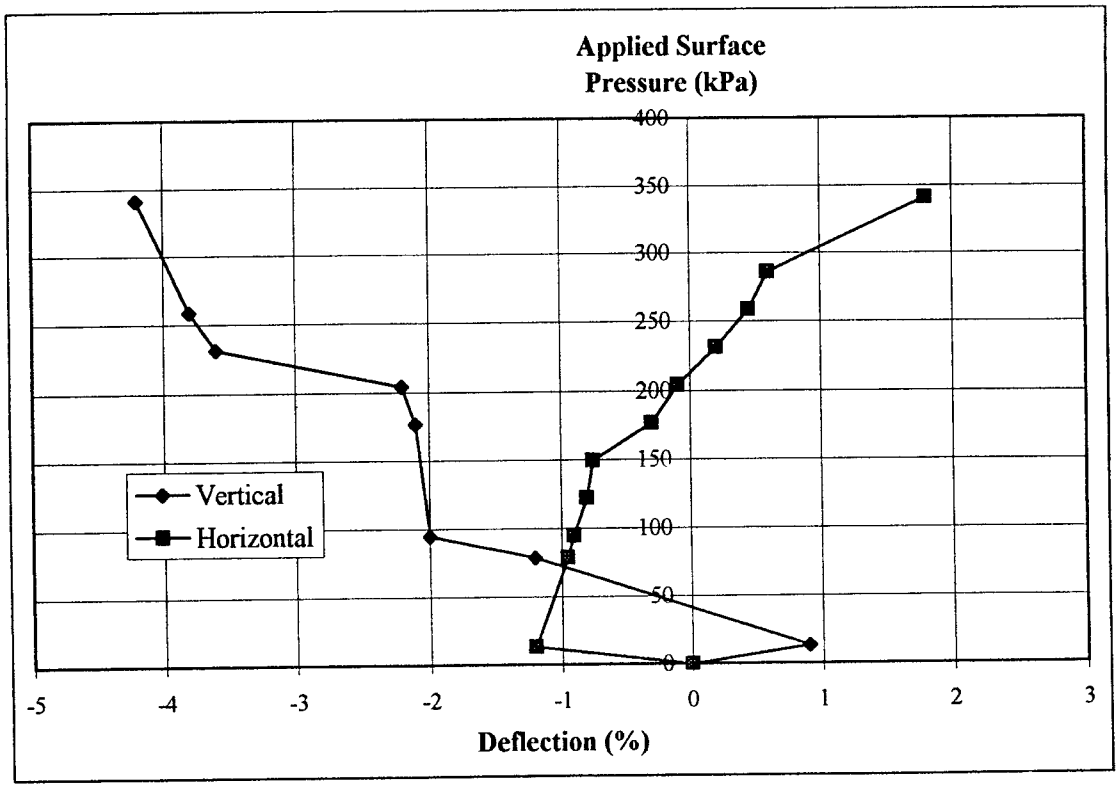

Figure 4.7 Deflections of the 610 mm Concrete Pipe for Test 2

Table 4.6. Experimental Deflections for 610 mm (24 in.) Diameter Reinforced Concrete Pipe — Test 2

Surface Pressure kPa (psi)	Horizontal Diameter mm (in.)	Vertical Diameter mm (in.)	Experimental Deflection		Ratio of Horizontal Deflection to Vertical Deflection
			Horizontal %	Vertical %	
0*	612.9 (24.13)	606.3 (23.87)	0	0	0
13.0 (1.9)	606.0 (23.86)	611.9 (24.09)	-1.13	0.93	1.22
78.5 (12.2)	607.3 (23.91)	599.4 (23.60)	-0.93	-1.13	0.82
94.9 (13.8)	607.3 (23.91)	594.4 (23.40)	-0.91	-1.98	0.46
122.2 (17.7)	607.8 (23.93)	----	-0.85	----	----
149.5 (21.7)	608.6 (23.96)	----	-0.73	----	----
176.8 (25.6)	611.4 (24.07)	593.6 (23.37)	-0.27	-2.11	0.13
204.1 (29.6)	612.6 (24.12)	592.8 (23.34)	-0.07	-2.23	0.03
231.3 (33.6)	614.2 (24.18)	584.5 (23.01)	0.02	-3.61	0.06
258.6 (37.5)	615.7 (24.24)	583.4 (22.97)	0.46	-3.78	0.12
285.9 (41.5)	617.0 (24.29)	----	0.64	----	----
341.3 (49.5)	624.3 (24.58)	581.2 (22.88)	1.85	-4.14	0.45

* Surface pressure includes the dead weight above the pipe.

above the crown. Vertical deflections in Test 2 were greater than in Test 1. This can be attributed to the lower compaction of Test 1, where the compaction was 84% at the springline. In contrast the compaction for Test 2 was 100% at the springline. Backfill compaction percent and location possibly affected the magnitude of pipe wall deflection. The deflection pattern for Test 2 was unsymmetrical. Again this may have been sensitive to the compaction as the last 610 mm (24 in.) was placed in two layers for Test 2 as compared to three layers for Test 3.

For Test 3 and Test 4, deflection measurements corresponded to observed distress in each pipe test. Deflection was insignificant for Test 3 until the first cracks were observed at load increment 4. At load increment 10, the last load increment where complete deflection measurements could be taken, the vertical deflection was -2.05% of diameter. Since deflections were so small, there was difficulty measuring the horizontal deflection in Test 3 with the rotating LVDT.

The manual LVDT was used for all horizontal and vertical deflection measurements in Test 4. When surface pressure was 97.1 kPa (14.1 psi), an equivalent height of 7.1 m (23 ft.) for Test 4, the percent vertical diameter change was -0.12% and the horizontal deflection was 0.23% of diameter. At the Load Increment 11, the last load increment before failure, the percent vertical diameter change was -2.53% and the corresponding horizontal diameter change was 1.84%. In the initial stage of testing Pipe 4 the ratios of horizontal to vertical deflections were less than -1.0. The final load reduced this ratio to -0.76. Detailed description of deflections is given in Table 4.7.

For Test 5 and Test 6, deflections were measured near the primary section as pipes were backfilled. The field data, comprised of output voltages, were processed using calibration factors determined in the laboratory. The deflections of vertical and horizontal diameters for both pipes

Table 4.7. Experimental Deflections for 1520 mm (60 in.) Diameter Reinforced Concrete Pipe — Test 3 and Test 4

Surface Pressure kPa (psi)	Experimental Vertical Deflection — Test 3		Experiment Deflection Test 4				
	Vertical Diameter mm (in.)	Vertical %	Vertical Diameter mm (in.)	Vertical %	Horizontal Diameter mm (in.)	Horizontal %	Ratio of Horizontal to Vertical
0	----	--	----	--	-----	--	--
Initial	1532.1 (60.32)	--	1523.7 (59.99)	--	1514.9 (59.64)	--	--
44.7 (6.5)	1536.4 (60.49)	0.28	1523.7 (59.99)	0	1516.6 (59.71)	0.12	--
67.1 (9.7)	1512.3 (59.54)	-1.29	1522.2 (59.93)	-0.10	1515.6 (59.67)	0.05	-0.50
97.1 (14.1) 119.7 (17.4)*	1512.1 (59.53)	-1.31	1522.0 (59.92)	-0.12	1516.4 (59.70)	0.10	-0.83
126.9 (18.4) 149.6(21.7)**	1512.8 (59.56)	-1.26	1522.0 (59.92)	-0.12	1518.4 (59.78)	0.23	-1.92
156.8 (22.7)	1501.9 (59.13)	-1.97	1519.7 (59.83)	-0.27	1519.9 (59.84)	0.34	-1.25
186.7 (27.1)	1506.5 (59.31)	-1.67	1517.6 (59.75)	-0.40	1522.2 (59.93)	0.49	-1.22
216.6 (31.4)	1500.6 (59.08)	-2.05	1514.3 (59.62)	-0.62	1524.8 (60.03)	0.65	-1.05

246.8 (35.8)	1503.7 (59.20)	-1.86	1508.8 (59.40)	-0.98	1529.3 (60.21)	0.96	-0.98
276.5 (40.1)	1498.3 (58.99)	-2.20	1505.5 (59.27)	-1.20	1532.6 (60.34)	1.17	-0.98
306.4 (44.4)	1488.4 (58.60)	-2.85	1450.0 (59.04)	-1.58	1537.7 (60.54)	1.51	-0.96
335.3 (48.8)	1511.0 (59.49)	-1.38	1485.1 (58.47)	-2.53	1542.8 (60.74)	1.84	-0.72
365.2 (53.1)	1480.8 (58.30)	-3.34	1462.8 (57.59)***	-4.00	1561.3 (61.47)***	3.07	-0.76

* Initial cracks in Test 3.
** Initial cracks in Test 4.
*** Readings were taken after the pipe was unloaded.

are shown in Figure 4.8a , Figure 4.8b and Table 4.8. The vertical and horizontal deflections were plotted as backfill height increased. Initial deflections, as shown in Figures 4.8a and 4.8b, are compressive in both vertical and horizontal directions.

4.7 SOIL PRESSURE AROUND PIPE

As described in Section 3.4, the soil pressure around the primary section of the pipe was monitored by four Geokon pressure cells for load cell tests as well as field tests (Figures 3.3 and 3.9). The relation between data and pressure is given as:

$$P = C_F(R_1 - R_0) + C_T\Delta_T \qquad (4.8)$$

where P is pressure, R_0 and R_1 are initial and current readings respectively, Δ_T is temperature difference and C_F, C_T are calibration factors for load and temperature, respectively. Before the test, all pressure cells were calibrated in the laboratory at room temperature to obtain the corresponding calibration factors. The temperature changes during all tests were small, and therefore, the temperature factor was ignored, resulting in a linear variation under test conditions. Figures 4.9a and 4.9b present the response of pressure cells for Test 1 and Test 2, respectively. A downward trend of the pressure can be observed in Test 1 for higher applied surface pressures at the crown. This point corresponds to pipe failure and has no further significance. Also, a difference in pressures at two springline locations is observed in both tests at the higher applied surface pressures. The pressure cell response at the crown was higher than applied surface pressure in Test 1, whereas in Test 2 pressure at the crown was almost equal to the applied surface pressure. This might correspond to the average compaction of the backfill where compaction was higher for Test 2. The well compacted soil would be expected to pick up load more uniformly.

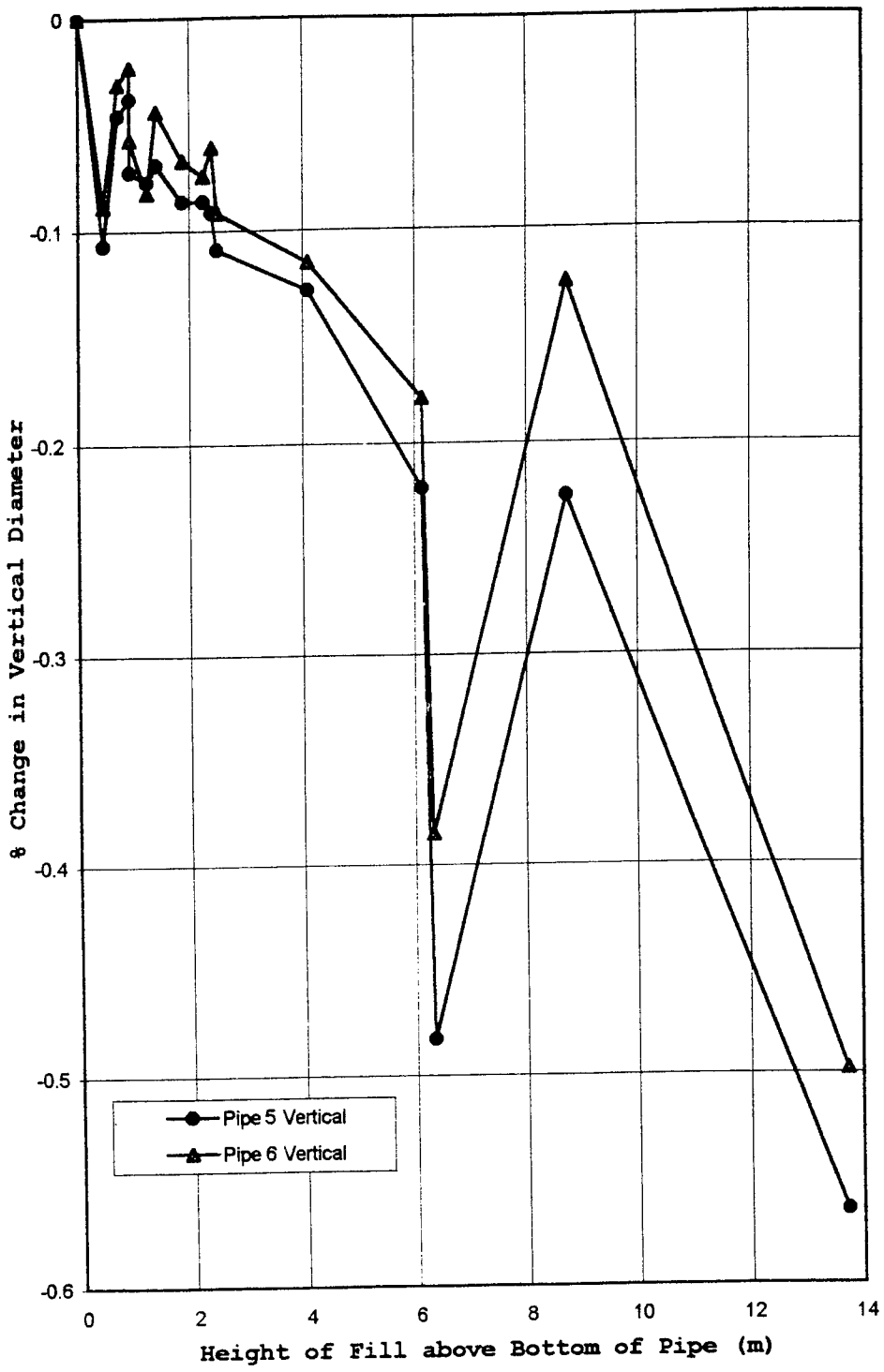

Figure 4.8a Correlation Between the Vertical Deflections with Change in Height of Fill For Test 5 and Test 6

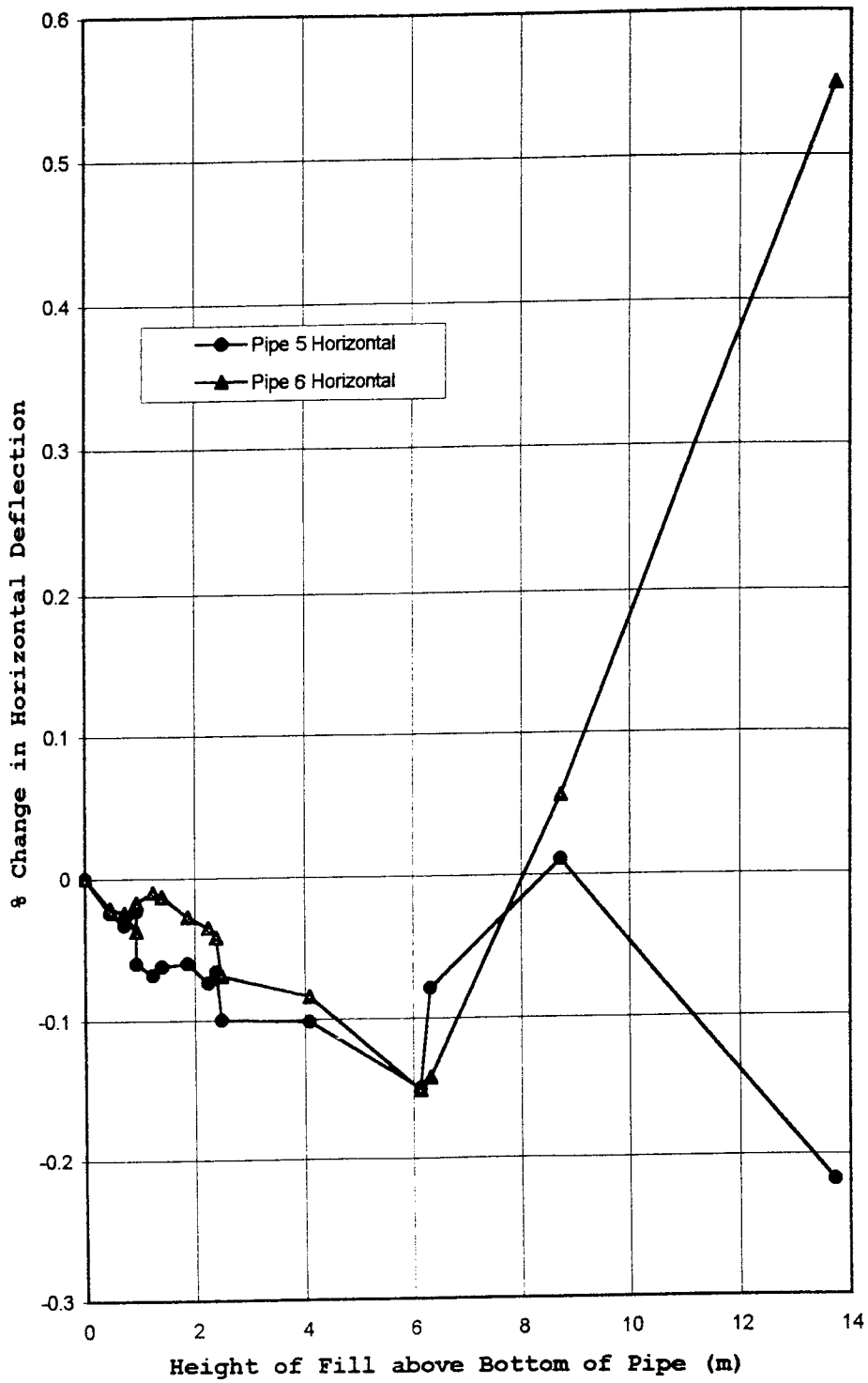

Figure 4.8b Correlation Between the Horizontal Deflections with Change in Height of Fill For Test 5 and Test 6

Table 4.8 Change in Vertical and Horizontal Deflections for Test 5 and Test 6

Fill Height m (ft)	Experimental Deflection - Test 5			Experimental Deflection - Test 6		
	Vertical %	Horizontal %	Ratio of Horizontal to Vertical	Vertical %	Horizontal %	Ratio of Horizontal to Vertical
0	0	0	--	0	0	--
1.87 (6.1)	-0.087	-0.060	0.69	-0.068	-0.027	0.40
2.23 (7.3)	-0.087	-0.074	0.85	-0.075	-0.035	0.47
2.38 (7.8)	-0.092	-0.066	0.72	-0.062	-0.042	0.68
2.48 (8.1)	-0.109	-0.100	0.92	-0.092	-0.069	0.75
4.10 (13.4)	-0.128	-0.102	0.80	-0.115	-0.084	0.73
6.13 (20.1)	-0.221	-0.150	0.68	-0.179	-0.151	0.84
6.31 (20.7)	-0.483	-0.079	0.16	-0.385	-0.142	0.37
8.72 (28.6)	-0.225	0.011	-0.05	-0.125	0.056	-0.45
13.72 (45.0)	-0.565	-0.218	0.38	-0.498	0.550	-1.10

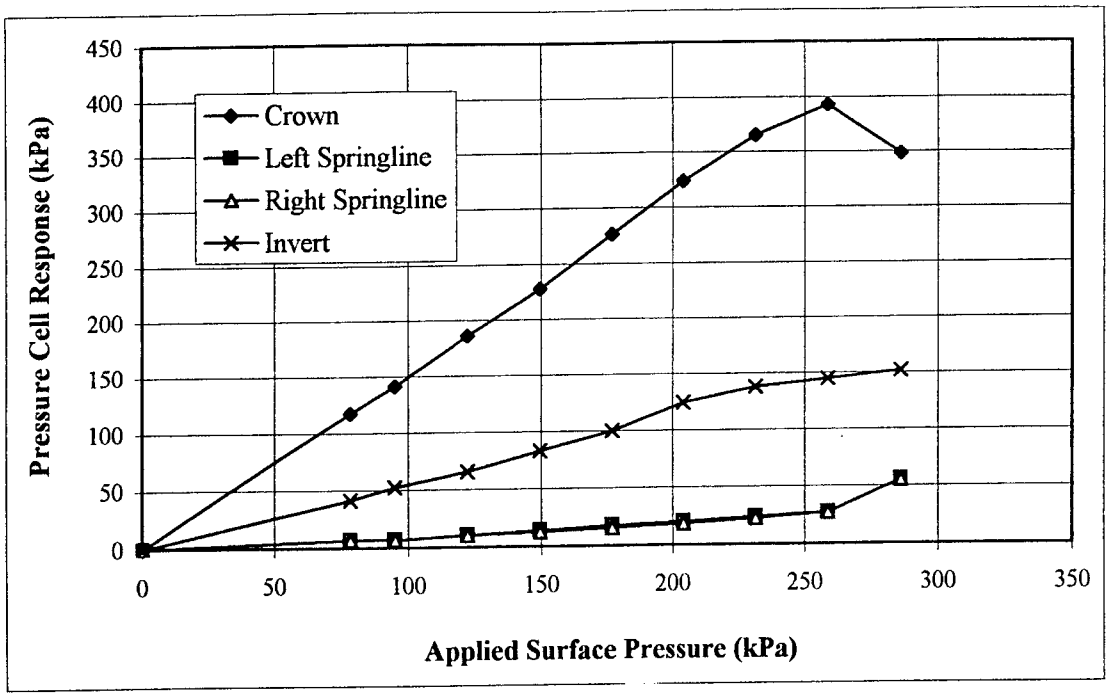

Figure 4.9a Response of the Pressure Cells of the 610 mm Concrete Pipe for Test 1

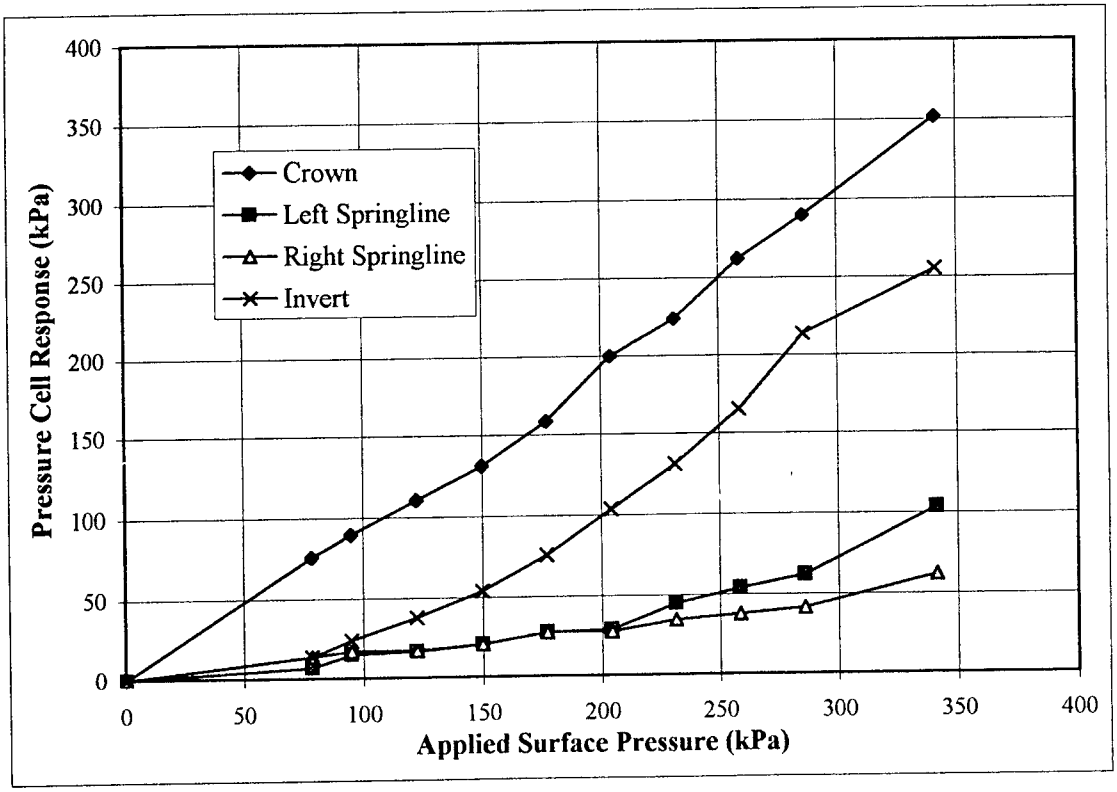

Figure 4.9b Response of the Pressure Cells of the 610 mm Concrete Pipe for Test 2

Pressures are shown in Figures 4.10a and 4.10b for Test 3 and Test 4, respectively. The values for the loading steps are shown. In the initial stage both pipes respond elastically, the crown pressure is approximately the same as the springline pressure, but the invert records about 2-3 times the applied pressure.

Higher measured pressures than applied pressure might be the result of the pressure cell being located near the rigid pipe, especially at the invert where there was only a 152 mm (6 in.) bedding layer between the pipe and bedrock. Averaged springline pressures look reasonable, which may indicate a sideways movement of the pipes. For Test 3, with a well compacted, Type 1 backfill, the pressures recorded at the crown and springlines were only about half of the values for Test 4, with Type 3 backfill. At the maximum load, for Test 4, the pressures appear to be hydrostatic, but still approximately three times the applied pressure.

For Test 5 and Test 6 the pressures at the top, bottom and springlines are shown, as related to fill height, in Figure 4.11. Comparing pressures measured with geostatic pressures calculated, several striking differences are apparent. In contrast with the general assumption, the pressure was not hydrostatic under deep burial for the concrete pipes instrumented. The springline pressures were approximately 27% of the geostatic pressure whereas the invert pressure was approximately 40% of the geostatic pressure. This may have resulted from the installation procedure where a 152 mm (6 in.) uncompacted layer of fill was placed under the center 1/3 of the pipe outside diameter. Since extreme care was exercised during pipe installation to properly locate the pressure cells, a conclusion drawn from consideration of vertical equilibrium is that a properly installed rigid pipe supports most of the overburden on its haunches.

There are several other interesting observations. There is a large difference in the invert

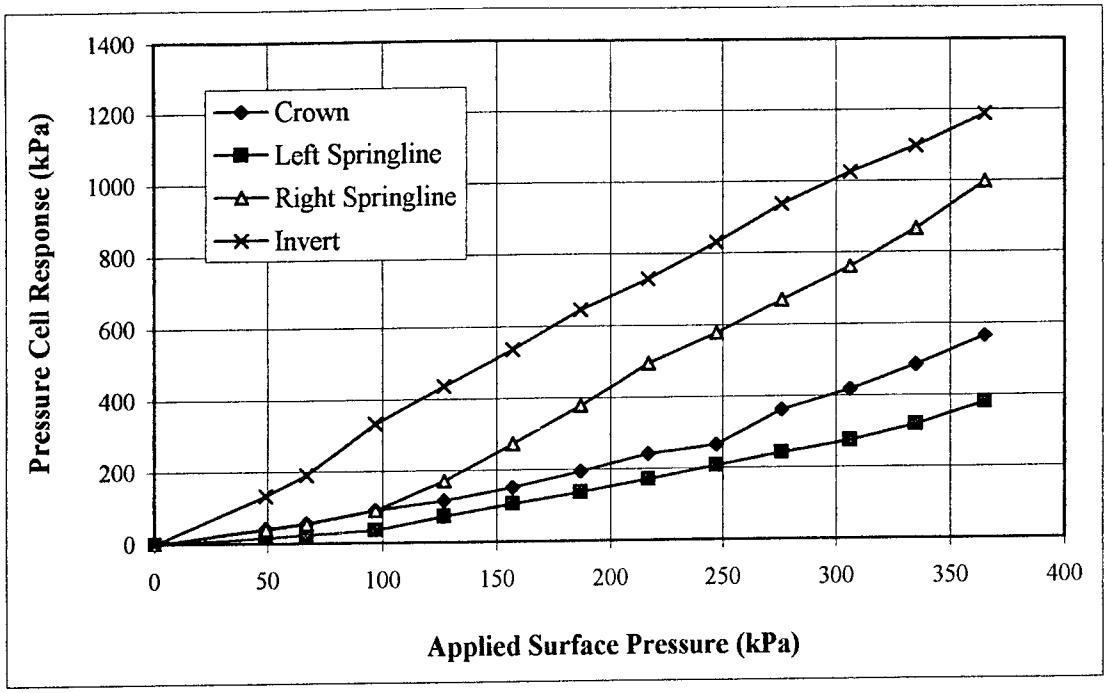

Figure 4.10a Response of the Pressure Cells of the 1520 mm Concrete Pipe for Test 3

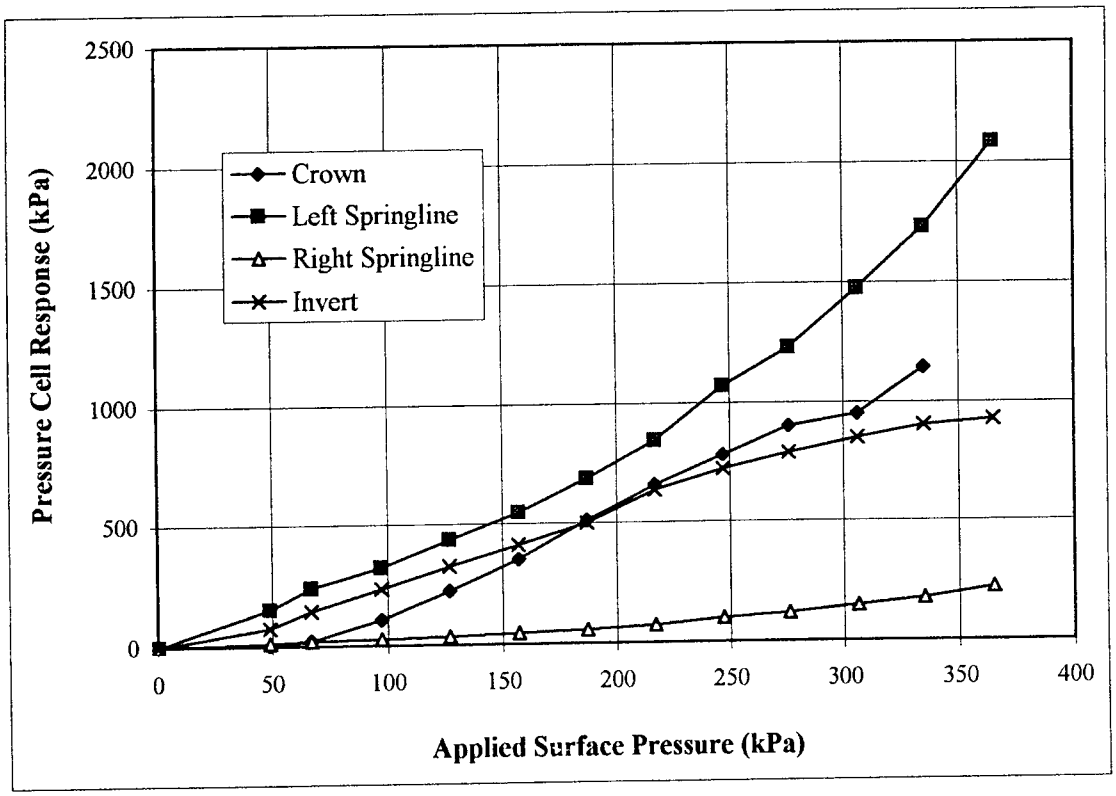

Figure 4.10b Response of the Pressure Cells of the 1520 mm Concrete Pipe for Test 4

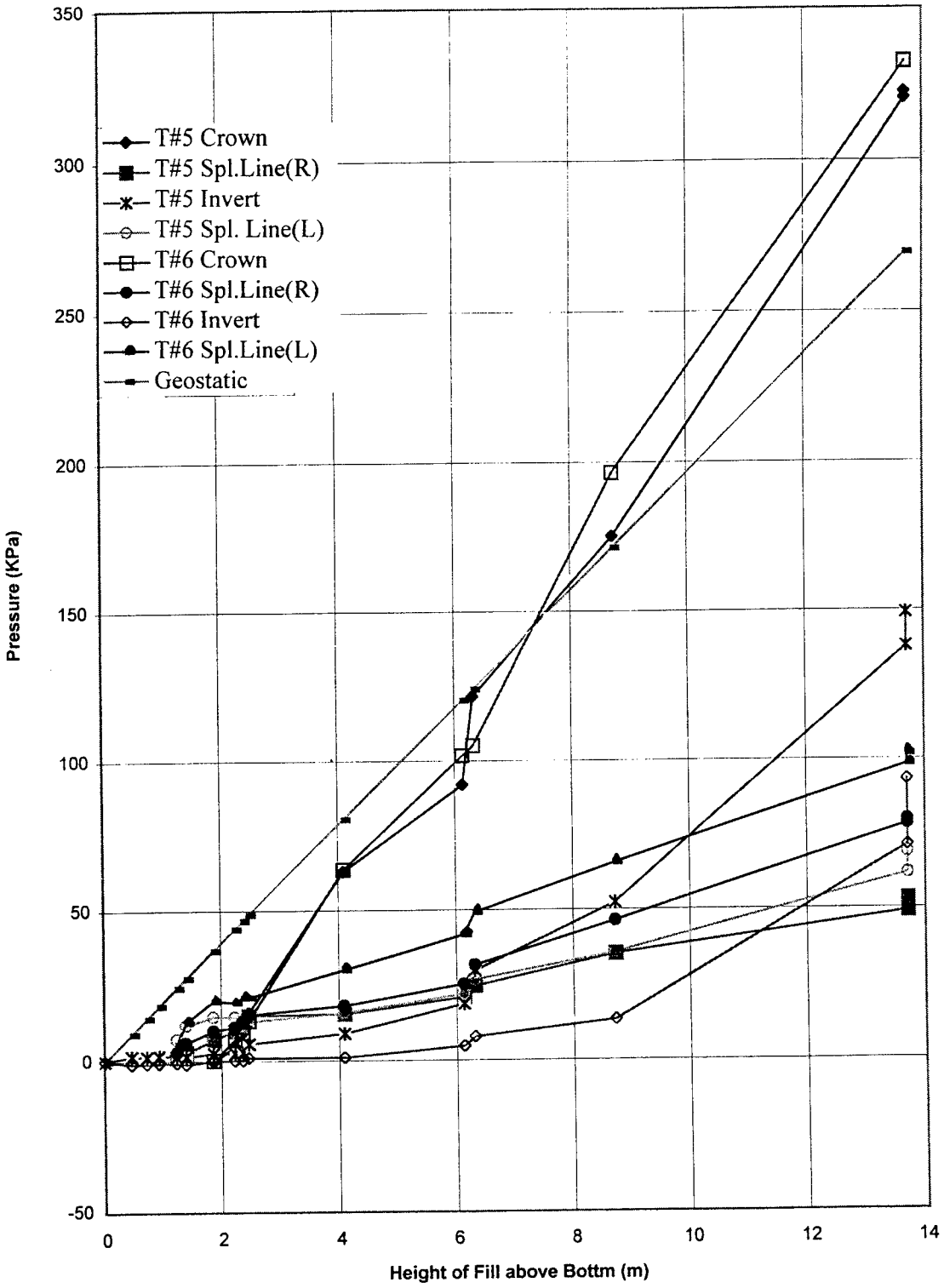

Figure 4.11 Pressure Increase in Test 5 and Test 6 at all Sections with Height of Fill Above Bottom

pressures of Test 5 and Test 6 with the pressure in Test 5 being about twice as large. Since the installation was identical, the same measured pressures would be expected. However, the springline pressure for Test 6 is higher than for Test 5. It is also interesting to note that the crown pressure becomes larger than the geostatic pressure for both tests, which may indicate negative soil arching.

4.8 MEASURED PIPE WALL RESPONSES TO LOADING

The strain in the pipe wall was experimentally determined using equations of Sections 4.2 and 4.3. The sign convention for strain is for tension to be positive. Test 1, Test 2, Test 3, and Test 4 are short term tests where each pipe was tested in a period of approximately four hours after backfilling was complete. Test 5 and Test 6 were field installations where the backfilling took place over a period of approximately six weeks. At the end of this period, soil pressures and deflections were recorded but further strains were not measured. In Chapter 5, bending moments and circumferential thrusts are calculated from strains using experimentally determined Young's modulus and Poisson's ratio. These calculated values are further compared with results obtained from SIDD and SIDD-HT software.

4.8.1 Measured Strain for Test 1

Electric strain gages were attached to the outside and inside of the pipe wall as well as the reinforcing cage. Measurements were taken at the crown, invert and both springlines. All plots are given with applied surface pressure as the independent variable. Results are shown in Figures 4.12 through 4.17 for Test 1. The strains plotted represent measured strains by the sensors which correspond to physical response of the pipe under load. Values of tensile strain above 100 με

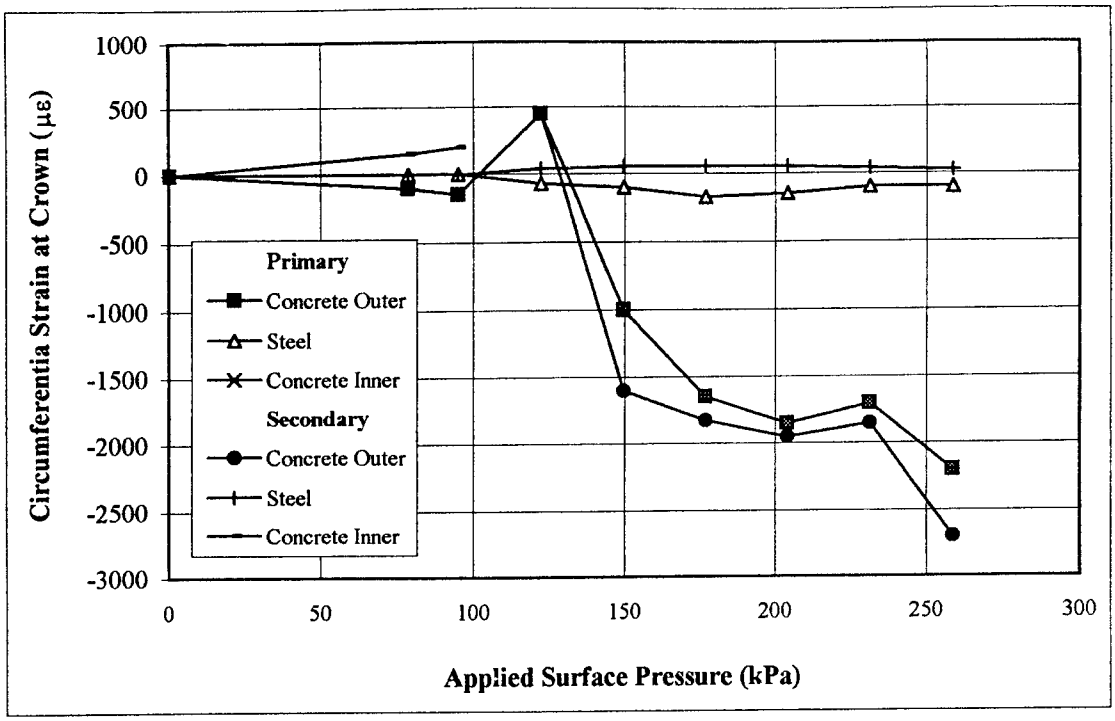

Figure 4.12 Cross-Sectional Strain at Crown of the 610 mm Concrete Pipe for Test 1

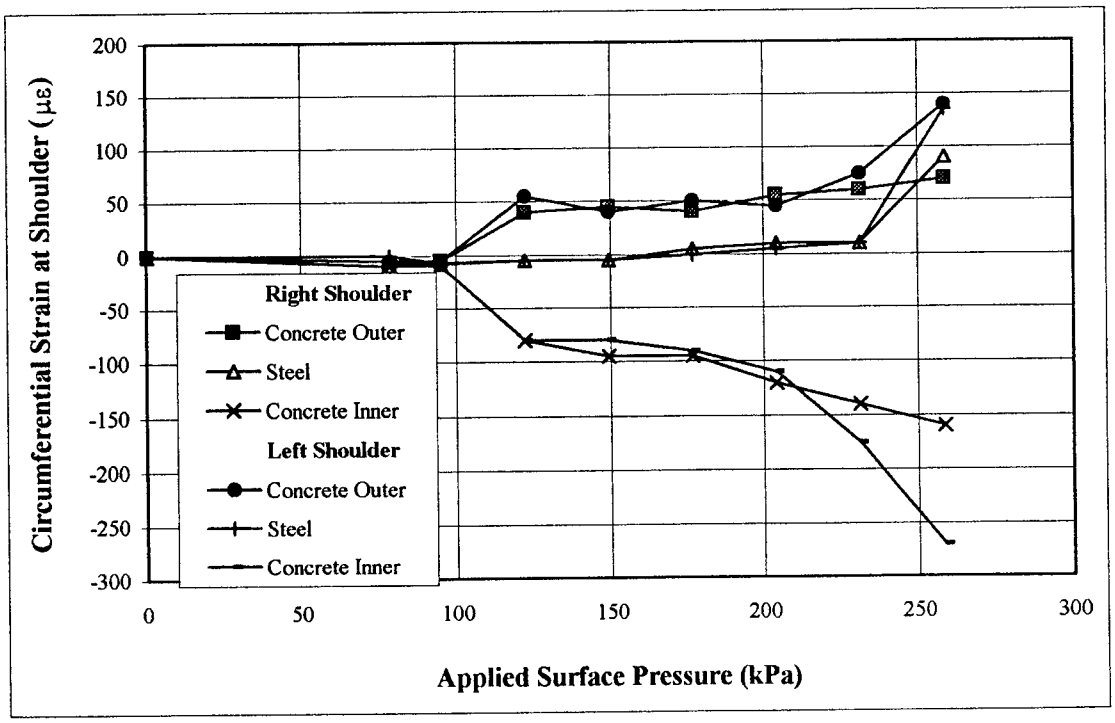

Figure 4.13 Cross-Sectional Strain at Right and Left Quarter points of the 610 mm Concrete Pipe for Test 1.

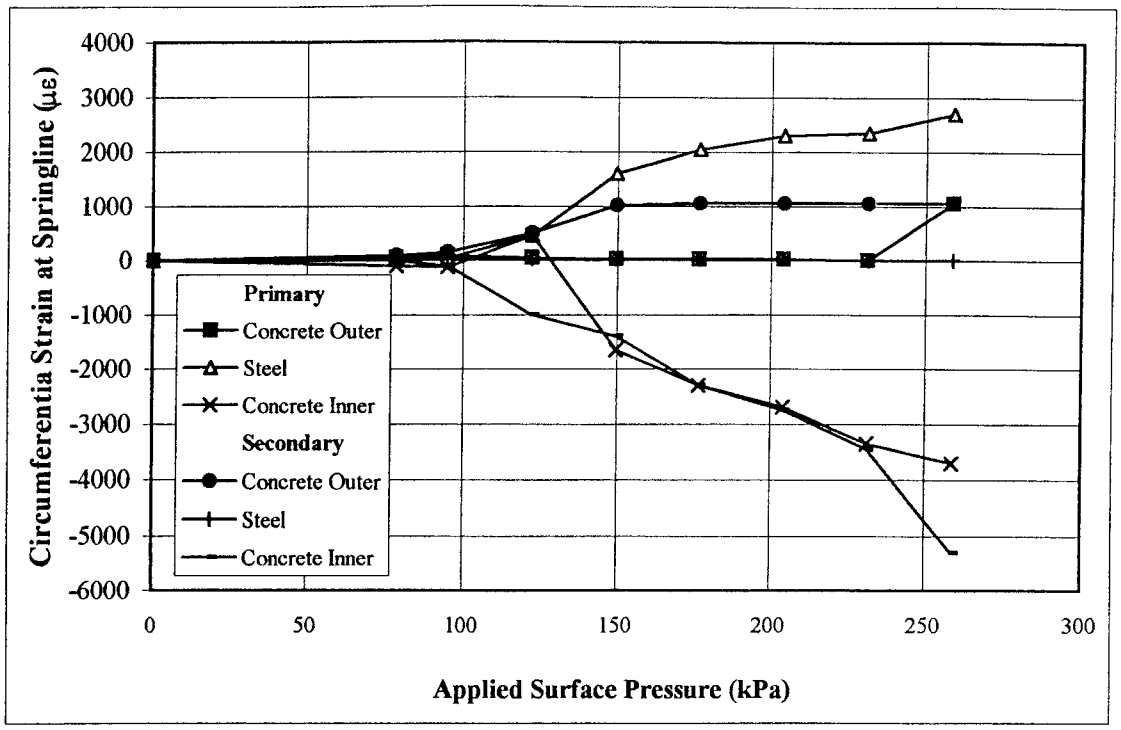

Figure 4.14 Cross-Sectional Strain at Right Springline of the 610 mm Concrete Pipe for Test 1

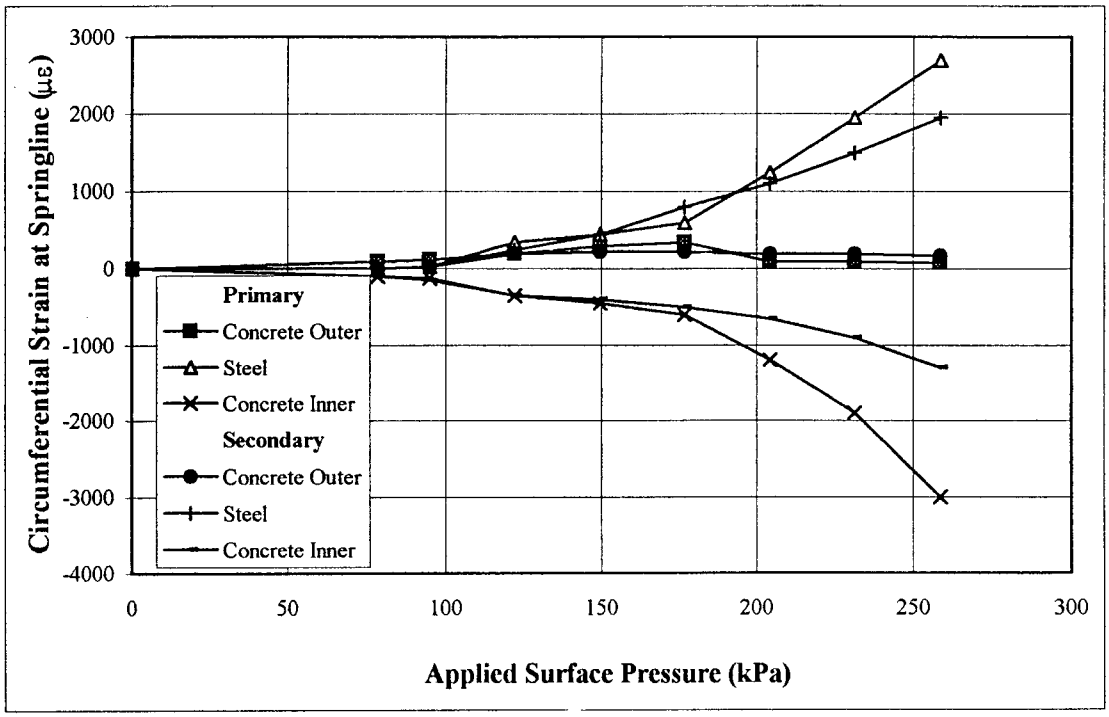

Figure 4.15 Cross-Sectional Strain at Left Springline of the 610 mm Concrete Pipe for Test 1

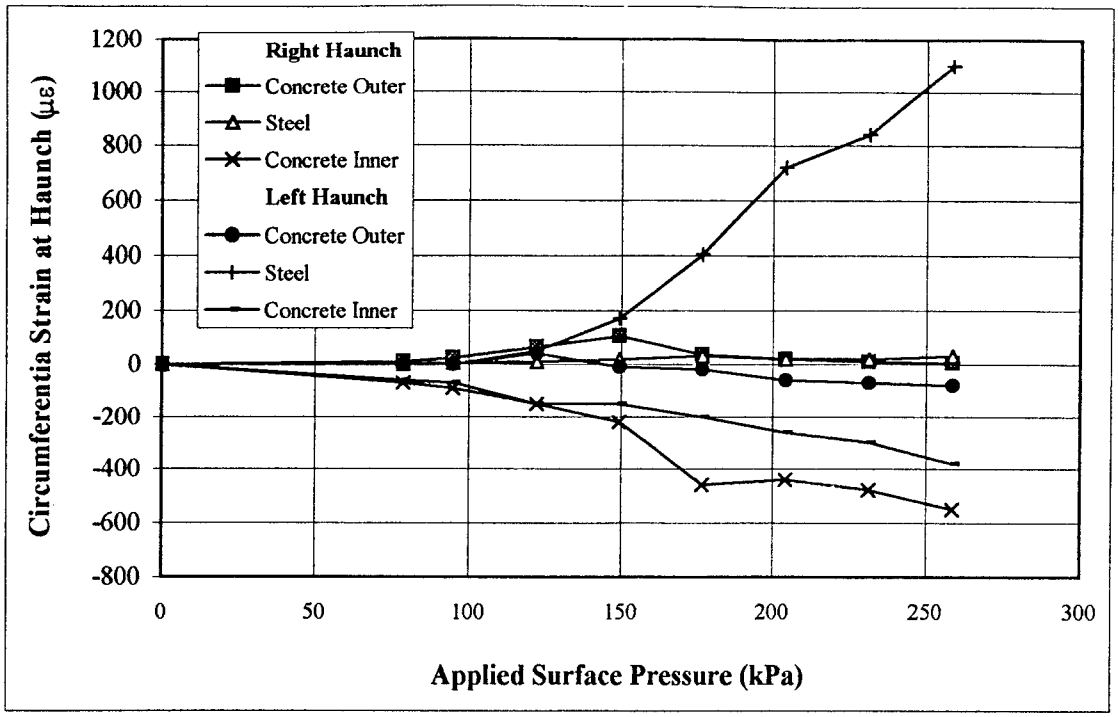

Figure 4.16 Cross-Sectional Strain at Right and Left Haunch of the 610 mm Concrete Pipe for Test 1

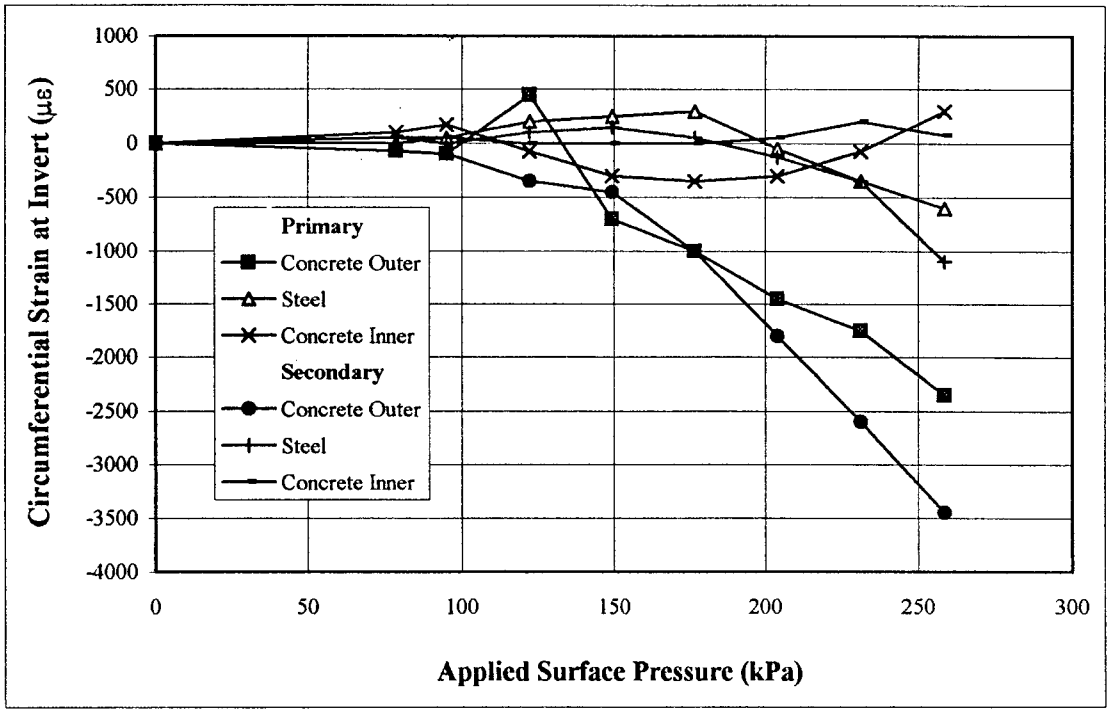

Figure 4.17 Cross-Sectional Strain at Invert of the 610 mm Concrete Pipe for Test 1

or compressive strains above 1000 με may represent inelastic response of the concrete pipe. The inner concrete gage, located at the crown, is an example of tensile failure (Figure 4.12). Surface pressure below 140 kPa (20 psi) show that the distress in the pipe is minimal for Test 1 with the Type 3 backfill. It is also interesting to note that the crown and invert record higher strain values than the springlines with the crown loading up more quickly in this test.

4.8.2 Measured Strain for Test 2

Strain values for Test 2 have been plotted in Figures 4.18 through 4.23. It is unusual to note that for Test 2 with a Type 1 backfill, the strain level at the crown remains high for a surface pressure of 140 kPa (20 psi). However, the strains in the other instrumented sections have been mitigated by the well-compacted backfill. For instance, the springline strain attained a value of 1000 με at a pressure of 280 kPa (40 psi), whereas for Test 1 the springline strain attained a value of 1000 με at a pressure of about 140 kPa (20 psi). Strains measured at the shoulders and haunches are in a transition area from positive to negative moments. For example, in Figure 4.19 the moment for right shoulder is obviously quite large negative value where the moment at the left is almost zero. There are examples of concrete failing in tension near strain gages. Examining Figure 4.22, the outer concrete gage indicates concrete failure at about loading of 120 kPa (17.4 psi). At initiation of concrete cracking, the gage records the release of tension.

4.8.3 Measured Strain for Test 3

Strains measured for Test 3 are shown in Figures 4.24 through 4.28. Table 4.11 gives magnitudes for strains measured. There were a number of strain gages for Test 3 and Test 4 that

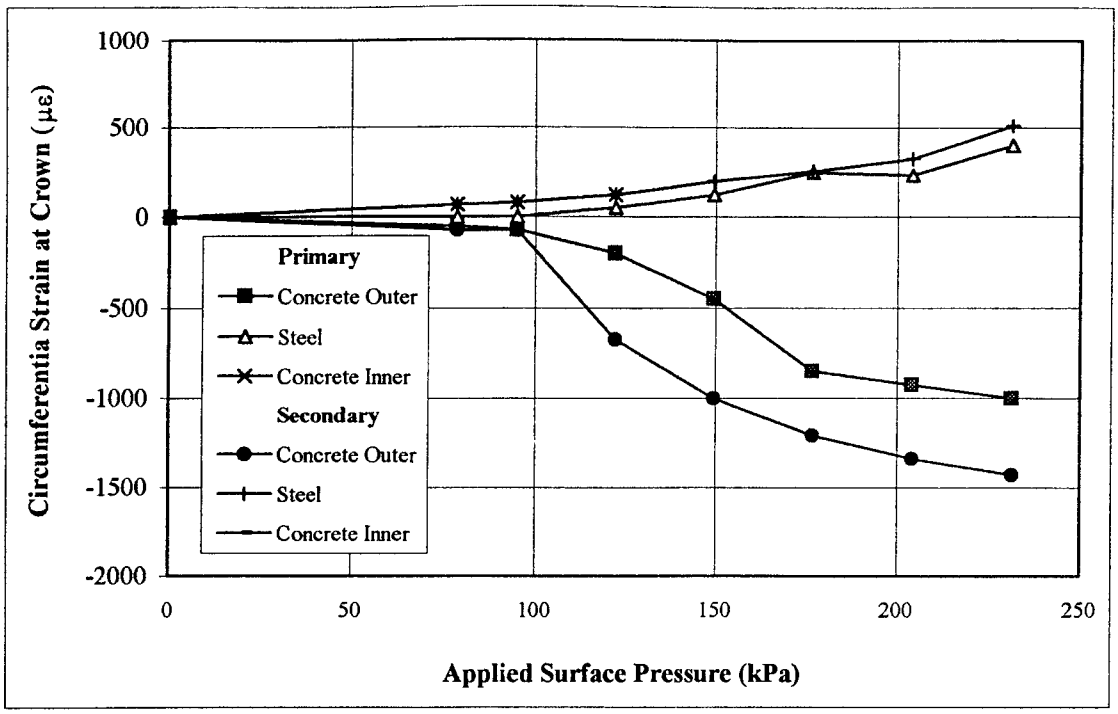

Figure 4.18 Cross-Sectional Strain at Crown of the 610 mm Concrete Pipe for Test 2

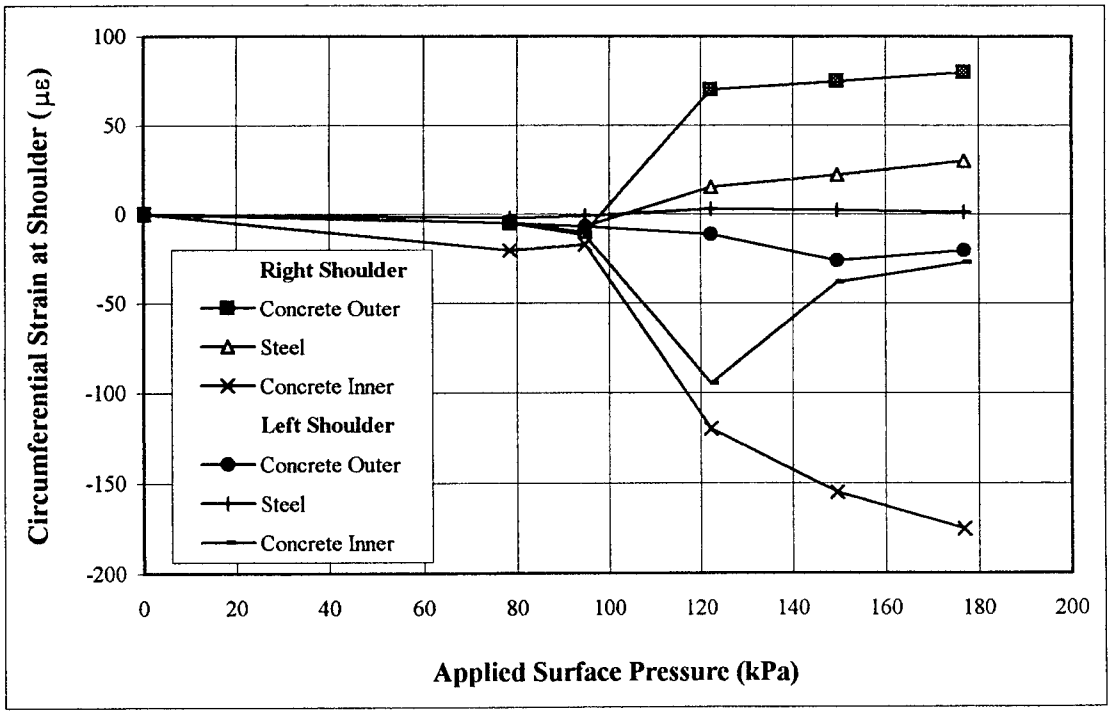

Figure 4.19 Cross-Sectional Strain at Right and Left Quarter points of the 610 mm Concrete Pipe for Test 2.

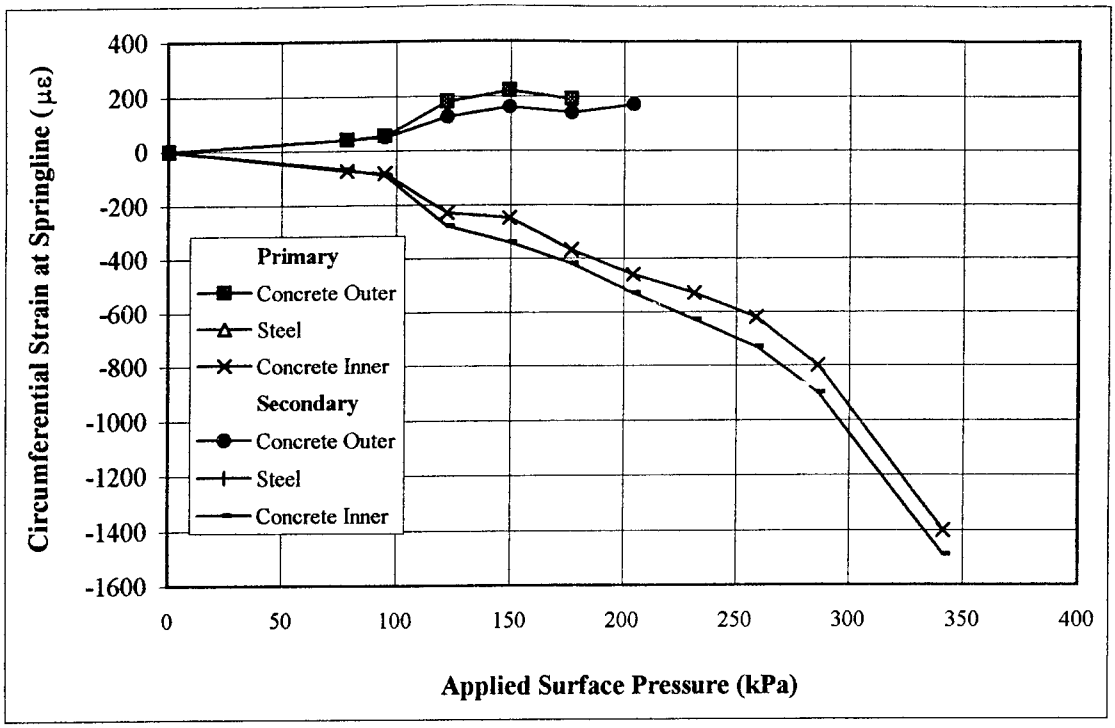

Figure 4.20 Cross-Sectional Strain at Right Springline of the 610 mm Concrete Pipe for Test 2

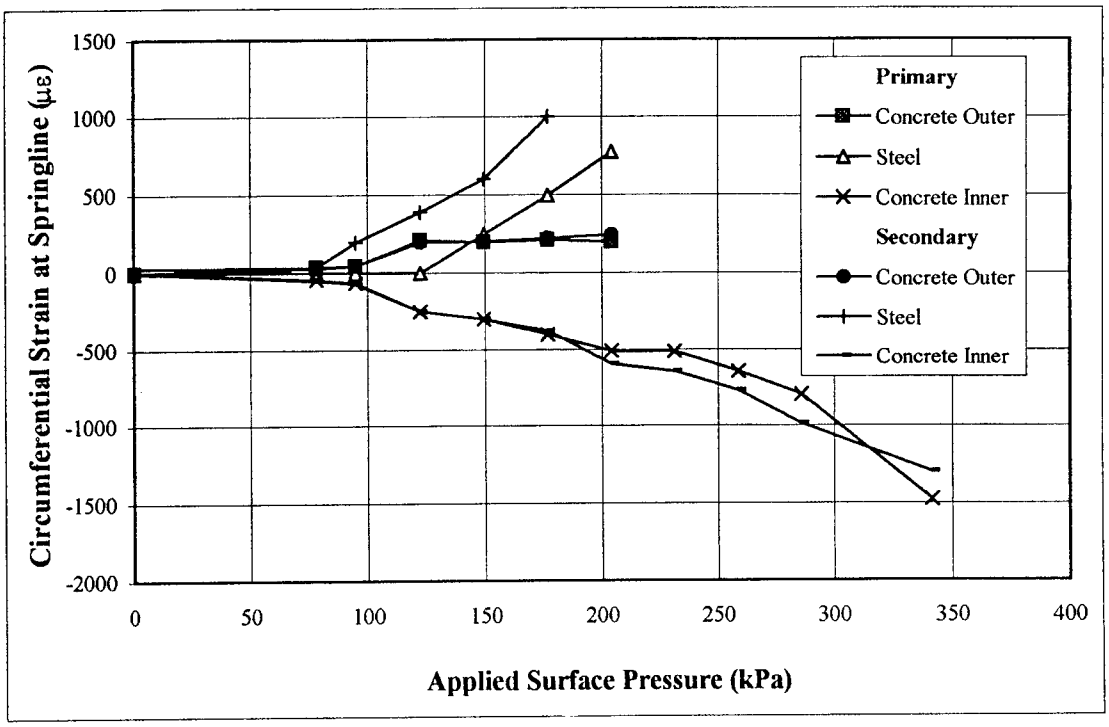

Figure 4.21 Cross-Sectional Strain at Left Springline of the 610 mm Concrete for Test 2

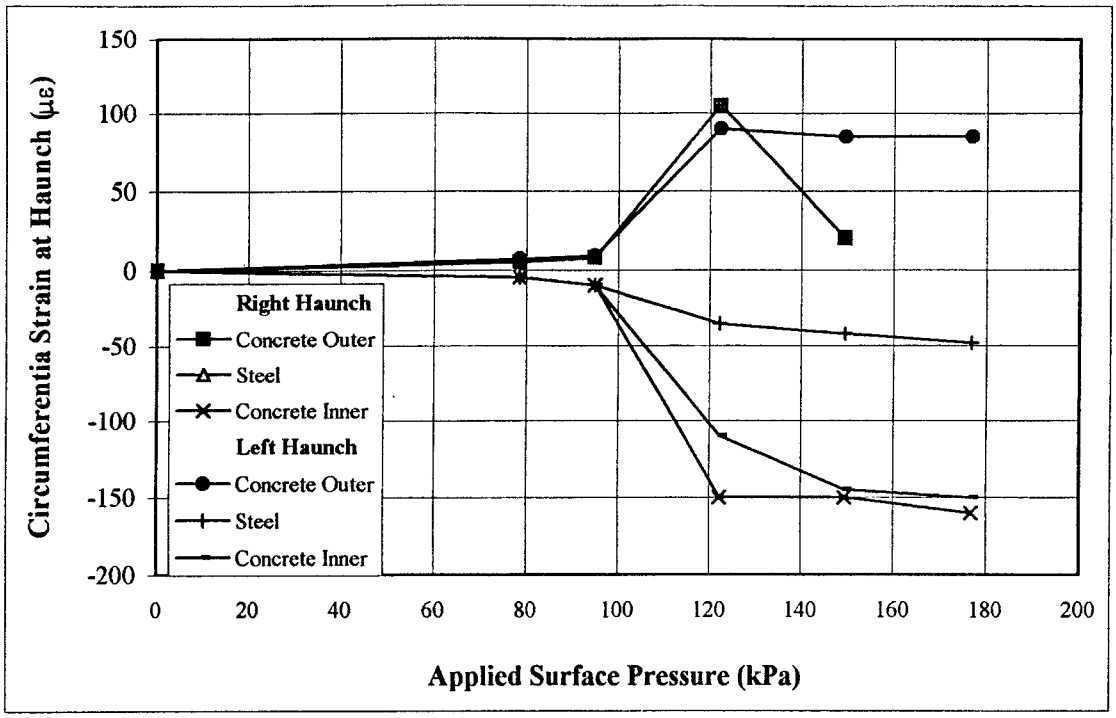

Figure 4.22 Cross-Sectional Strain at Right and Left Haunch of the 610 mm Concrete Pipe for Test 2

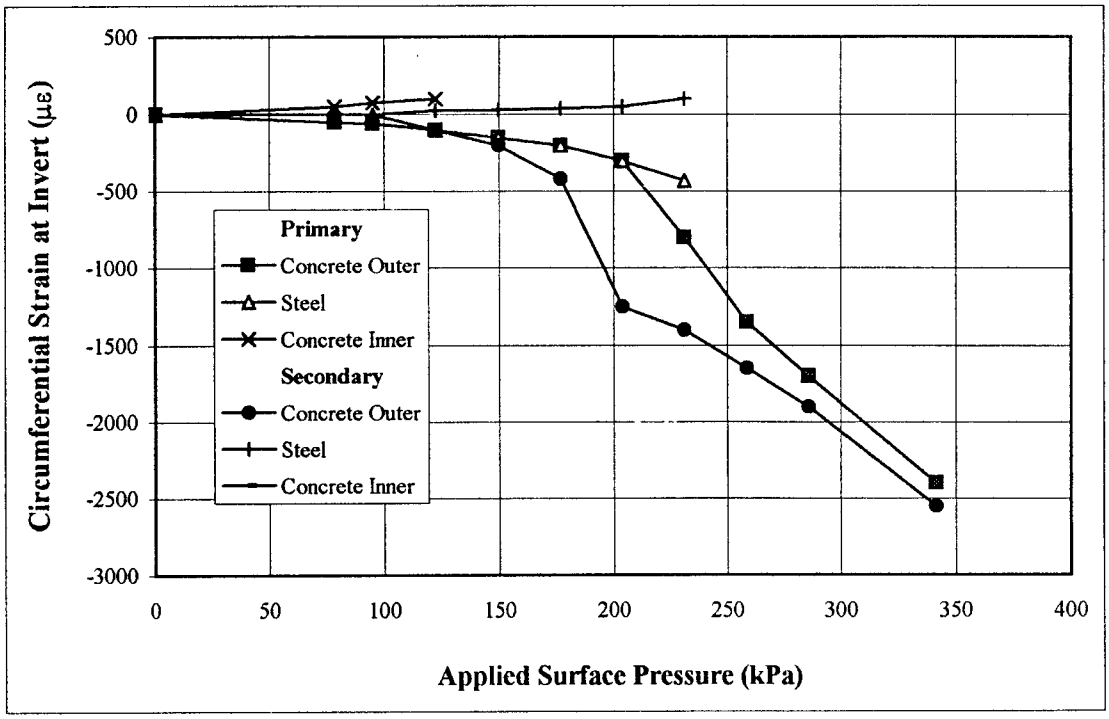

Figure 4.23 Cross-Sectional Strain at Invert of the 610 mm Concrete Pipe for Test 2

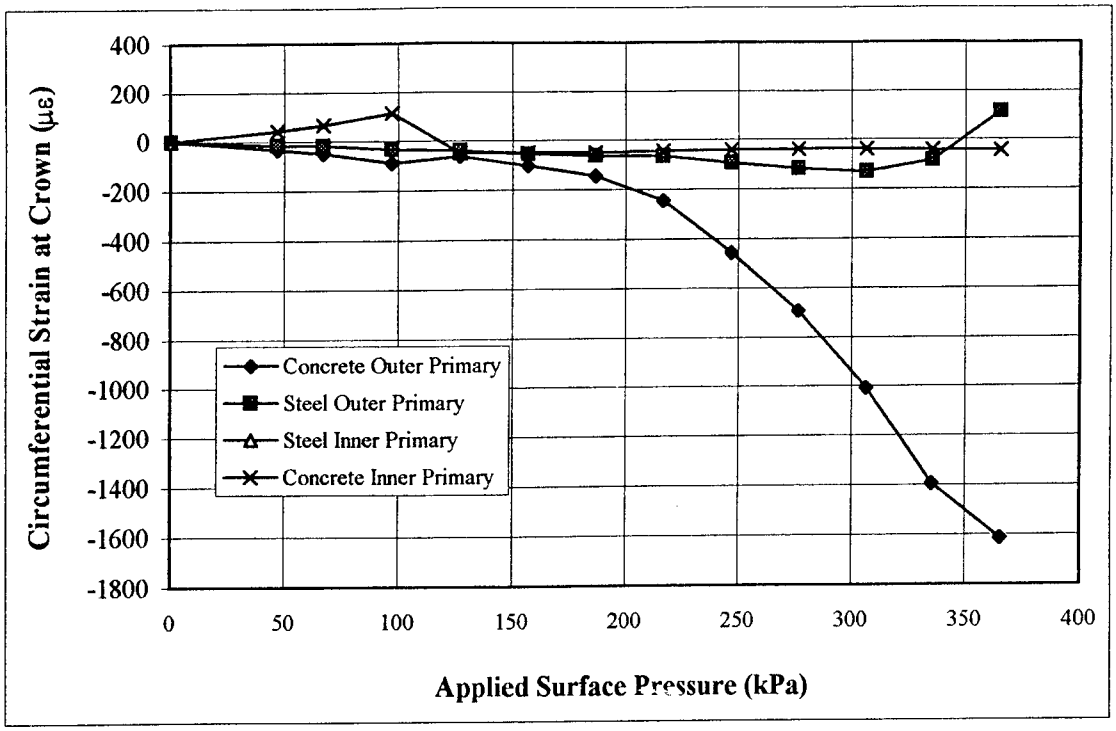

Figure 4.24a Cross-Sectional Strain at Crown of the 1520 mm Concrete Pipe for Test 3

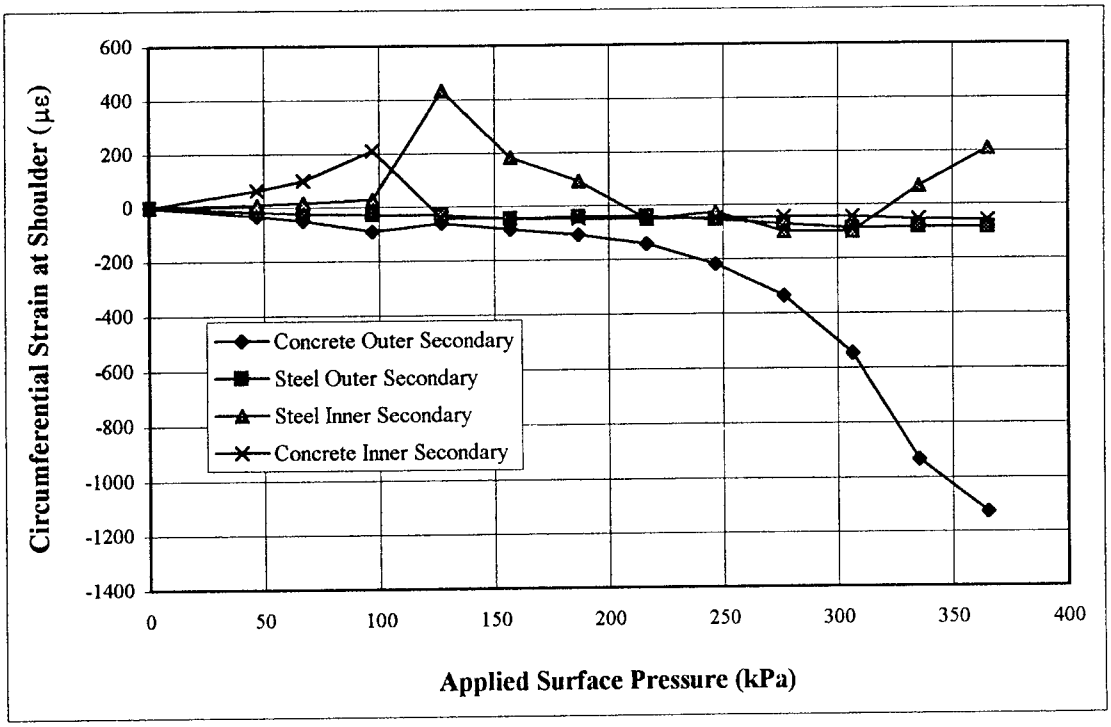

Figure 4.24b Cross-Sectional Strain at Crown of the 1520 mm Concrete Pipe for Test 3

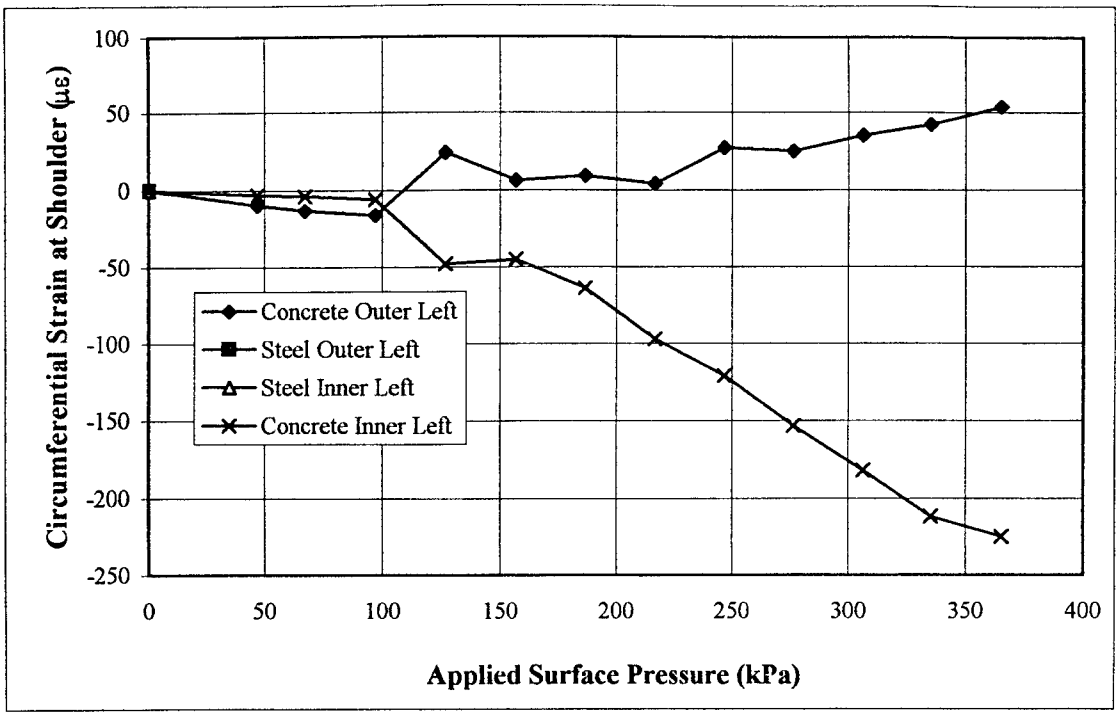

Figure 4.25a Cross-Sectional Strain at Shoulder of the 1520 mm Concrete Pipe for Test 3

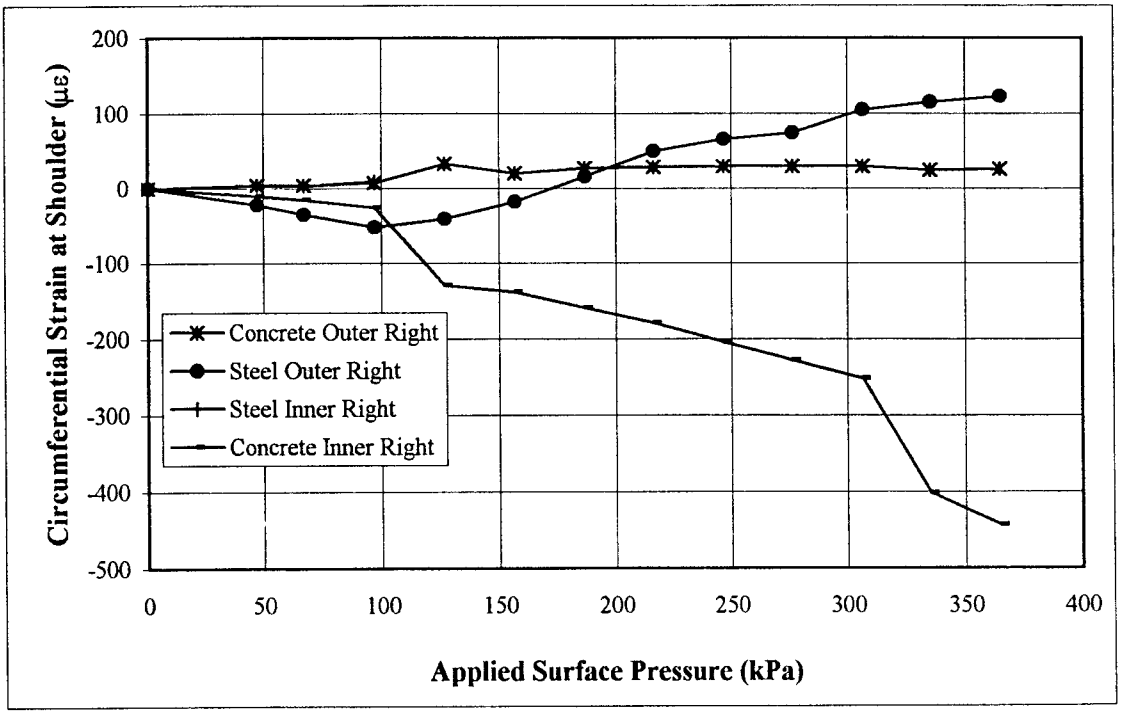

Figure 4.25b Cross-Sectional Strain at Shoulder of the 1520 mm Concrete Pipe for Test 3

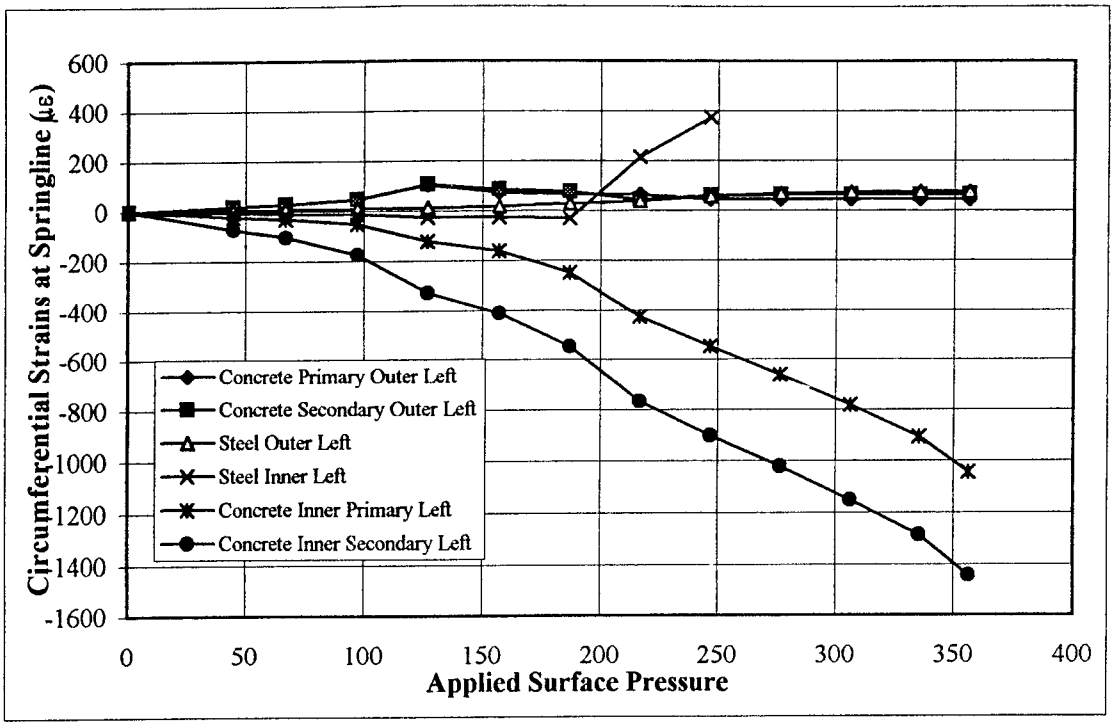

Figure 4.26a Cross-Sectional Strain at Springline of the 1520 mm Concrete Pipe for Test 3

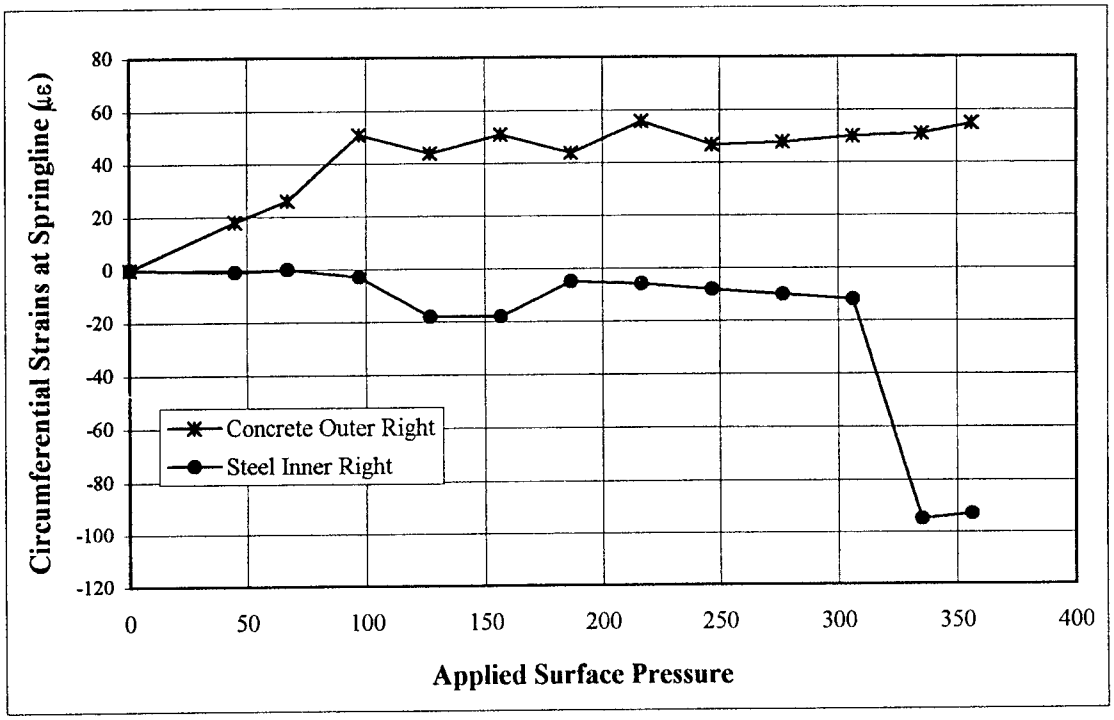

Figure 4.26b Cross-Sectional Strain at Springline of the 1520 mm Concrete Pipe for Test 3

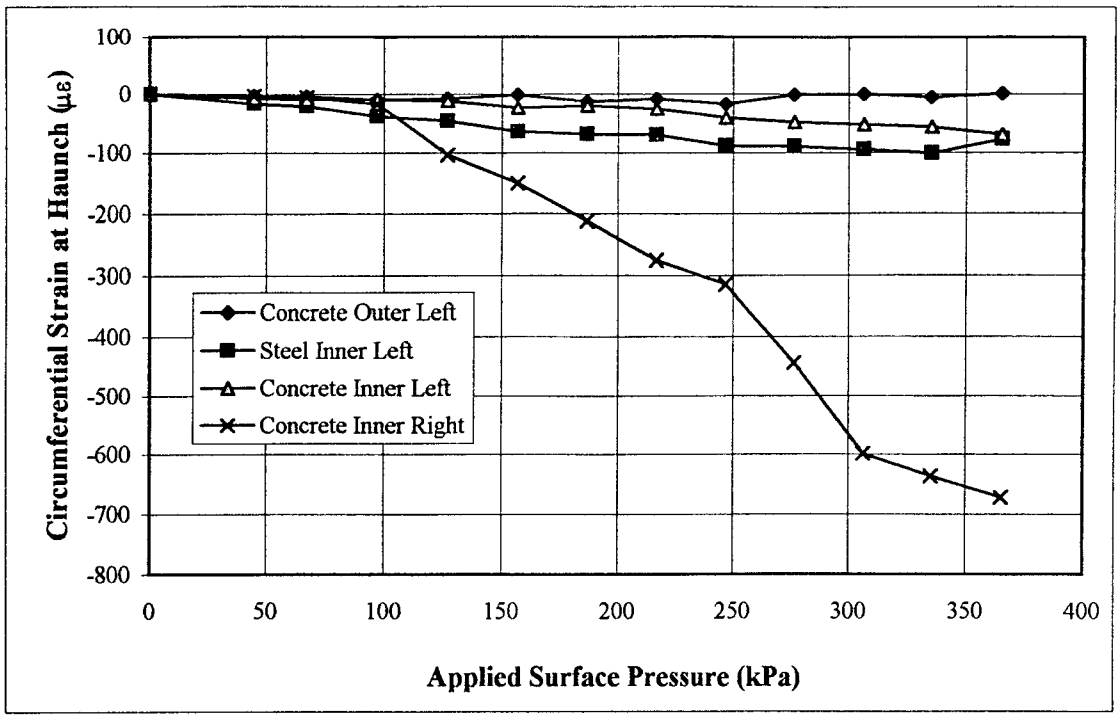

Figure 4.27 Cross-Sectional Strain at Haunch of the 1520 mm Concrete Pipe for Test 3

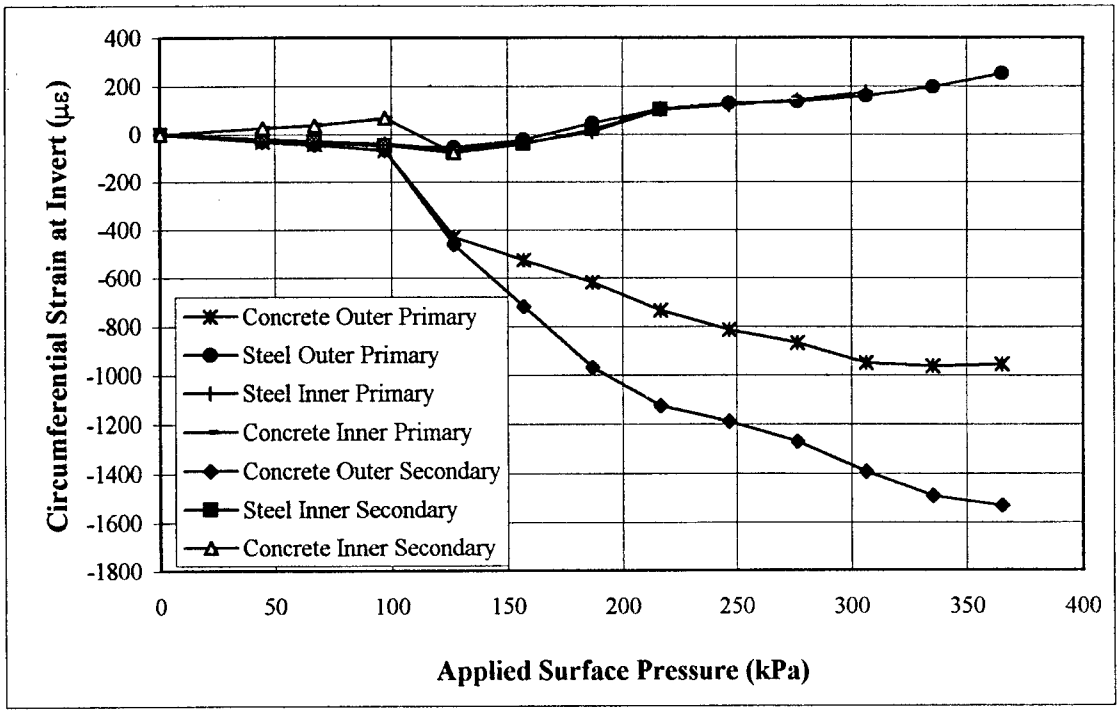

Figure 4.28 Cross-Sectional Strain at Invert of the 1520 mm Concrete Pipe for Test 3

Table 4.11 Cross-Sectional Strain at Springlines of the 1520 mm Concrete Pipe for Test 3

Surface Pressure for Test 3 kPa	Springlines							
	Left						Right	
	Outer Concrete		Outer Steel	Inner Steel	Inner Concrete		Outer Concrete	Inner Steel
	Prim.	Sec.			Prim.	Sec.		
0	0	0	0	0	0	0	0	0
44.7	18	18	5	-5	-23	-73	18	-1
67.1	28	28	8	-10	-33	-106	26	0
97.1	47	47	10	-14	-53	-174	51	-3
126.9	104	105	11	-27	-122	-328	44	-18
156.8	73	86	18	-28	-162	-412	51	-18
186.7	64	75	27	-32	-250	-546	44	-5
216.6	65	43	37	216	-428	-764	56	-6
246.8	43	60	56	374	-546	-900	47	-8
276.5	44	61	67		-662	-1020	48	-10
306.4	44	62	73		-781	-1149	50	-12
335.3	43	62	74		-906	-1286	51	-95
356.2	43	65	74		-1044	-1441	55	-93

could not be read. Pipes for Test 3 and Test 4 could not be tested when delivered because of scheduling difficulties. Subsequently, during storage the pipes were subject to vandalism and most of the leads to the electric strain gages were detached and many gages destroyed. Gages on the concrete surfaces were replaced prior to testing but the steel cages were inaccessible.

Examining Figure 4.24, crown strains on the outside increase in magnitude beyond the range where cracking was observed. Compressive shoulder strains, shown along the inside of the pipe in Figure 4.25, are about 30% of the crown compressive strains. In contrast to the crown, compressive stresses along the springlines respond almost immediately to surface loading. Haunch strains as shown in Figure 4.27 are quite small. And again the invert strains appear to respond to cracking of the concrete. The magnitudes of strains at the crown, invert and springlines indicate the 1520 mm (60 in.) pipe was close to failure when the test ended.

4.8.4 Measured Strain for Test 4

Strains measured for Test 4 are shown in Figures 4.29 through 4.31. Magnitudes measured at the load steps are given in Table 4.12. The strains measured at the secondary section should duplicate strains measured at the primary section. An example is shown in Figure 4.29 where the strains measured at the concrete outer primary can be compared to strains measured at the concrete outer secondary. The readings are very similar. Consequently, in most cases secondary circumferential strains are equivalent to primary circumferential strains. The springline strains are more difficult to interpret. Examining Figure 4.31a and Figure 4.31b, the tensile strains on the concrete outer primary right are almost zero whereas the concrete outer primary left and concrete outer secondary left show magnitudes around 100 με to 200 με.

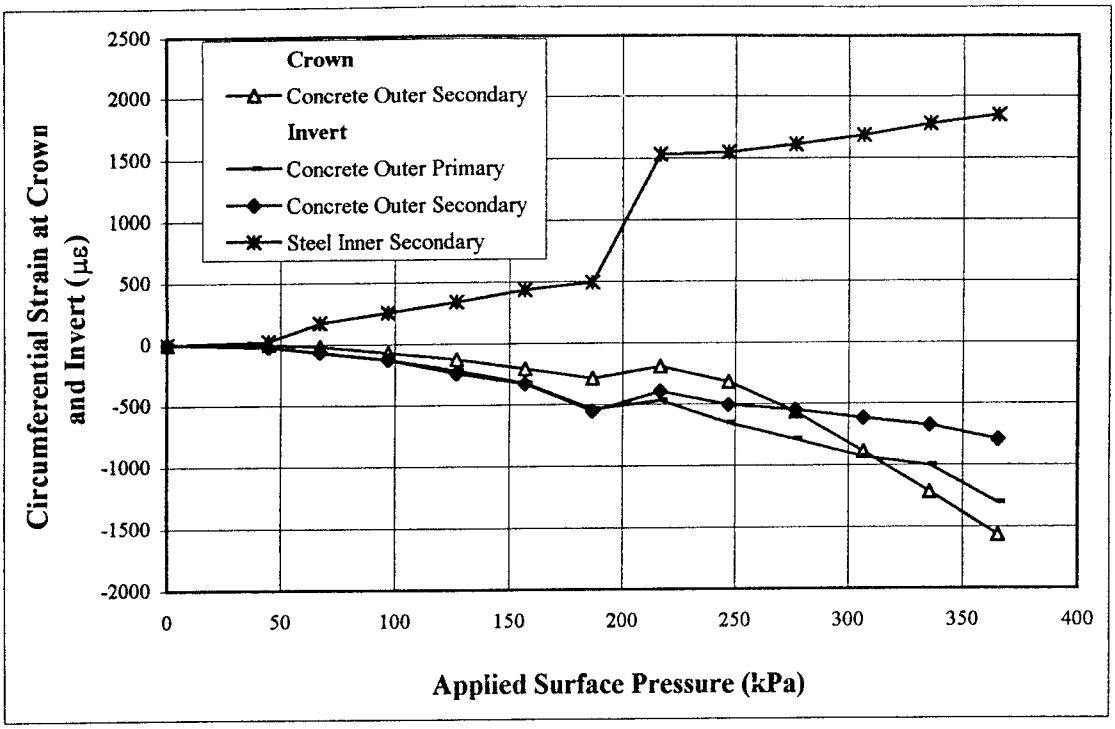

Figure 4.29 Cross-Sectional Strain at Crown and Invert of the1520 mm Concrete Pipe for Test 4

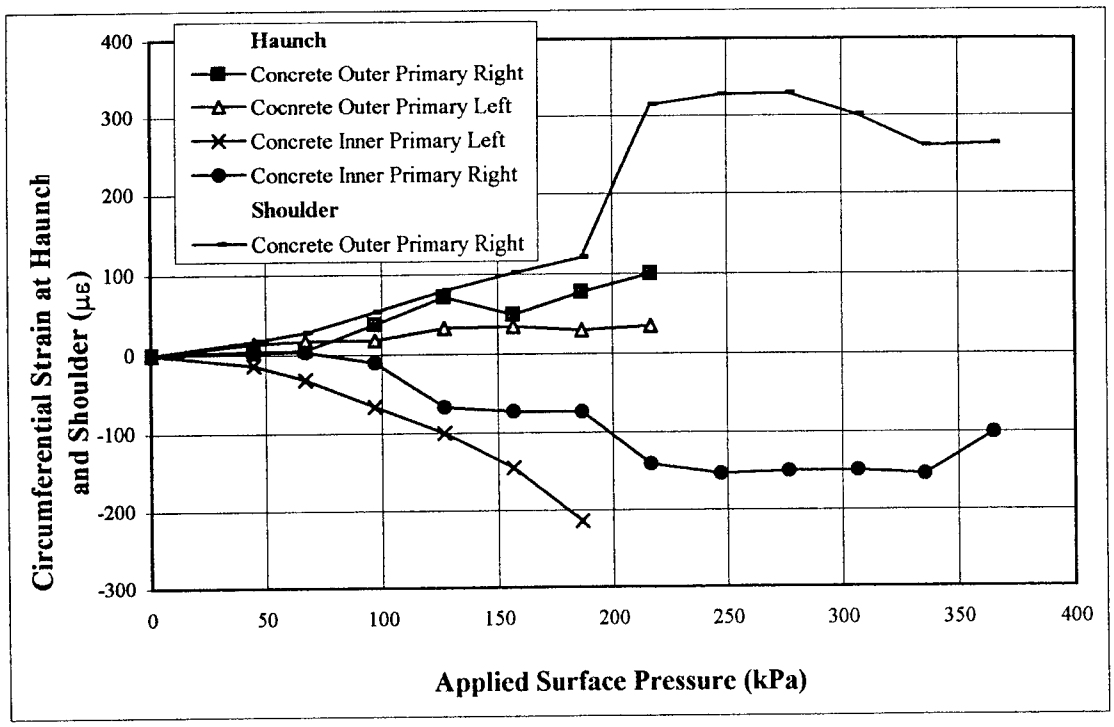

Figure 4.30 Cross-Sectional Strain at Quarter Points of the 1520 mm Concrete Pipe for Test 4

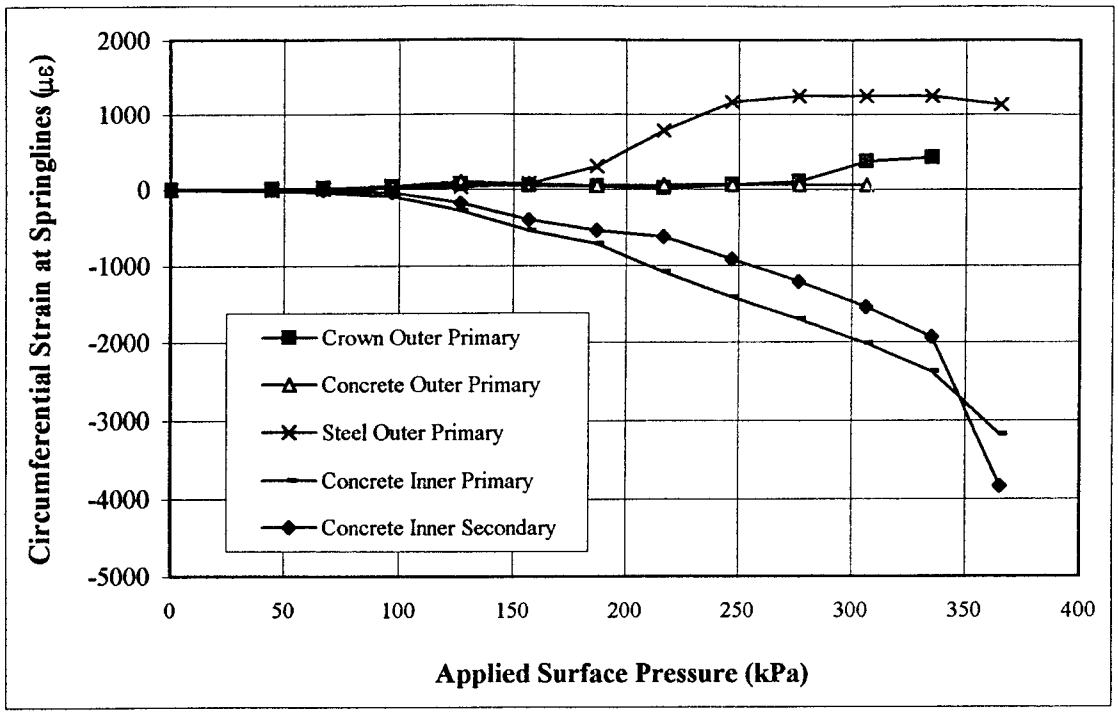

Figure 4.31a Cross-Sectional Strain at Right Springline of the 1520 mm Concrete Pipe for Test 4

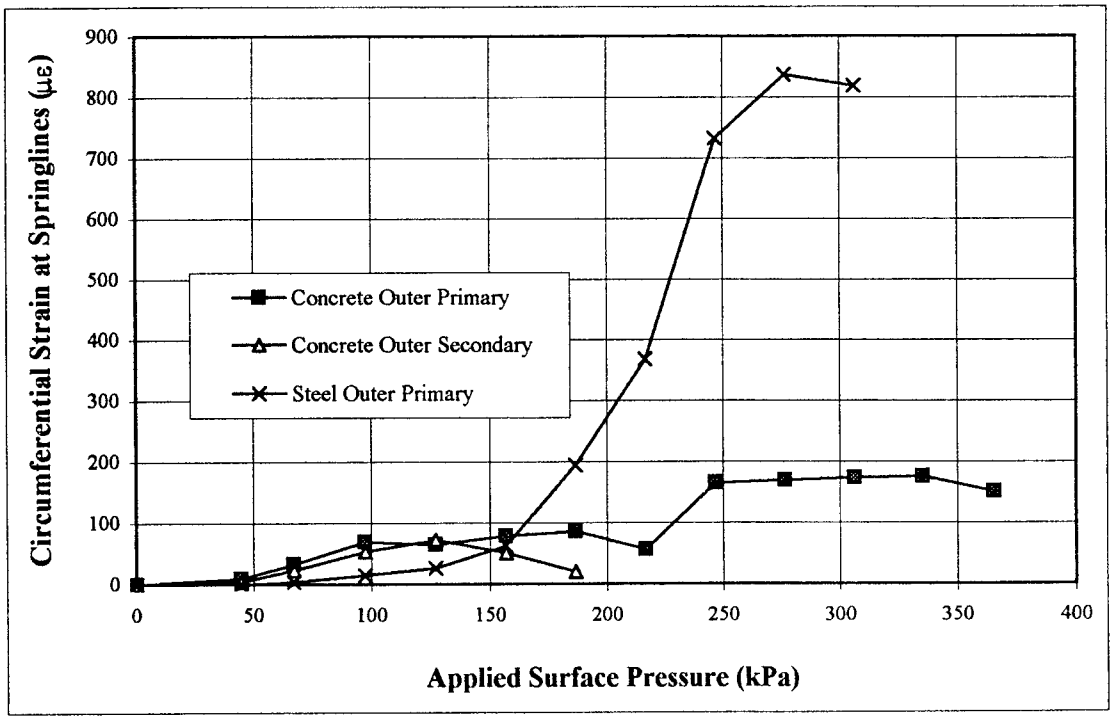

Figure 4.31b Cross-Sectional Strain at Left Springline of the 1520 mm Concrete Pipe for Test 4

Table 4.12 Cross-Sectional Strain at Springlines of the 1520 mm Concrete Pipe for Test 4.

Applied Surface Pressure	**Concrete Outer Primary**	**Concrete Outer Secondary**	**Steel Outer Primary**	**Concrete Inner Primary**	**Concrete Inner Secondary**	**Concrete Outer Primary**	**Concrete Outer Secondary**	**Steel Outer Primary**
(kPa)	Right	Right	Right	Right	Right	Left	Left	Left
0	0	0	0	0	0	0	0	0
44.7	6	7	-7	-16	-3	10	4	0
67.1	16	17	3	-42	-13	33	23	4
97.1	33	41	17	-98	-43	69	53	15
126.9	68	99	29	-277	-179	65	72	27
156.8	52	75	75	-545	-402	79	51	63
186.7	39	52	302	-717	-544	86	20	195
216.6	17	53	784	-1090	-623	56		368
246.8	56	60	1165	-1418	-922	165		733
276.5	101	59	1255	-1702	-1215	169		837
306.4	367	54	1247	-2011	-1542	173		819
335.3	416		1255	-2371	-1928	176		
365.2			1133	-3172	-3827	151		

Strains measured at the shoulder and haunch indicate no distress in these regions as shown in Figures 4.29 and 4.31. Strains at the crown and invert respond to surface loading in a similar fashion as Test 3. The compaction does not appear to affect these locations substantially. Compressive strains at the crown and invert were approximately the same magnitude as for Test 3. Springline strains increased rapidly and were at magnitudes that could be associated with local cracking, when the loading was about 50% of the surface pressure and the springline walls had crushed. Examination of Table 4.11 indicates that the steel cage provides an important reinforcement mechanism in the tension zone.

4.8.5 Measured Strains for Test 5 and Test 6

Strains measured for Test 5 and Test 6 are plotted in Figures 4.32 through 4.35. Examining tensile strains at the springline in Figure 4.34, we see that at the final depth of cover a maximum of the tensile strain is about 250 με. This would indicate possible cracking has occurred on the outside at the springline of Test 6. Since the springline compressive strains did not exceed 300 με in either pipe, as shown in Figures 4.32 and 4.34, the pipes are in no danger of collapse. A similar pattern is noted at the invert, Figures 4.33 and 4.35, where the tensile strains exceed 190 με for either pipe.

Longitudinal strains measured at the invert exceeded -400 με for Test 5, as shown in Figure 4.33. Tensile strains were of a similar magnitude, although tensile strains in concrete are difficult to quantify. As the standard installation procedure was followed, strains of this magnitude indicate that further study is warranted. All measured strains are given in the Appendix.

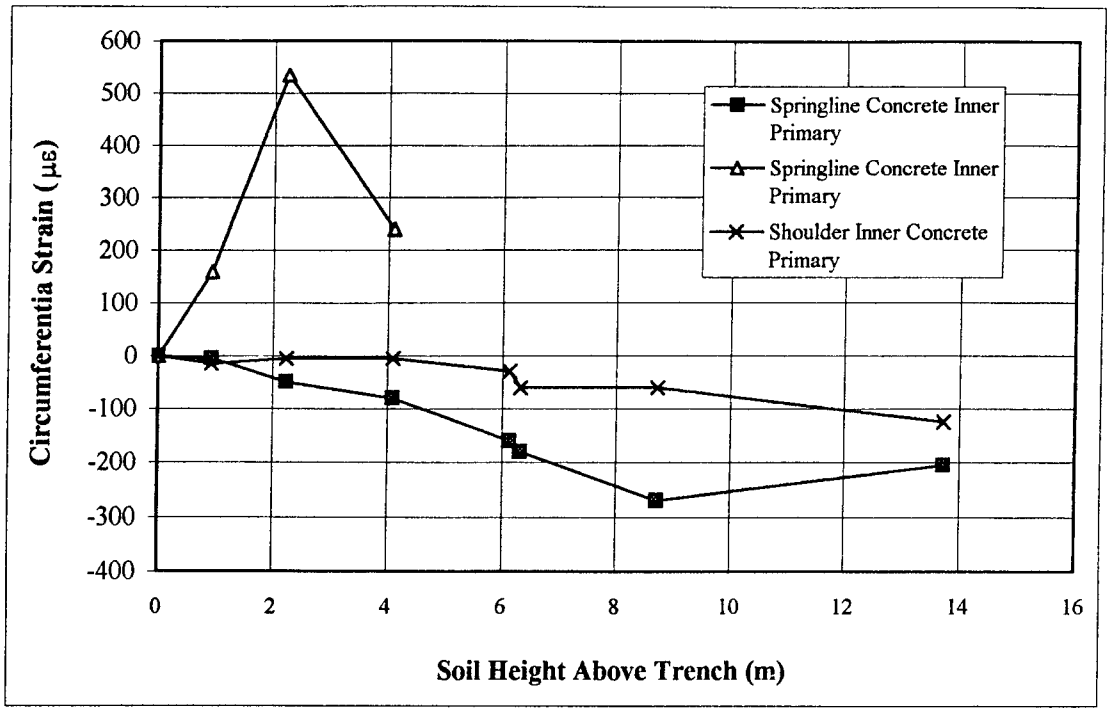

Figure 4.32 Cross-Sectional Strain at Springline and Shoulder of the 1520 mm Concrete Pipe for Test 5

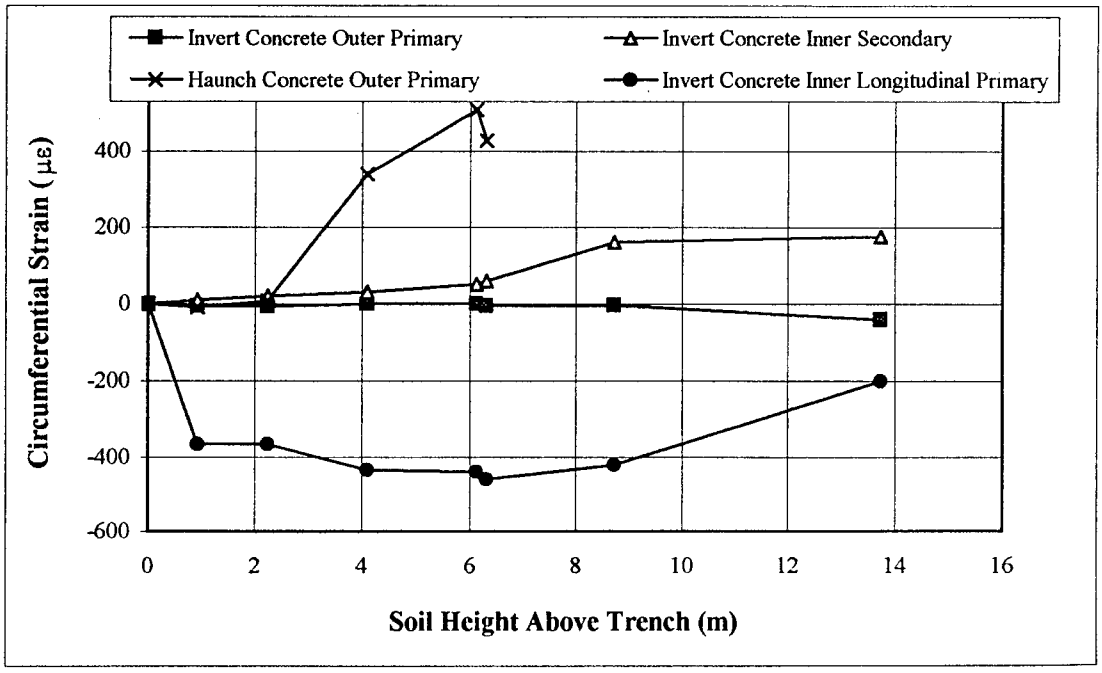

Figure 4.33 Cross-Sectional Strain at Haunch and Invert of the 1520 mm Concrete Pipe for Test 5

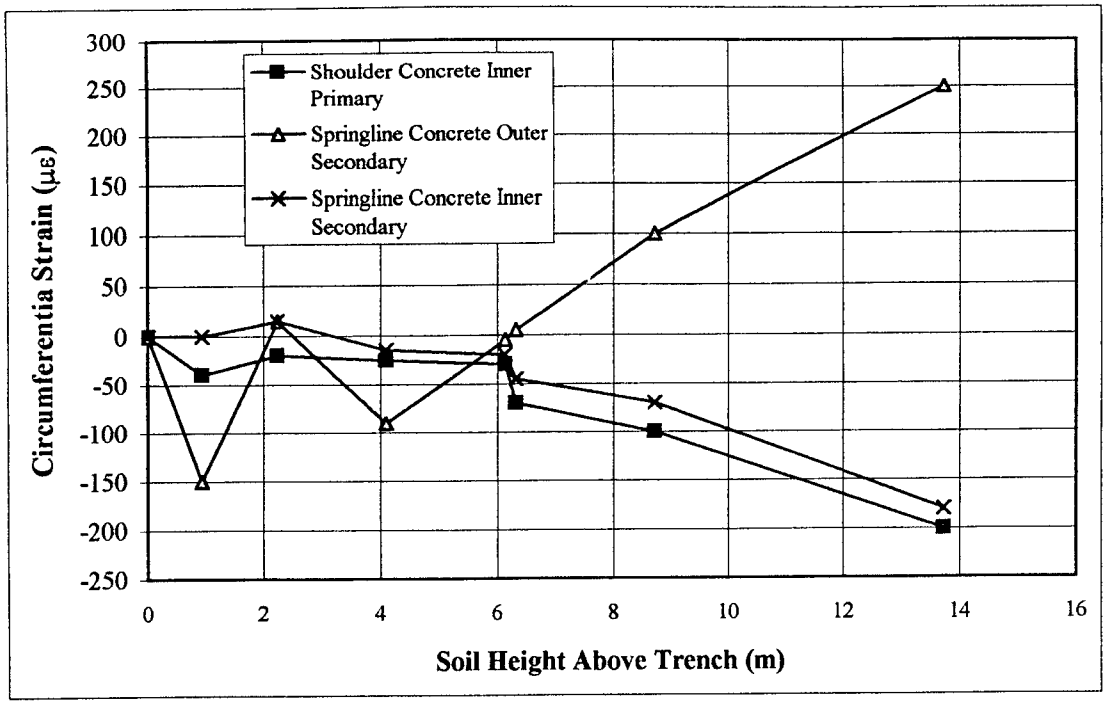

Figure 4.34 Cross-Sectional Strain at Springline and Shoulder of the 1520 mm Concrete Pipe for Test 6

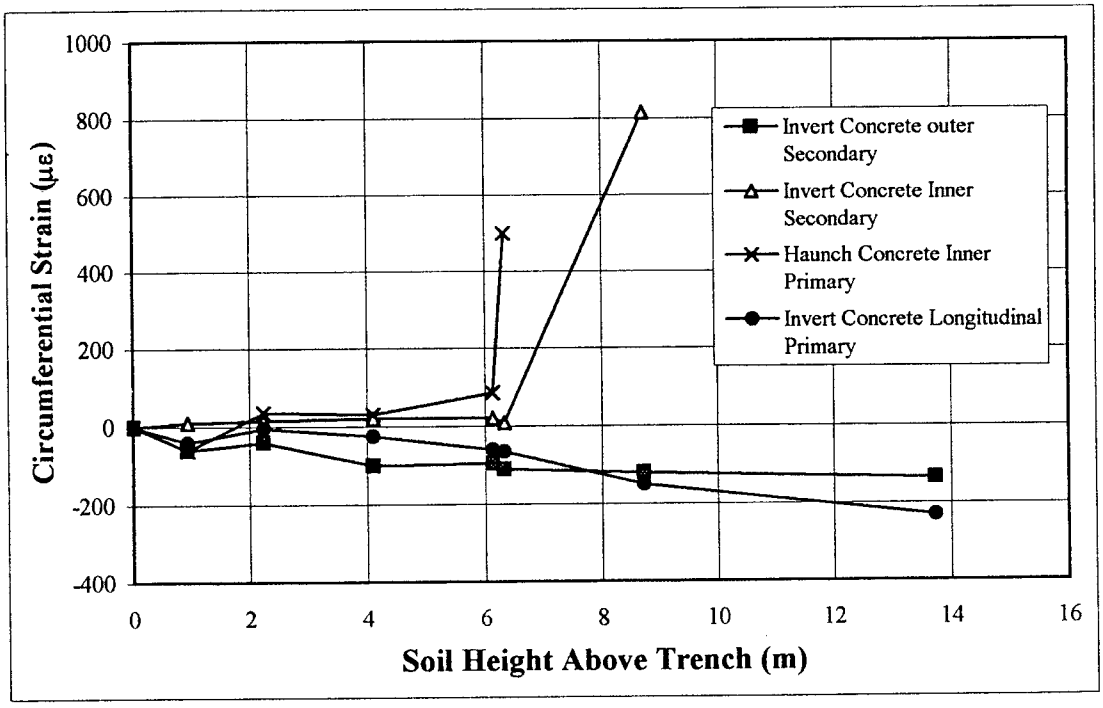

Figure 4.35 Cross-Sectional Strain at Haunch and Invert of the 1520 mm Concrete Pipe for Test 6

4.9 SUMMARY

The deformation response of the 610 mm(24 in.) pipe tested in Test 1 (Type 3) gave a maximum vertical deformation of 3.2 % at failure. A similar pipe in Test 2 (Type 1) gave a maximum vertical deformation of 4.1 % but did not collapse. Deformation response of the 1520 mm (60 in.) pipes were less. The maximum vertical deflection was 1.38 % in Test 3 (Type 1) whereas the maximum vertical deflection was 2.5 % when the pipe wall at the springlines crushed.

Soil pressure and strain values measured at the invert show no difference for the procedure for placing bedding utilized in Tests 1 and 2. It is concluded that since the sandy bedding material was compacted, except for a width, $D_o / 3$, after the pipe was placed, the procedure for placing a layer of sand in the bottom of the trench is similar to excavating a smaller trench, $D_o / 3$ wide, and filling with sand.

Pressures measured at the deep burial site, Test 5 and Test 6, do not show a hydrostatic response, which would indicate that the load cell apparatus approximates well the deep burial situation for these rigid pipes.

Change in the vertical diameter for all tests was approximately twice as large as the change in horizontal diameter. For Test 5 and Test 6, the overall change in diameter was less than 8 mm. Evidence of concrete wall cracking was observed in all pipe tests. This affected tensile strain reading in the concrete wall in the latter stages of loading or backfilling.

It was difficult to judge the damage to the springlines as load or backfill was applied since direct observations could not be made. However, from springline concrete outer strain measurements, it is noted that the springlines can be the critical regions of the pipe design. While cracking was observed at the crown concrete inner and invert concrete inner locations, strain

measurements at the springlines display magnitudes that would indicate cracking at springlines concrete outer for all pipes tested. All pipes removed from the loading frame showed evidence of springline wall cracking. The collapse of pipe in Test 1 (Type 3) and the springline wall crushing of the pipe in Test 3 (Type 3), both pipes placed with lower compaction, indicates the importance of proper backfilling procedures for rigid pipe.

CHAPTER 5

VERIFICATION OF SIDD METHOD

5.1 BACKGROUND

Wall thrust and moment were calculated from electric strain gage readings using Equations 4.5 and 4.6. The moduli of concrete were determined from concrete cylinder tests: 36 GPa (5.2E6 psi) for Tests 1, 2; 33.8 GPa (4.9E6 psi) for Tests 3, and 4; 31 GPa (4.5E6 psi) for Tests 5 and 6. The Poisson's ratio used in all calculations was 0.13. The steel modulus was taken as 200 Mpa (29E6 psi). The moment of inertia was calculated from the dimensions of the pipe wall.

In this chapter experimental values determined for thrust and moment are compared to values calculated by SIDD. The SIDD model used for this analysis is shown in Figure 5.1. Because the SIDD model assumes symmetry, the analysis is done on one half of the pipe where the crown boundary is approximated by a vertical roller, and the invert boundary is held fixed.

5.2 LOAD CELL VERIFICATION OF SIDD METHOD FOR 610 mm (24 in.) PIPE

For Test 1 and Test 2 the 610 mm (24 in.) pipes were designed with a wall thickness of 73 mm (2.875 in.). The pipes were reinforced at the center of the wall thickness with a single circular wire cage, which was fabricated by welding 5.1 mm (0.20 in.) diameter, smooth, steel wires. Longitudinal steel wires were spaced at 150 mm (6 in.) in the circumferential direction. Circumferential wires were spaced at 50 mm (2 in.) in the longitudinal direction.

The moments were calculated from the field data given in Figures 4.12 through 4.23. All

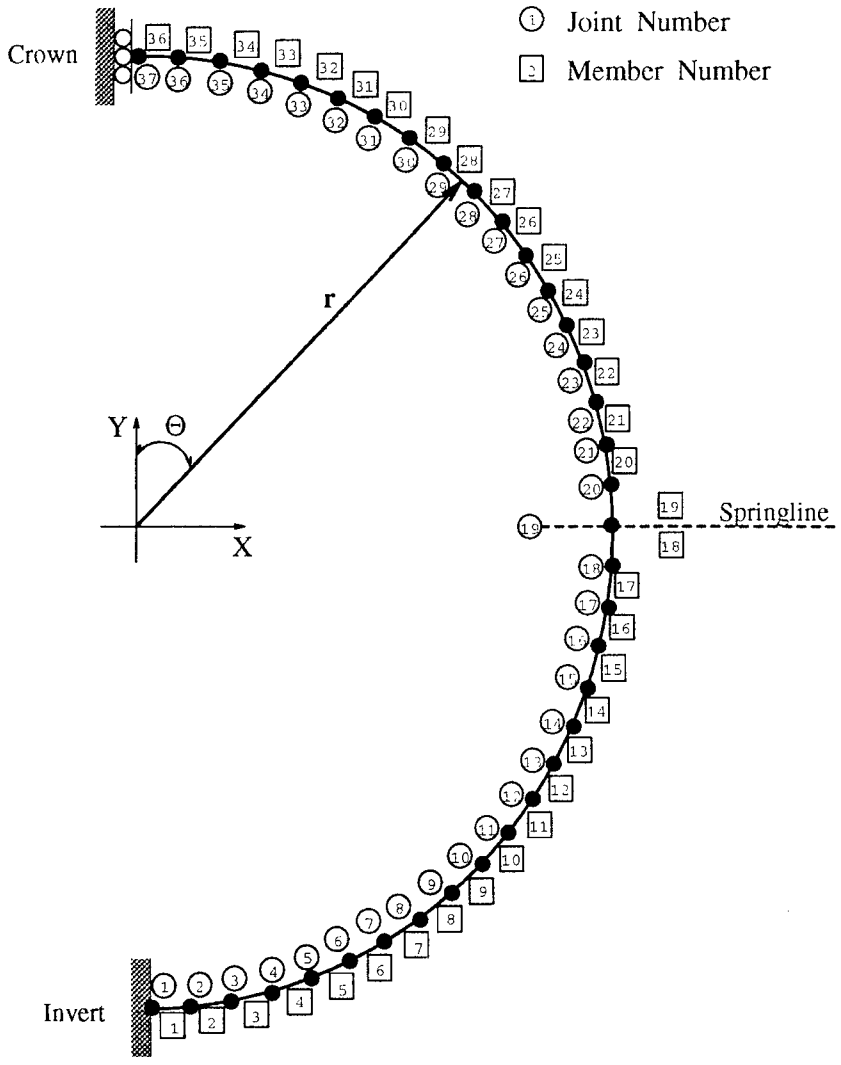

Figure 5.1 Frame Model Used for Computer Analysis of Pipe Sections in SIDD

moments and thrusts were plotted along the centerline of the pipe circumference starting from the crown in the clockwise direction for 360°.

In Figures 5.2 through 5.4, the comparison is made for a Type 3 installation which corresponded to Test 1 and a Type 1 installation which corresponded to Test 2. The comparisons with SIDD predicted moments are excellent for initial load steps of 65.5 kPa (9.5 psi) and 81.9 kPa (11.88 psi). The moment at the crown has a larger magnitude and is more concentrated than predicted by SIDD. For 137 kPa (19.8 psi) surface pressure in Test 1, longitudinal cracking was observed for the inner concrete surface at the crown and springline, which may have induced the sudden increase in the value of the moment as illustrated in Figure 5.4. Obviously, moments were calculated from strains measured at the location of sensors for the sections of the pipe wall indicated. After formation of cracks, an additional load was applied to determine the failure mode of the pipe. At the maximum applied load, the pipe in Test 1 deflected substantially; however, the reinforcing steel did not rupture, which was true for all pipes tested. The comparison with the SIDD prediction is not expected to be good after cracks form because SIDD accounts for crack formation in the concrete only when designing for reinforcement and not when service load forces are computed. Consequently, after the development of cracks, the moments and thrusts calculated by SIDD should not be relied on.

The agreement with SIDD is much better when the pipe is embedded in a well-compacted backfill, as shown in Figure 5.4 for Pipe 2. Despite the high load with a significant concrete crack pattern in the pipe, there is reasonable agreement between SIDD and the load cell tests. It is also interesting to note that SIDD predicted values which were bracketed by the Type 1 and Type 3 tests except for the high pressure. SIDD results were shown to be conservative for the Type 1 installation in the loading design range.

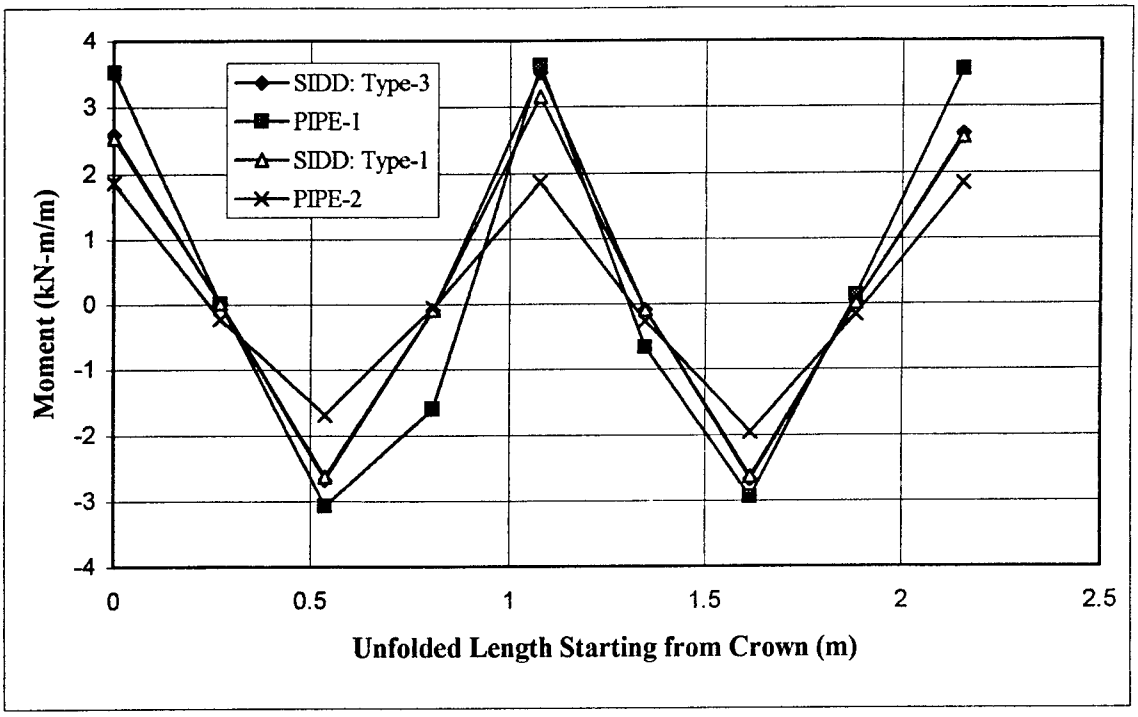

Figure 5.2 Comparison of Bending Moments in the 610 mm Concrete Pipe for Test 1 and Test 2 at Surface Pressures of 65.5 kPa and 71.0 kPa.

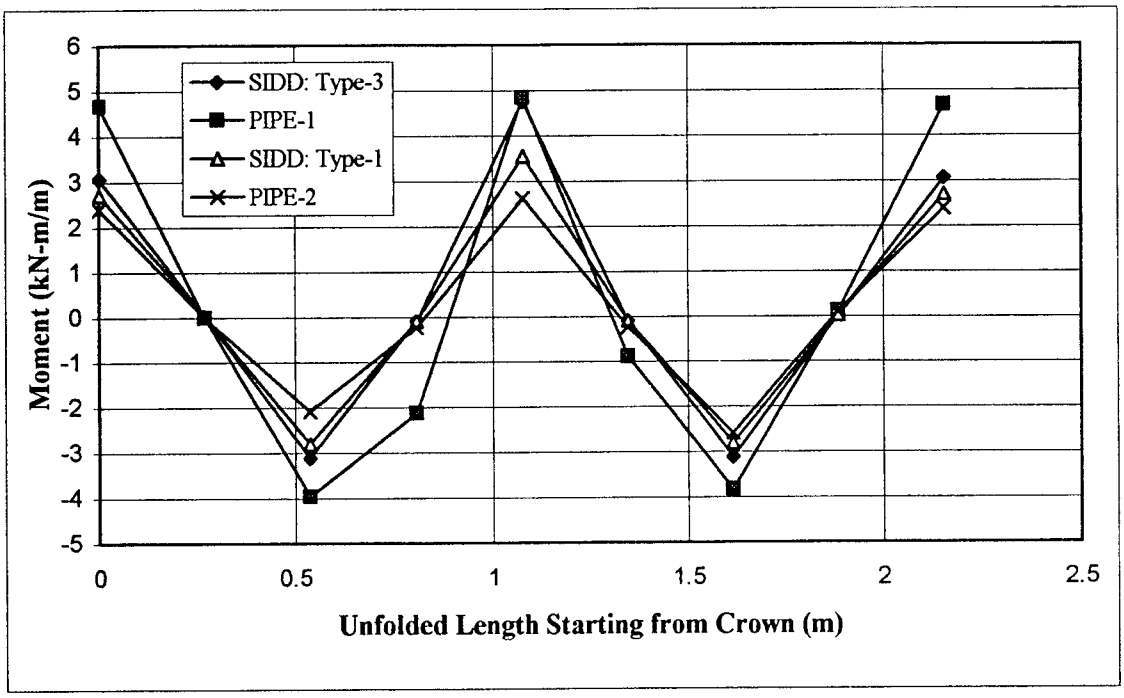

Figure 5.3 Comparison of Bending Moments in the 610 mm Concrete Pipe for Test 1 and Test 2 at Surface Pressures of 81.9 kPa.

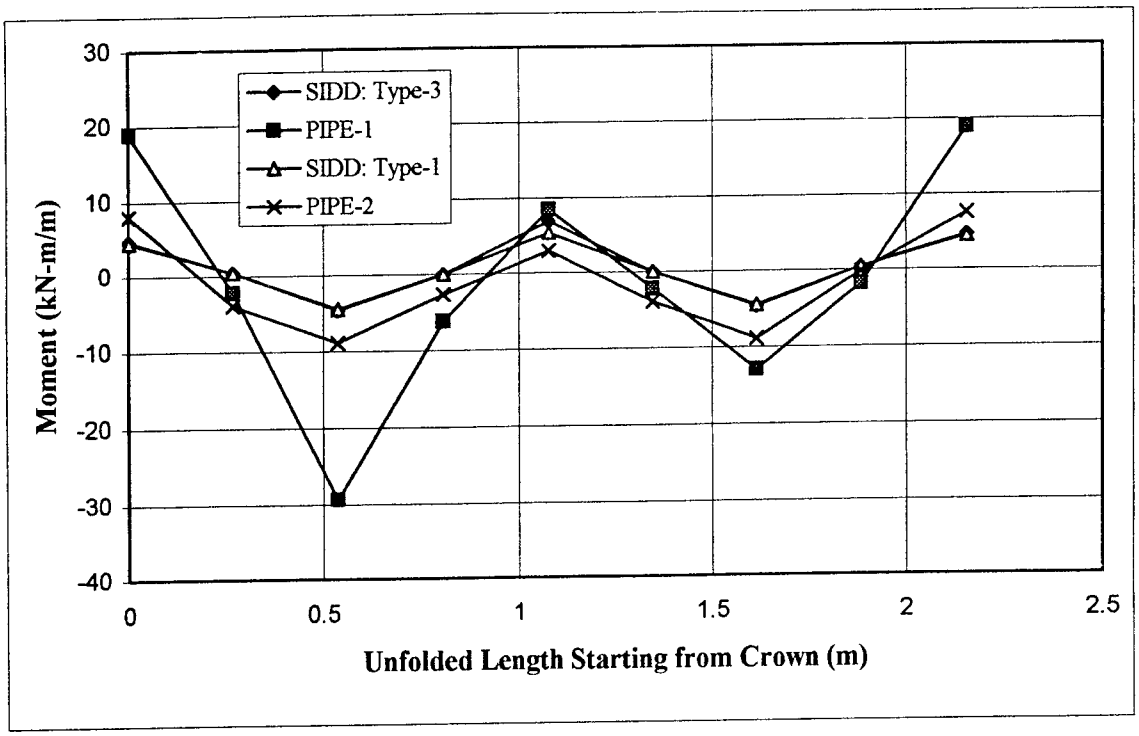

Figure 5.4 Comparison of Bending Moments in the 610 mm Concrete Pipe for Test 1 and Test 2 at Surface Pressure of 137 kPa.

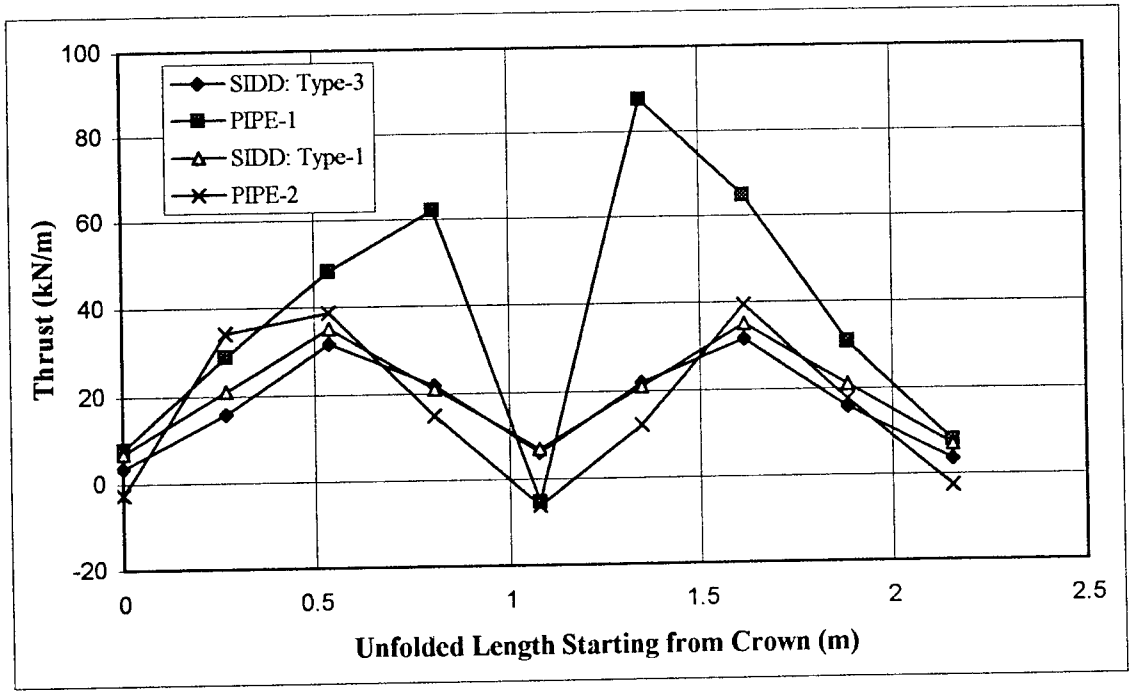

Figure 5.5 Comparison of Circumferential Thrust in the 610 mm Concrete Pipe for Test 1 and Test 2 at Surface Pressures of 65.5 kPa and 71.0 kPa.

Thrust forces in the concrete pipe, for Test 1 and Test 2, are shown in Figures 5.5 through 5.7. Except at the invert, thrust comparisons with SIDD are good at low surface pressures for the Pipe 2 (Type 1) installation, as shown in Figures 5.5 and 5.6. At 137 kPa (19.8 psi), Figure 5.7, SIDD no longer calculates reasonable values for thrust. There was significant crack formation at the invert and crown for this load, which was approximately equal to 7.0 m (23 ft) of fill.

In contrast to the Type 1 installation, the examination of Test 1 (Type 3), in Figures 5.4 to 5.7, reveals that the SIDD calculations are not comparable. Whereas the thrust values measured for the load cell tests are consistent with results reported in the literature by Roschke and Davis [10].

When the pipe in Test 1 was removed from the trench, cracks were found at the outer surface of the crown, invert, and springlines. The cracks that formed at the inner surface of the invert branched in to two directions. During production this location was damaged and repaired, which may have weakened the invert. Tensile stress during the latter loading stages resulted in severe cracking which caused pieces of concrete to break away. High strain values, as seen in Figures 4.12 to 4.17, were recorded on the inside of the invert and on the pipe surfaces not subject to cracking, during the final load steps. In contrast to the pipe in Test 1, the pipe in the well-compacted fill was essentially intact when removed from the trench with the pipe wall collapse confined to the springlines.

For this installation, there is some question as to accuracy of the boundary condition at the invert as shown in Figure 5.1. The moments, as shown in Figures 5.2 and 5.3, and the thrust for a Type 1 installation, as shown in Figures 5.5 and 5.6, could be improved at the crown and invert with a more realistic boundary condition.

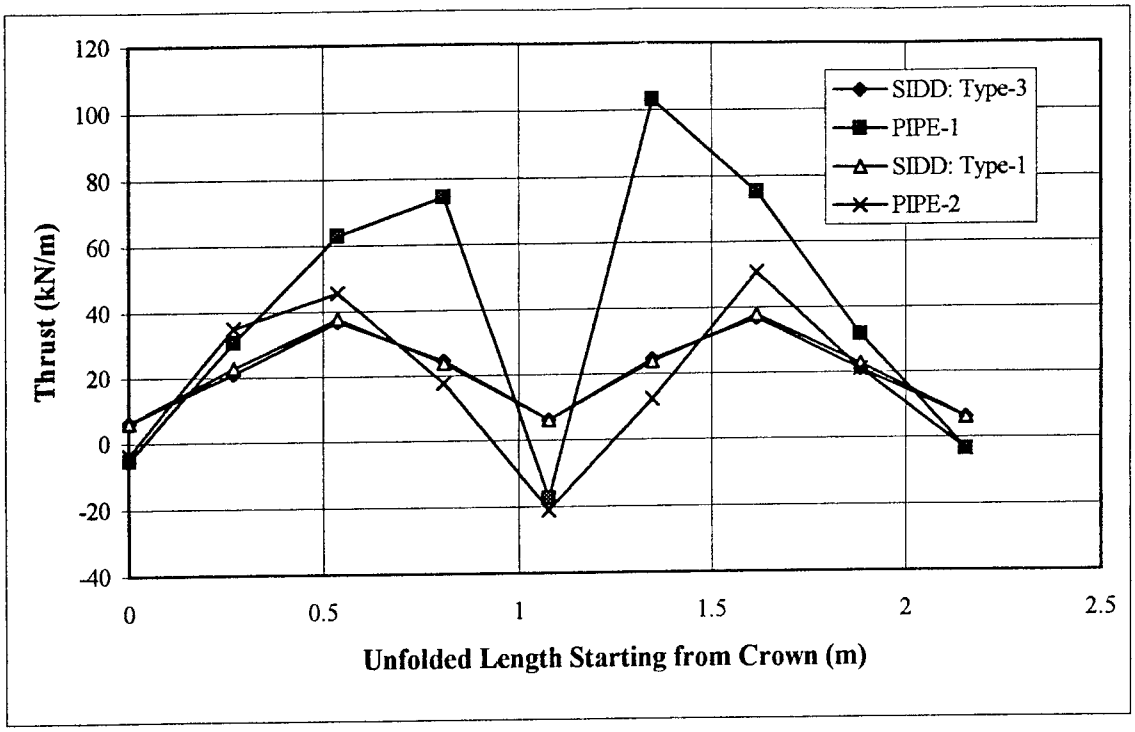

Figure 5.6 Comparison of Circumferential Thrust in the 610 mm Concrete Pipe for Test 1 and Test 2 at Surface Pressure of 81.9 kPa.

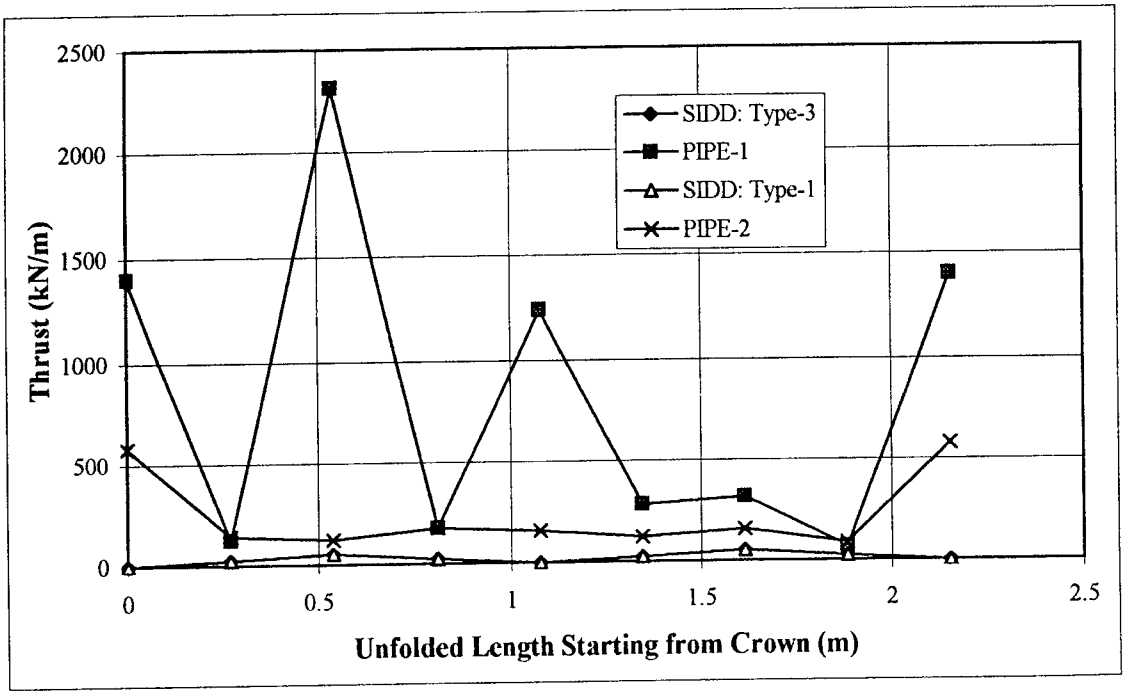

Figure 5.7 Comparison of Circumferential Thrust in the 610 mm Concrete Pipe for Test 1 and Test 2 at Surface Pressure of 137 kPa.

5.3 LOAD CELL VERIFICATION OF SIDD METHOD FOR 1520 mm (60 in.) PIPE

For Test 3 and Test 4 the 1520 mm (60 in.) pipes were designed with a wall thickness of 172 mm (6.75 in.). Circumferential wires in the cages were installed 32 mm (1.25 in.) from the inside and outside concrete surfaces. The cages were fabricated from wires spaced 50 mm (2 in.) in the longitudinal direction and 203 mm (8 in.) in the circumferential direction. For the inner steel cage, the circumferential steel wire was 7.8 mm (0.305 in.) in diameter and the longitudinal steel wire was 5.7 mm (0.225 in.) in diameter. Similarly, for the outside cage, the circumferential steel wire was 5.5 mm (0.215 in.) in diameter and the longitudinal steel wire was 5.1 mm (0.200 in.) in diameter.

Moments and thrusts were calculated from electric strain gage readings given in Figures 4.24 through 4.31. Data is also listed in Tables 4.11 and 4.12. Bending moments for Test 3 and Test 4 are presented in Figures 5.8 and 5.9. Bending moments and thrusts are further compared to results calculated from SIDD.

The bending moments are compared to SIDD design calculations in Figure 5.8. There is good agreement at the crown for Pipe 3 and springline for Pipe 4 with the SIDD design calculation. The SIDD design calculation is high for the Invert of Pipe 3. Experimental values are lower for the initial loading steps at the invert of Pipe 3 as the loose bedding layer compacts. The bending moment is shown in Figure 5.8 for the load step when crack formation was first noticed at the invert (119.7 kPa (17.4 psi)). At this load step the experimental moment increases noticeably but the values may be suspect. Strain readings are reliable for the crown and invert regions only before cracking is observed or noticed in the gage reading.

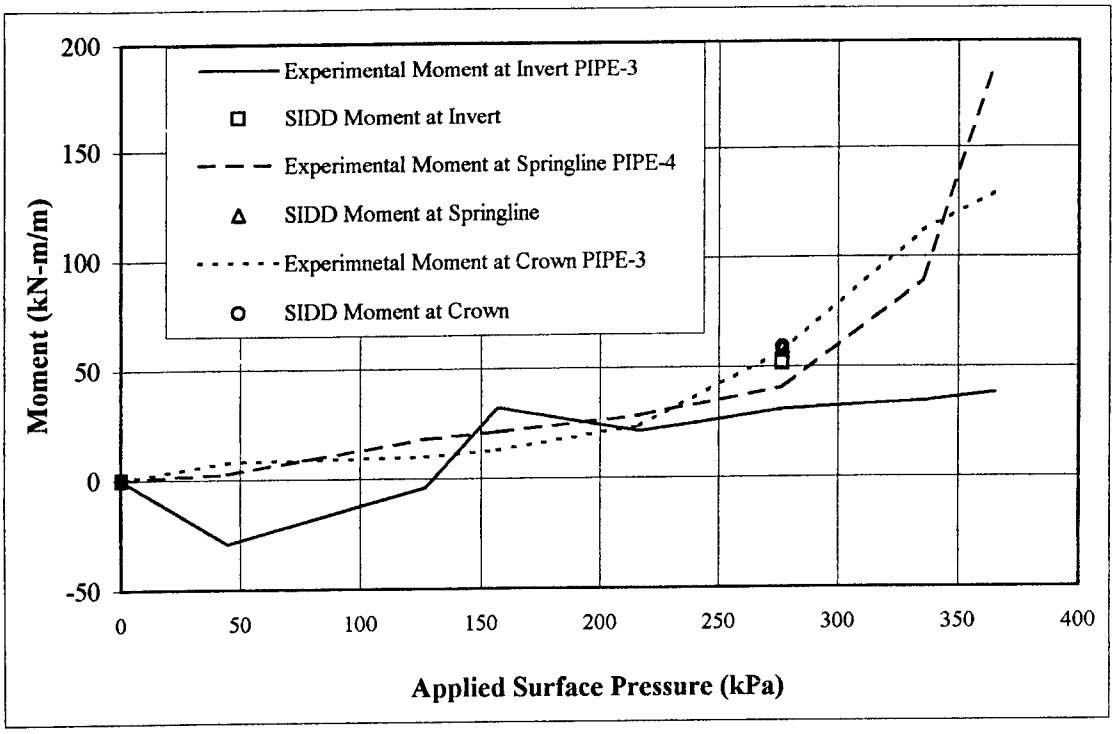

Figure 5.8 Comparison of Bending Moments at the Crown, Springline and Invert in the 1520 mm Concrete Pipe for Test 3 and Test 4

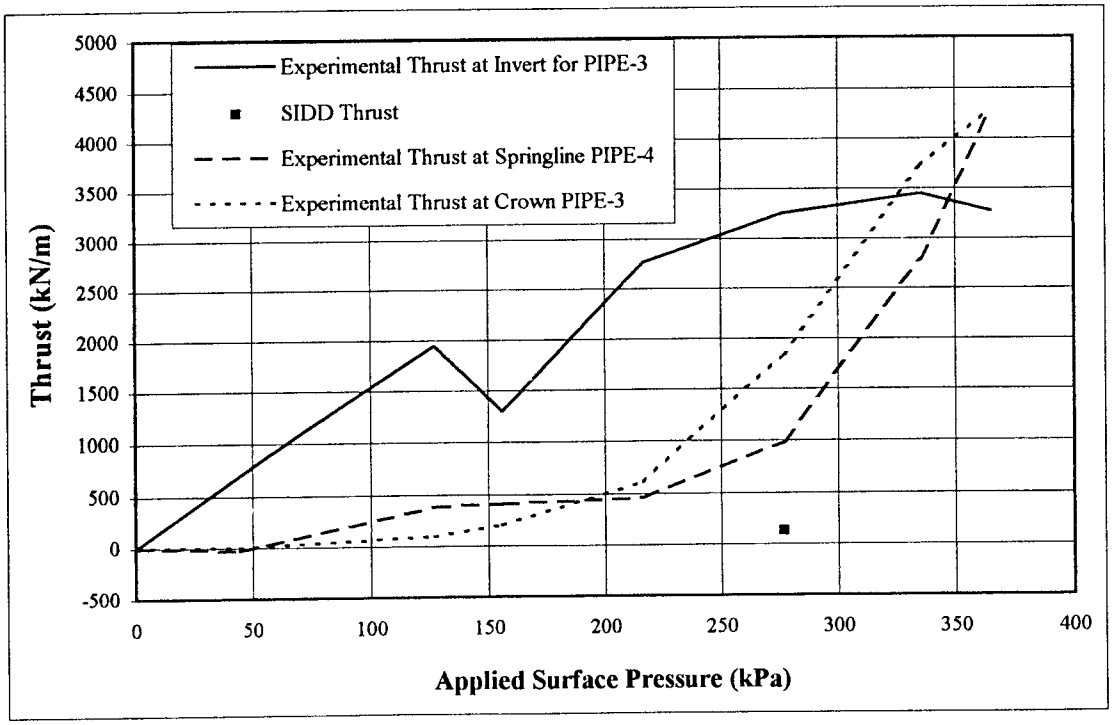

Figure 5.9 Comparison of Thrust at the Crown, Springline and Invert in the 1520mm Concrete Pipe for Test 3 and Test 4

Beyond the design depth experimental bending moment magnitudes become considerably larger with the increase of load.

There is no agreement between the thrust measurements versus values calculated by SIDD in the pipe wall. The experimental value for thrust at the invert of pipe 3 drops as the concrete fractures in the pipe wall at 119.7 kPa (17.4 psi). Since the magnitude of thrust is large, it will have a large influence on the failure mechanism. It is also interesting that in contrast to the bending moment comparison, the experimental values for thrust rise sharply before the design pressure is attained.

The comparison of field values of thrust to SIDD calculations corresponds to the previous discussion on the 610 mm (24 in.) pipes. However, the agreement with moment is somewhat better for Pipes 3 and 4 when compared to Pipes 1 and 2.

5.4 FIELD VERIFICATION OF SIDD AND CANDE METHODS FOR 1520 mm (60 in.) PIPE

For Test 5 and Test 6 the 1520 mm (60 in.) pipes were designed with a wall thickness of 172 mm (6.75 in.). Circumferential wires in the cages were installed 32 mm (1.25 in.) from the inside and outside concrete surfaces. The cages were fabricated from wires spaced 50 mm (2 in.) in the longitudinal direction and 203 mm (8 in.) in the circumferential direction. For the inner steel cage, the circumferential steel wire was 8.7 mm (0.341 in.) in diameter and the longitudinal steel wire was 5.9 mm (0.232 in.) in diameter. Similarly, for the outside cage, the circumferential steel wire was 6.7 mm (0.262 in.) in diameter and the longitudinal steel wire was 5.1 mm (0.200 in.) in diameter.

For Test 5 and Test 6 the 1520 mm (60 in.) pipes were designed by SIDD for a Type 1

standard installation. The steel areas that were required by SIDD are shown in Table 5.1.

Table 5.1 Initial SIDD Design for 1520 mm (60 in.) Field Installation

Location	Reinforcing Steel Cage	Design Area Required (mm/m)
Invert	Inside	1365
Springlines	Outside	542
Crown	Inside	876

To match the required areas a double circular cage configuration with and without mats was considered. After some discussion, it was decided to produce the pipe with full circular cages. This design presented a better analysis and instrumentation plan for the experimental studies since wiring to strain gages would be simplified.

After the preliminary design, several input values were adjusted to conform more closely to the actual installation. First, the design strength of concrete was adjusted closer to the actual value. Second, to account for deep burial the factor of live load (thrust) was reduced from 1.3 to 1.0, and the factor on internal pressure (thrust) was increased from 1.5 to 1.8. Third, since the pressure distribution on the pipe was not known, the flexure strength reduction factor was decreased to 0.95, and the limiting crack width factor was decreased to 0.9. The final design is shown in Table 5.2.

Table 5.2 Final SIDD Design Area with Steel Cage Areas Adopted in Test 3, Test 4 and Test 5, Test 6

Location of Steel Cage	SIDD Design (mm/m)	Load Cell Installation Test 3 and Test 4 (mm/m)	Field Installation Test 5 and Test 6 (mm/m)
Inside	1124	928	1160
Outside	536	461	684

CANDE is a finite element method for design and analysis of culverts of different materials and different shapes. Simulation can be performed more closely in CANDE than in SIDD with field data. SIDD response is elastic and there is no option to place the construction increment and different soil types at different levels of height of fill as usually occurs in field installations. In CANDE it is possible to make a user defined mesh and also to place construction increments and soil properties as they occur in the field. The comparison of results is of particular value for the vertical and horizontal deflection and the pressure distribution around the pipe perimeter.

Figure 5.10 and 5.11 compare the theoretical calculations for deflection with measured values. Examining the vertical deflections plotted in Figure 5.10, the comparison experimental to calculated deflections is good. The increase in vertical diameter at 8.72 m (28.6 ft) of backfill may have resulted from a hairline crack observed in the right shoulder region at this measurement. The final vertical deflections are substantially larger than those calculated by CANDE or SIDD where SIDD gives a value of final deflection that is 57% of the average measured value at 13.7 m (45 ft) of backfill.

In contrast to the expected deformation from CANDE and SIDD, the horizontal diameter shortened until the depth of 6.13 m (20.1 ft). With crack initiation in the inner wall of the

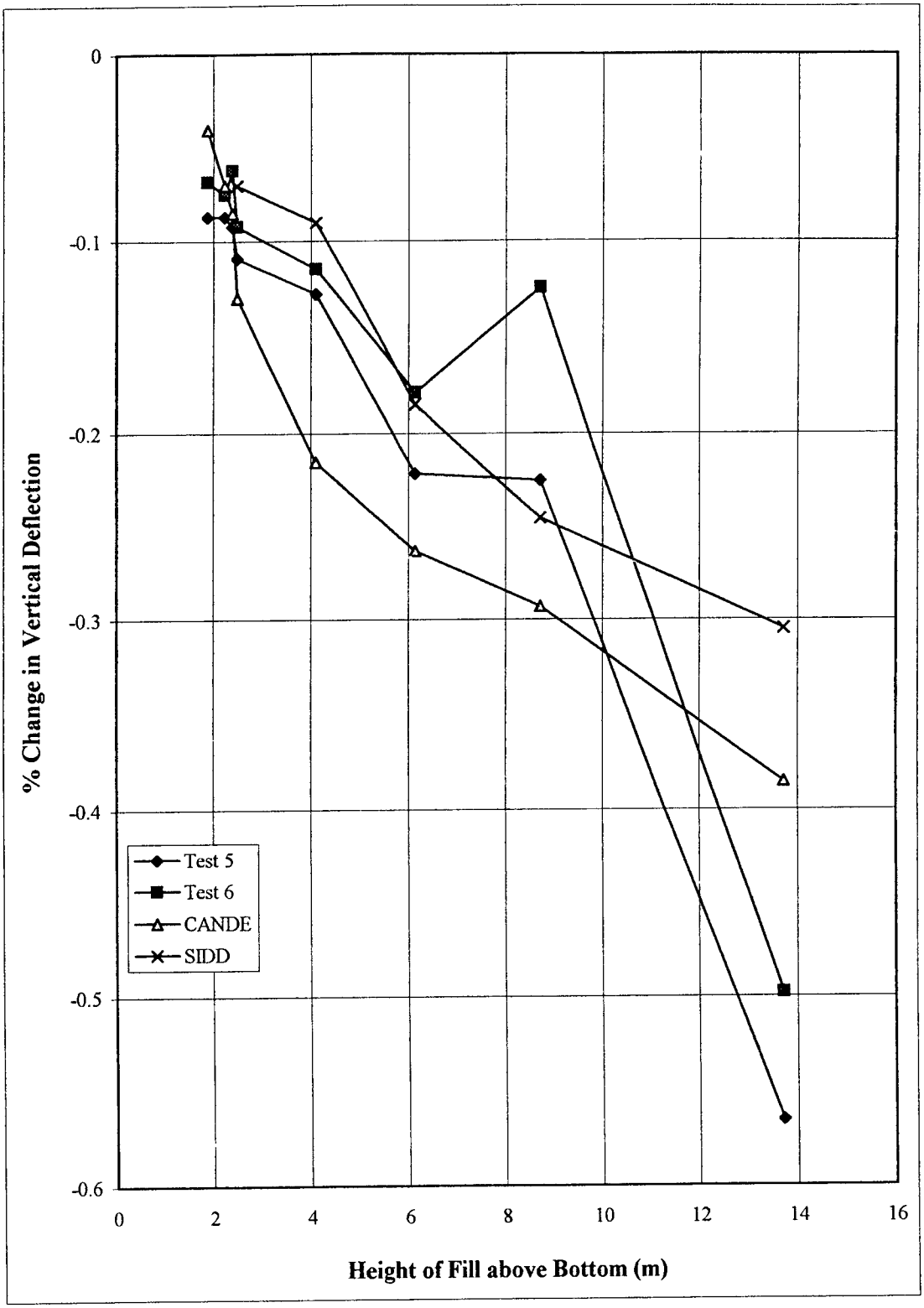

Figure 5.10 Comparison of Vertical Deflection with CANDE, SIDD and Field Data for Test 5 and Test 6

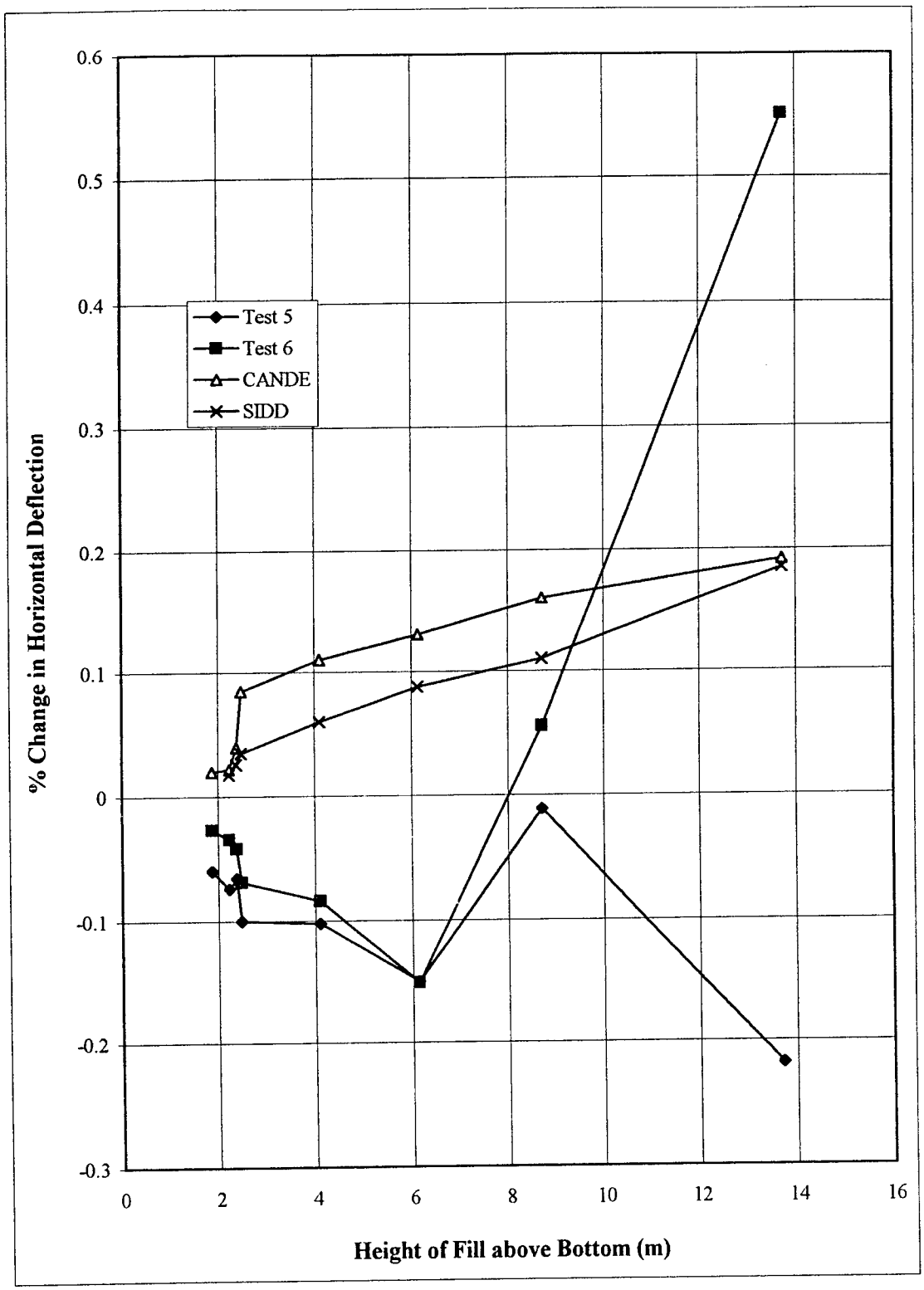

Figure 5.11 Comparison of Horizontal Deflection with CANDE, SIDD and Field Data for Test 5 and Test 6

shoulder, both horizontal diameters increased. The horizontal diameter of Test 6 continued to increase while that of Test 5 shortened. An explanation for the different pipe responses is that possibly the pipe deforms in reaction to the concrete crack pattern. Horizontal deflection was approximately the same magnitude as the vertical deflection.

Experimental pressures measured at the crown, springlines, and invert are compared to theoretical values in Figures 5.12 through 5.14. The pressure at the crown (Figure 5.12) compares well, field measurements, SIDD, and CANDE all give about the same pressures. The average pressure at the crown of the pipes for 13.5 m (44.3 ft) height of soil above bottom was 322 kPa (46.7 psi) in field measurements and was found for CANDE and SIDD to be 256 kPa (37.1 psi) and 300 kPa (43.5 psi), respectively.

The pressures at the springlines are significantly less than the CANDE and SIDD design pressures. The same trend continues for the invert. SIDD and CANDE design pressures always exceeded the geostatic pressures as shown in Table 5.3.

Table 5.3 Comparison of Pressure Measurements with Pressure Calculated at the Invert for Test 5 and Test 6

Geostatic (kPa)	SIDD (kPa)	CANDE (kPa)	Test 5 (kPa)	Test 6 (kPa)
258	354	307	144	73

The pressure on these pipes in not hydrostatic as measurements at the springlines were about 30% of geostatic pressure and measurement at the invert was about 60% of geostatic pressure.

Figures 5.15 through 5.18 show a comparison of experimental thrust and moment with

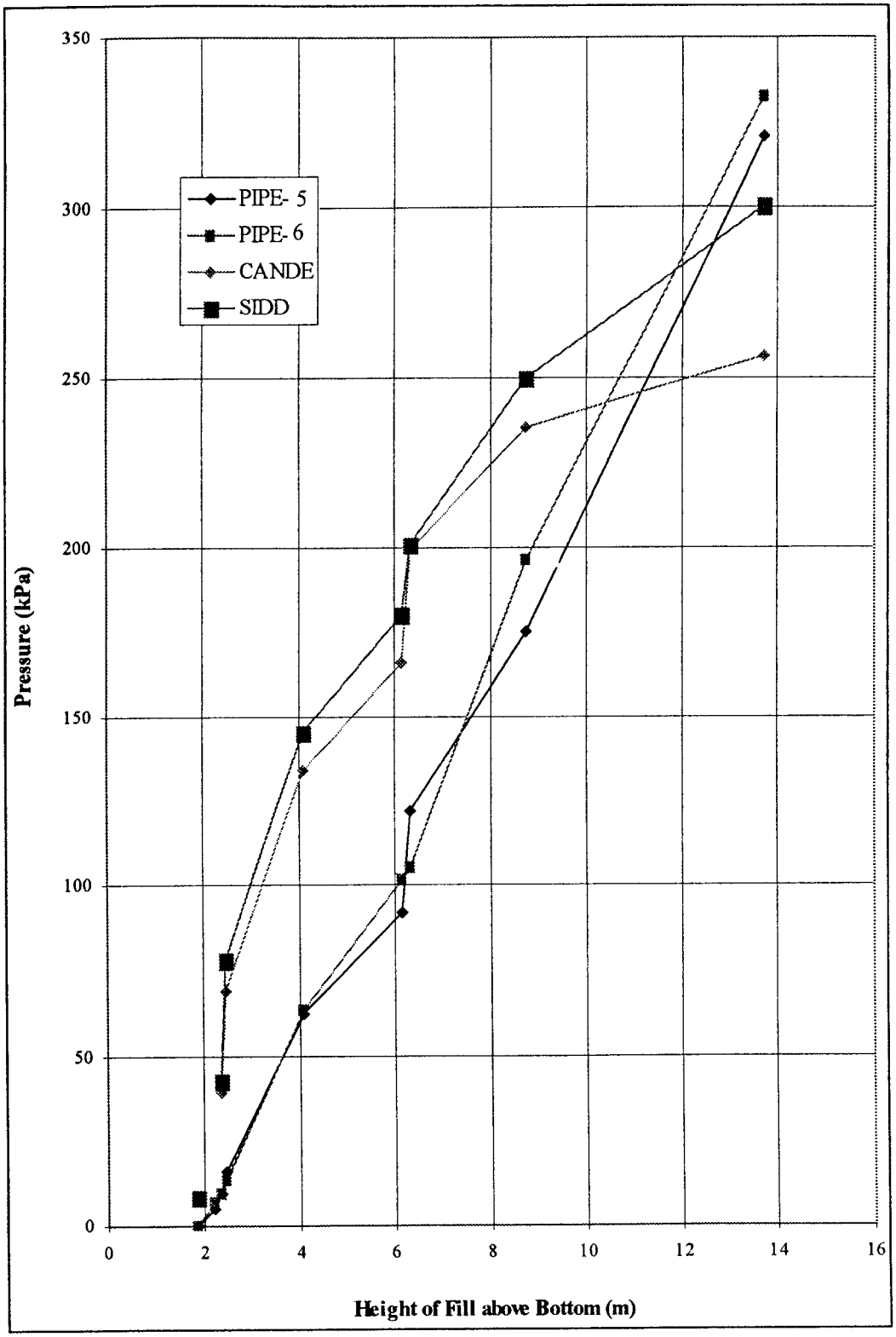

Figure 5.12 Comparison of Crown Pressure with CANDE, SIDD and Field Data for Test 5 and Test 6

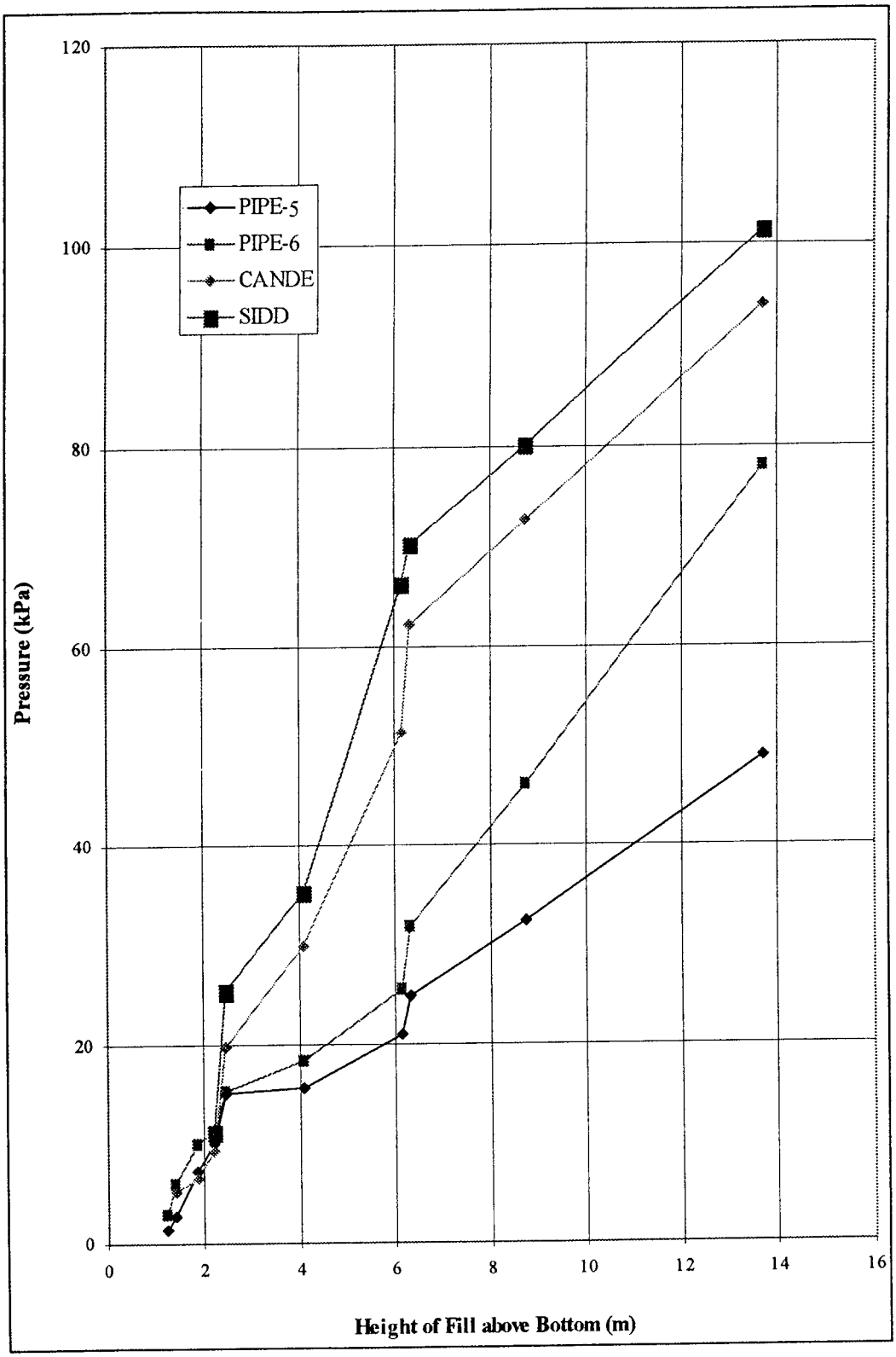

Figure 5.13 Comparison of Springline Pressure with CANDE, SIDD and Field Data for Test 5 and Test 6

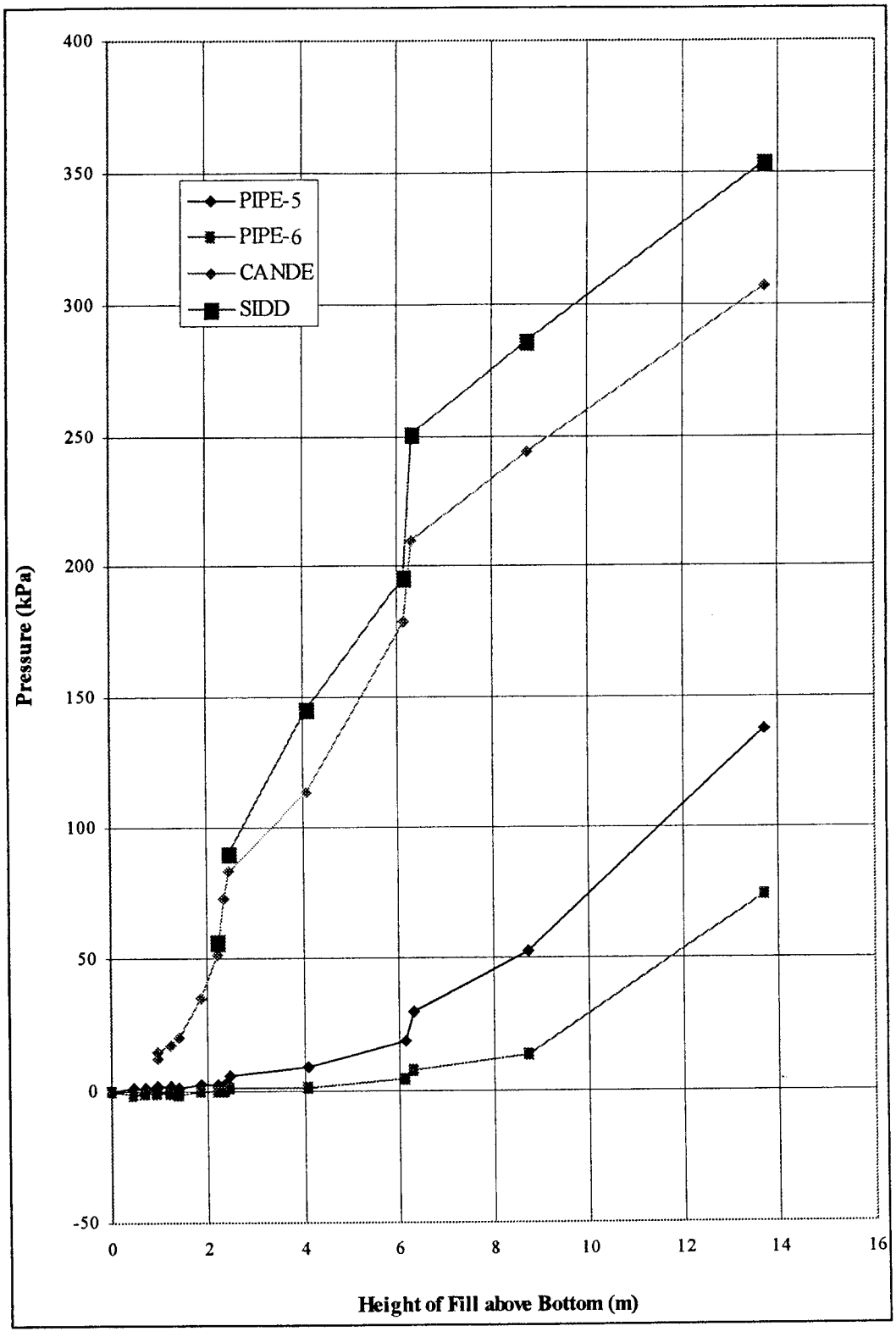

Figure 5.14 Comparison of Invert Pressure with CANDE, SIDD and Field Data for Test 5 and Test 6

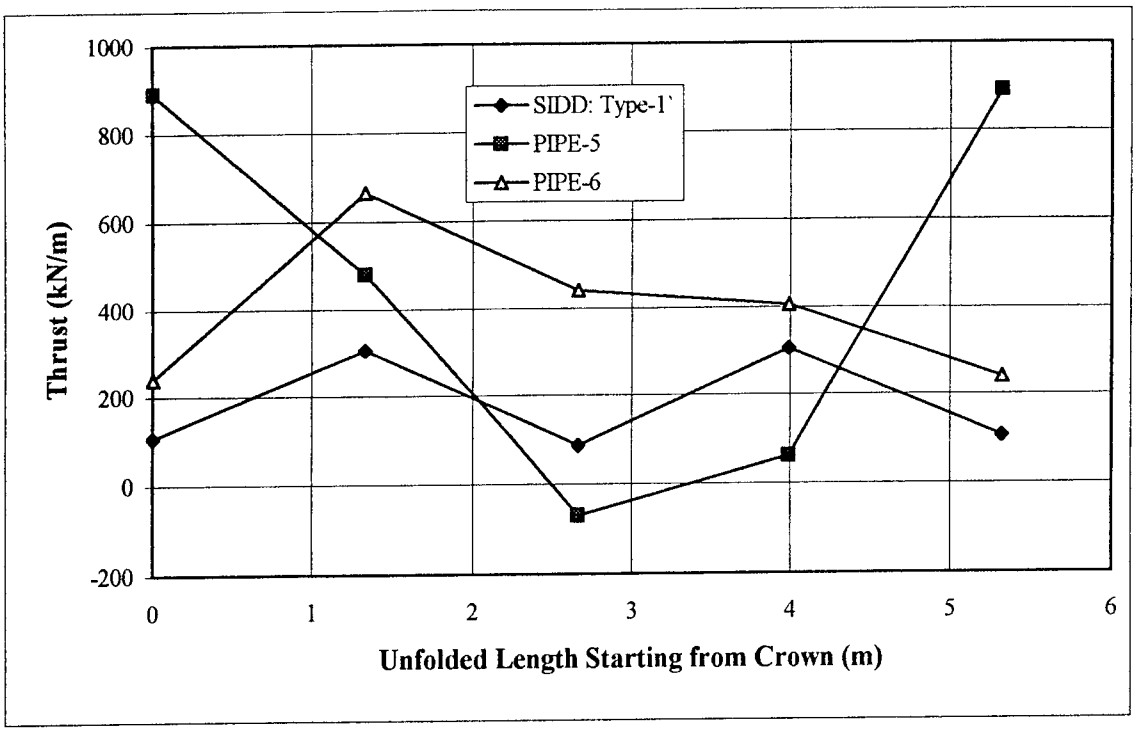

Figure 5. 15 Comparison of Field Data for Circumferential Thrust with SIDD Calculations for 6.3 m of Backfill Above the Trench for Test 5 and Test 6

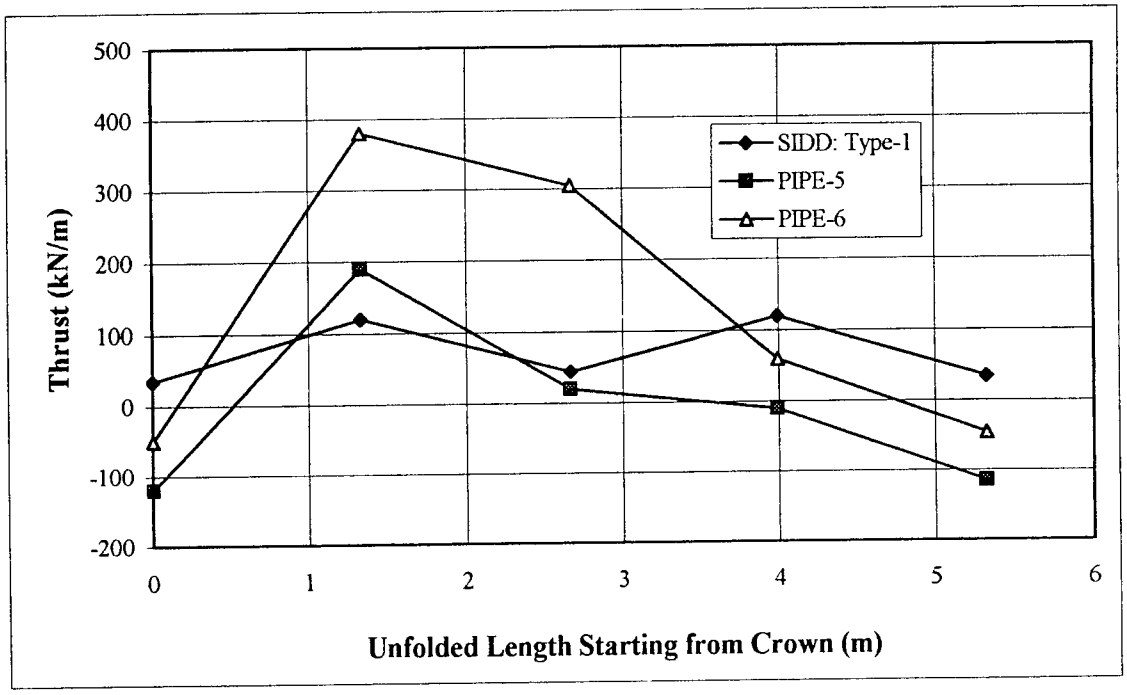

Figure 5. 16 Comparison of Field Data for Circumferential Thrust with SIDD Calculations for 13.7 m of Backfill Above the Trench Bottom for Test 5 and Test 6.

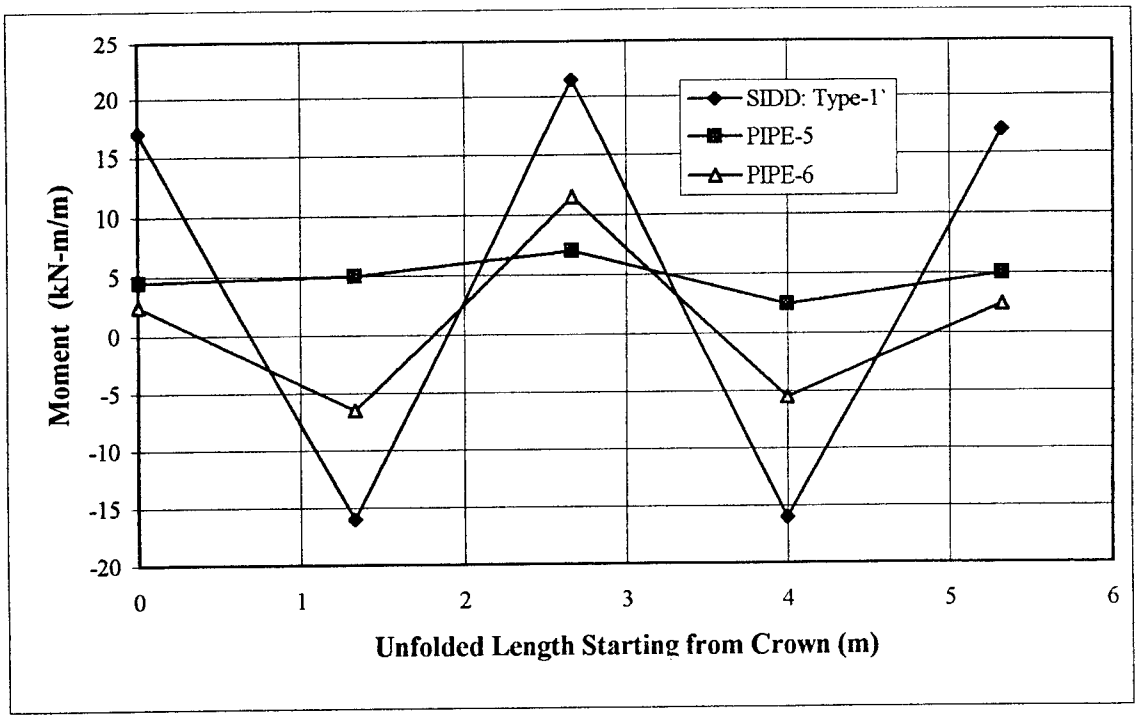

Figure 5.17 Comparison of Field Data for Bending Moment with SIDD Calculations for 6.3 m of Backfill Above the Trench for Test 5 and Test 6

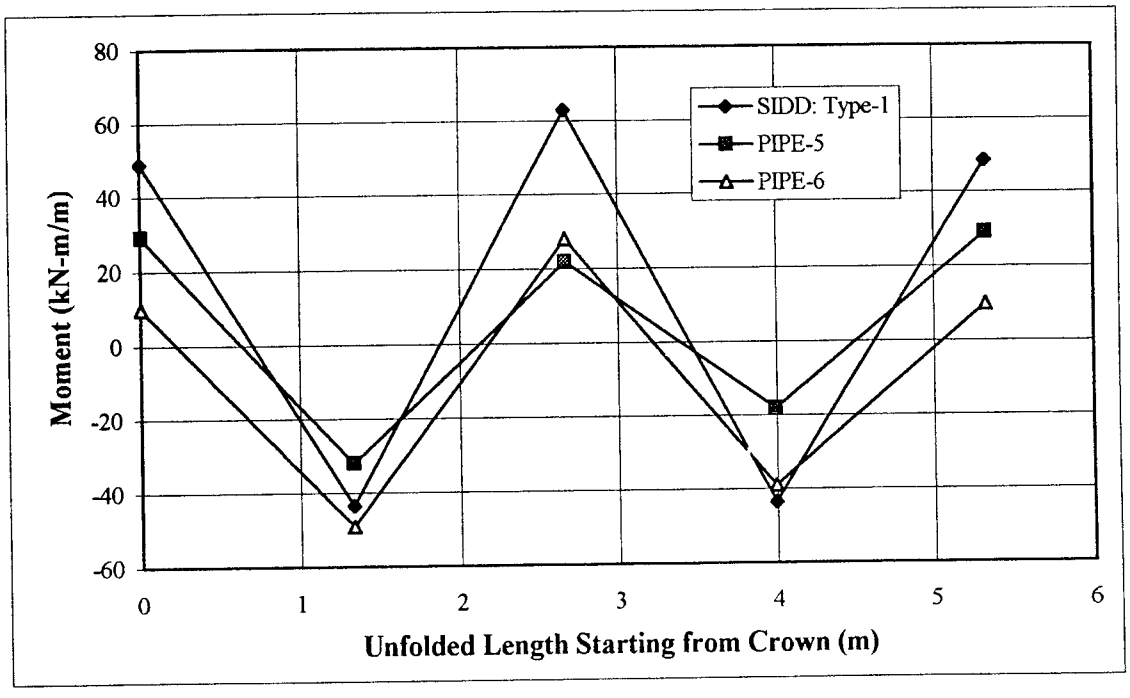

Figure 5.18 Comparison of Field Data for Bending Moment with SIDD Calculations for 13.7 m of Backfill Above the Trench Bottom for Test 5 and Test 6.

SIDD calculated results at 6.3 m (20.7 ft) and 13.7 m (45 ft) backfill steps. Thrust and moment were calculated by taking a least square fit through the profile strains. Stress used in force and moment calculations were obtained as previously with Equations 4.6 and 4.7 and the laboratory determined moduli.

Examining the pipes when backfill was at 6.3 m (20.7 ft) in Figure 5.15, the average of the thrust values at the springlines is approximately equal to the overburden force. However, the thrust calculated in neither pipe was symmetric. The large average thrust in the horizontal direction would be consistent with the decrease in horizontal deflections of Test 5 and Test 6 at this load step.

At a backfill load corresponding to 13.7 m (45 ft) of fill, as shown in Figure 5.16, thrust values again approximated equilibrium at the springlines. Thrust in the springline was 120 kN/m (0.69 kip/in.) in SIDD and 111 kN/m (0.63 kip/in.) in CANDE. However, the average field thrust was measured at 92.5 kN/m (0.53 kip/in.) in Test 5 and 220 kN/m (1.26 kip/in.) in Test 6. The low values of horizontal thrust at invert and crown is again consistent with deformation for Test 6. The thrust values found in the invert for 13.7 m (45 ft) of fill were 45 kN/m (0.26 kip/in.) and 52 kN/m (0.30 kip/in.) in SIDD and CANDE calculations, respectively. The thrust at the invert for Test 5 was 20 kN/m 0.11 kip/in.) and that in Test 6 was 300 kN/m (1.71 kip/in.).

Measured moments were conservative in comparison to SIDD predicted moments at 6.3 m (20.7 ft) as shown in Figures 5.17 and 5.18. SIDD predictions were a good fit to experimental data at 6.3 m (20.7 ft) and a very good fit at 13.7 m (45 ft) of fill. The additional design capacity may offset the larger measured thrusts. At the springlines, for 13.7 m (45 ft) of fill, moments in SIDD and CANDE were 45 kN-m/m (10.1 kip-in./in.) and 31.5 kN-m/m (7.1 kip-in./in), respectively. The average field moment was calculated to be 25.5 kN-m/m (5.7 kip-in./in.) and

44 kN-m/m (9.9 kip-in./in.) in Test 5 and Test 6, respectively. The difference between predicted and measured moments is consistent with the differences between the predicted and measured soil pressures at the pipe invert: the lower invert pressures resulting in lower springline moments. In examining the calculations at the crown and invert, substantial differences are apparent. However, SIDD calculations are conservative.

The comparison of data illustrates the difficulty of simulating field conditions in a computer model. The variation of thrust and moment in SIDD and CANDE were approximately linear with respect to fill height. However, both programs provide reasonable values for moment. The field simulation is more easily accomplished in CANDE, but the advantage of using CANDE was not apparent when comparing to field data.

5.5 SUMMARY

Comparison of the four load cell tests on two different diameter pipes and two pipes instrumented in the field shows a number of similarities for rigid pipe. Displacements, before cracks appear in the pipe wall, are so infinitesimal that an LVDT system must be employed to obtain reasonable results. Deflection and pressure are influenced by crack patterns in the concrete. This is especially apparent in the field studies. Pressure distribution in deep burial is not hydrostatic, but compares favorably to the load cell test. Bedding the pipe in uncompacted fill appears to greatly reduce the invert pressure in the field and, in the initial load steps, when tested at the load cell. This change in pressure was not adequately accounted for in either computer model. The uncompacted sandy trench with $D_o/3$ uncompacted appeared to give similar response to SIDD. SIDD is based on an assumption that the specified loosely compacted soil under the invert for $D_o/3$ may actually end up at 85% of the standard proctor density.

Computer models adequately predict the design moment for both the load cell and the field tests. Before cracking, and for well compacted fill, moments predicted by CANDE and SIDD corresponded closely to test results. Thrusts agreed to the field results only for low applied pressures. Both pipes tested under Type 3 installation failed at the springlines when the design loads had been exceeded and subsequent to significant cracking.

CHAPTER 6

CONCLUSIONS AND RECOMMENDATIONS

6.1 CONCLUSIONS

The mode of failure of a reinforced concrete pipe varies with backfill conditions. Interpretation of the failure mode under various backfill conditions will help engineers design with more confidence to guard against such failure modes. This report contains six comparisons of test data with the SIDD computer program. Four comparisons are made with results from load cell tests; two SIDD backfill types were simulated and two pipe diameters were tested. A field comparison was also made on State Route 7 in Meigs County. Two pipes were field instrumented and results recorded for a fill height of 13.7 m (45 ft). The pipe performance was monitored in terms of diameter deflection, pipe/soil contact pressure, strains in the reinforcing cages, and strains at the concrete surface. Two cross sections were instrumented in each pipe. Readings were taken during test loading and construction loading periods. For the field installation, deflection of the diameter and pipe/soil pressures continued to be monitored for six months after the final fill was placed.

Based on load cell Tests 1 and 2, and predicted results from SIDD, the performance of two 610 mm (24 in.) was examined. The pipes in both the Type 1 installation and Type 3 installation performed according to design. Design loads were about 150 kPa (22 psi) for 610 mm (24 in.) pipe and 220 kPa (32 psi) for the 1520-mm pipe. Before formation of cracks, moments were well correlated by SIDD results. After formation of cracks in the concrete pipe, moments were not comparable to SIDD results. Thrusts, on the other hand, were consistent with SIDD capabilities only for initial applied pressures (below design). Cracks formed in the

locations that experienced the maximum moments, which were predicted by SIDD. Substantial loading capacity was remained in the pipes when concrete cracking was observed. Pipe failure occurred at approximately twice the load of initial cracking. For the Type 3 installation, tensile stress exceeded the design during the latter loading stages and resulted in excessive cracking and pieces of concrete breaking away. High strain values were recorded on the inside at the invert and other locations not subject to cracking during the final load steps.

For Test 3 and 4, the 1520 mm (60 in.) concrete pipes, the loading procedure was similar to that used in Tests 1 and 2, where 610 mm (24 in.) pipes were tested. However, to prevent soil failure, a larger loading platform was fabricated.

SIDD calculations were in good agreement with experimental measurements when compared to loading before cracks appeared. About 50% of the load capacity of the pipe remained when concrete wall cracks were first observed. Furthermore, at an applied pressure corresponding to the design depth of fill (12 m), the agreement with the moment was excellent. Invert contact pressures measured in the study were substantially larger than crown contact pressures. Pipes tested for Type 1 and Type 3 loading performed well under applied pressure. This study again shows the importance of backfill construction during the installation of rigid pipe designed in accordance with the SIDD methodology.

For Tests 5 and 6 the 1520 mm (60 in.) concrete pipes performed according to design. The change in diameter was less than 9 mm (0.35 in.). Evidence of concrete cracking was observed which affected pipe deflection in the latter stages of backfill. Pressures matched those assumed in SIDD calculations for the crown and springlines. There was a large difference at the invert with experimental measurements lower than the SIDD assumption which may require more correlation with field studies. From consideration of vertical forces, it can be concluded

that a properly installed rigid pipe probably supports most of the overburden on its haunches.

Profile strains showed a nonlinear response to overburden load. SIDD calculations for the moment were conservative at the initial stage of backfill. The agreement was better in comparison to field measured values at the conclusion of backfilling. SIDD moments are conservative in comparison to the measured moments. This is consistent with the fact that the assumed invert pressure was less than that measured.

6.2 RECOMMENDATIONS

The following recommendations are made regarding the use of SIDD design of concrete pipe installations:

- An uncompacted bedding layer is recommended when rigid pipe is placed over bedrock. When this is done, the invert soil pressure matches the assumed SIDD distribution.
- One possible method of applying bedding is to place it uniformly in the trench and compact all except the middle $D_0/3$. No difference in pipe performance was noted in the load cell when the bedding layer was spread over the trench bottom as contrasted with excavating a bedding region in the trench, as long as the compaction requirement was observed.
- The SIDD invert pressure distribution should be further refined with more field data.
- The SIDD Type 1 backfill gives additional load carrying capacity to rigid pipes placed in deep fills or subjected to large loads.
- As longitudinal stresses were found to be significant only in the field tests, a load cell investigation should be devised to examine this phenomenon.

REFERENCES

1. Katona, M.B., et al., *CANDE - A Modern Approach for Structural Design and Analysis of Buried Culvert: User Manual,* and Reports: *FHWA-RD-77-5, 77-6,* US Naval Civil Engineering Laboratory, 1977.

2. Simpson, Gumpertz and Heger, Consulting Engineers, *Users Instruction for SIDD and SIDD-HT,* Arlington, Mass.

3. American Concrete Pipe Association, *Concrete Pipe Technology Handbook,* Vienna, Virginia, 1993.

4. American Concrete Pipe Association, *Concrete Pipe Technology Handbook,* Vienna, Virginia, 1980.

5. Krizek, R.J. and McQuade, P.V., "Behavior of Buried Concrete Pipe," *Journal of the Geotechnical Engineering Division, ASCE,* Vol. 99, No. GT7, July 1978, pp. 815-836.

6. Anderson, J.E., "A Model for Evaluating the Response of Buried Circular Concrete Pipe," Ph.D. Dissertation, Northwestern University, 1974.

7. Selig, E.T. and D.L. Packard, "Buried Concrete Pipe Embankment Installation Analysis," *Journal of Transportation Engineering, ASCE,* Vol. 112, No. 6, November 1986, pp. 576-592.

8. Roschke, P.K. and Davis, R.E., "Rigid Culvert Finite Element Analysis," *Journal of Geotechnical Engineering,* Vol. 112, No. 8, August 1986, pp. 749-767.

9. Penman, A.D.M, Charles, J.A. Nash, J.K. and Humphreys, J.D., "Performance of Culvert under Winscar Dam, *Geotechnique,* Vol 25, No. 4, 1975, pp. 713-730.

APPENDIX

Field Strain Data Presentation for Test 5 and Test 6

Table A.1 Strain at Outside Concrete Top at Different Levels of Soil Height above Bottom of Pipe.

Soil Height above Bottom (m)	Pipe 5				Pipe 6			
	OPC(L)	OPC(C)	OSC(C)	Shoulder (R)	OPC(L)	OPC(C)	OSC(C)	Shoulder (R)
0.00	17*	-6	16	37	-39	1341	3	60
0.461	24	-21	26	54	-46	2312	20	81
0.720	43	-3	43	61	-24	2515	47	95
0.933	62	50	62	34	-102	2578	68	74
0.933	6	20	24	41	-172	3023	16	56
1.238	8	4	20	31	-157	3274	17	65
1.400	12	-1	23	23	-149	3511	25	78
1.867	17	35	30	8	-171	3923	52	65
2.235	-4	18	19	9	-188	3996	44	59
2.375	-18	12	17	8	-189	4036	45	59
2.476	**	**	**	**	**	**	**	**
4.092	109	19	0	81	61	16109	329	53
6.134	117	6	39	80	392	***	746	19
6.317	127	-26	14	75	498	***	4323	-48
8.725	211	139	73	112	2282	***	4612	38
13.724	353	322	188	120		***	***	268

*Strains are measured in micro strain
OPC=Outer Primary concrete OSP=Outer Secondary Concrete
(L)= Longitudinal (C)=Circumferential

Table A.2 Strain at Inside Concrete Top at Different Levels of Soil Height above Bottom of Pipe.

Soil Height above Bottom (m)	Pipe 5				Pipe 6			
	IPC(L)	IPC(C)	ISC(C)	Shoulder (R)	IPC(L)	IPC(C)	ISC(C)	Shoulder (R)
0.000	-7*	-7	7	157	8	1777	-11	3
0.461	-23	-15	-7	459	-5	2868	-23	6
0.720	-27	-16	-12	413	-14	3420	-28	-1
0.933	-24	-11	-39	372	-43	3677	-23	-7
0.933	-10	-19	-30	508	-9	4704	-17	11
1.238	-15	-11	-16	603	5	5104	-20	18
1.400	-24	-18	-20	747	2	5521	-35	22
1.867	-18	-1	-20	887	-21	6755	-10	14
2.235	-17	-10	-25	958	-16	7090	-11	18
2.375	-17	-10	-25	1030	-18	5256	-11	18
2.476	**	**	**	**	**	**	**	**
4.092	11	30	13	989	6	7470	8	56
6.134	19	54	23	1063	9	7516	18	117
6.317	5	50	28	1192	-3	8609	26	107
8.725	28	84	36	1291	12	8541	76	337
13.724	30	90	-43	1273	6	8109	90	355

* Strains are measured in micro Strain.
IPC= Inner Primary Concrete ; ISC= Inner Secondary Concrete;
(L)= Longitudinal Direction; (C)=Circumferential Direction;

Table A.3 Strain at Outside Springline(R) of Concrete at Different Levels of Soil Height above Bottom of Pipe.

Soil Height above Bottom (m)	Pipe 5				Pipe 6			
	OPC(L)	OPC(C)	OSC(C)	Haunch (R)	OPC(L)	OPC(C)	OSC(C)	Haunch (R)
0.000	35*	41	27	**	60	520	71	-8
0.461	30	52	36	**	65	604	93	31749
0.720	**	68	37	**	71	748	106	2131
0.933	**	-13	15	**	75	-71	62	845
0.933	**	11	18	**	83	1008	79	1144
1.238	**	1	19	**	83	1015	77	1190
1.400	**	-4	21	**	70	1087	85	1190
1.867	**	-31	22	**	39	1080	83	1051
2.235	**	-53	18	**	42	1045	88	1026
2.375	**	-58	14	**	46	1057	87	772
2.476	**	**	**	**	**	**	*	**
4.092	**	326	38	**	-74	1079	13	-6
6.134	**	653	64	**	47	1248	55	566
6.317	**	494	83	**	46	1759	30	593
8.725	**	581	145	**	67	2793	231	707
13.724	**	301	302	**	108	4078	314	1139

* Strains are measured in micro Strain.
OPC= Outer Primary Concrete ; OSC= Outer Secondary Concrete;
(L)= Longitudinal Direction; (C)=Circumferential Direction;

Table A.4 Strain at Inside Springline(R) of Concrete at Different Levels of Soil Height above Bottom of Pipe.

Soil Height above Bottom (m)	Pipe 5				Pipe 6			
	IPC(L)	IPC(C)	ISC(C)	Haunch (R)	IPC(L)	IPC(C)	ISC(C)	Haunch (R)
0.000	-18*	442	-11	-12	13	705	53	54
0.461	-22	1203	-21	-20	14	1173	96	99
0.720	-28	1397	-22	-20	17	1453	113	106
0.933	-38	1303	-19	-2	7	1578	23	18
0.933	-14	2368	-4	-9	46	2332	29	23
1.238	-9	2647	-4	-18	57	2581	61	49
1.400	-1	2821	-1	-19	57	2724	81	63
1.867	-15	3282	-13	-8	45	3163	59	51
2.235	-16	3373	-1	-8	49	3287	56	48
2.375	-13	3450	0	-10	52	3355	58	49
2.476	**	**	**	**	**	**	**	**
4.092	-37	3632	-4	-22	64	3887	47	12
6.134	-16	4020	-14	-30	72	4185	48	-17
6.317	-26	4378	-40	-47	59	4702	48	-27
8.725	-61	4428	-64	-124	85	4699	5	-120
13.724	-314	4140	-145	-133	96	4773	3	-191

* Strains are measured in micro Strain.
IPC= Inner Primary Concrete ; ISC=Inner Secondary Concrete;
(L)= Longitudinal Direction; (C)=Circumferential Direction;

Table A.5 Strains at Outside Bottom of Concrete at Different Levels of Soil Height above Bottom of Pipe.

Soil Height above Bottom (m)	Pipe 5				Pipe 6			
	OPC(L)	OPC(C)	OSC(C)	Haunch (L)	OPC(L)	OPC(C)	OSC(C)	Haunch (L)
0.000	**	-6*	1	-2	14	**	12	12
0.461	**	-7	1	-3	12	**	7	4
0.720	**	-5	1	-5	13	**	9	7
0.933	**	-14	-8	-18	-6	**	-48	-65
0.933	**	-18	-3	13	14	**	-15	5
1.238	**	-17	-1	11	24	**	0	14
1.400	**	-17	-1	14	30	**	3	18
1.867	**	-15	-11	12	7	**	-30	16
2.235	**	-14	-9	14	15	**	-25	23
2.375	**	-12	-7	14	15	**	-26	26
2.476	**	**	**	**	**	**	**	**
4.092	**	22	4	345	24	**	-99	-79
6.134	**	28	1	515	22	**	-86	74
6.317	**	20	-9	434	16	**	-128	125
8.725	**	24	-4	419	-905	**	-132	285
13.724	**	7	-39	-163	-3416	**	-142	601

*Strains are measured in micro Strain.
** Data not Available
OPC= Outer Primary Concrete ; OSC= Outer Secondary Concrete;
(L)= Longitudinal Direction; (C)=Circumferential Direction;

Table A.6 Strain at Inside Bottom of Concrete at Different Levels of Soil Height above Bottom of Pipe.

Soil Height above Bottom (m)	Pipe 5				Pipe 6			
	IPC(L)	IPC(C)	ISC(C)	Haunch (L)	IPC(L)	IPC(C)	ISC(C)	Haunch (L)
0.000	84*	67	3	17	49	83	3	29
0.461	52	25	3	24	89	166	4	23
0.720	-24	-49	2	26	94	210	8	42
0.933	-279	-314	15	-2	8	-6	20	-33
0.933	-245	-276	11	1	18	7	17	51
1.238	-213	-250	7	13	46	92	9	57
1.400	-188	-227	7	14	58	155	7	61
1.867	-278	-300	18	7	41	36	28	77
2.235	-282	-312	18	11	40	32	23	74
2.375	-283	313	16	12	41	33	26	77
2.476	**	**	**	**	**	**	**	**
4.092	-356	-343	36	71	12	-42	34	63
6.134	-363	-330	50	97	-16	-85	41	116
6.317	-375	-327	54	103	-25	-93	17	116
8.725	-339	-318	155	109	-111	-202	833	623
13724	-115	-359	177	2480	-187	-303	812	969

*Strains are measured in micro Strain.

**

IPC= Inner Primary Concrete; ISC= Inner Secondary Concrete;

(L)= Longitudinal Direction; (C)= Circumferential Direction;

Table A.7 Strain at Outside Springline (L) of Concrete at Different Levels of Soil Height above Bottom of Pipe.

Soil Height above Bottom (m)	Pipe 5				Pipe 6			
	OPC(L)	OPC(C)	OSC(C)	Shoulder (L)	OPC(L)	OPC(C)	OSC(C)	Shoulder (L)
0.000	2*	-2	-15	11	-19	181	-34	-47
0.461	**	-11	**	-11	7	385	-99	-89
0.720	**	9	**	4	7	497	-335	-20
0.933	**	-14	**	26	-22	566	-188	70
0.933	**	-23	**	668	-15	814	-43	**
1.238	**	-40	**	-15	-17	881	-71	**
1.400	**	-38	**	-6	-19	949	-59	**
1.867	**	-54	**	3973	-13	1207	-13	**
2.235	**	-53	**	1935	-15	1312	-22	**
2.375	**	-55	**	2227	-13	1385	-23	**
2.476	**	**	**	**	**	**	**	**
4.092	**	-92	**	**	166	1142	-120	**
6.134	**	-155	**	20914	435	1890	-41	**
6.317	**	-178	**	**	546	3172	-29	**
8.725	**	-274	**	**	794	3684	67	**
13.724	**	-209	**	**	1192	5425	221	**

* Strains are measured in micro Strain.
** Data Not Available
OPC= Outer Primary Concrete ; OSC= Outer Secondary Concrete;
(L)= Longitudinal Direction; (C)= Circumferential Direction;

Table A.8 Strain at Inside Springline (L) of Concrete at Different Levels of Soil Height above Bottom of Pipe.

Soil Height above Bottom (m)	Pipe 5				Pipe 6			
	IPC(L)	IPC(C)	ISC(C)	Shoulder (L)	IPC(L)	IPC(C)	ISC(C)	Shoulder (L)
0.000	17*	160	14	2	**	-2041	15	6
0.461	15	317	24	-10	**	24808	13	-2
0.720	22	350	19	-20	**	29189	13	-5
0.933	-6	325	-4	-20	**	29315	15	-33
0.933	26	493	1	7	**	29281	24	-3
1.238	37	543	14	14	**	29293	30	-1
1.400	45	574	16	14	**	29331	32	-12
1.867	36	666	11	-13	**	29360	12	-18
2.235	37	698	14	-1	**	29397	24	-10
2.375	41	713	13	-2	**	29369	23	-6
2.476	**	**	**	**	**	**	**	**
4.092	36	431	28	-9	**	29369	0	-19
6.134	52	96	24	-28	**	29343	-5	-35
6.317	5	-55	7	-60	**	28806	-29	-63
8.725	0	-479	-17	-60	**	29116	-56	-92
13.724	-47	-879	-89	-132	**	29169	-169	-199

* Strains are measured in micro Strain.
** Data Not Available.
IPC= Inner Primary Concrete ; ISC= Inner Secondary Concrete;
(L)= Longitudinal Direction; (C)= Circumferential Direction;